Mutational-kinetic Analysis Reveals the Roles of Arginines and Aromatics in the Core of the GABAA Receptor Ligand-binding Pocket

Phu Tran
Marquette University

MUTATIONAL-KINETIC ANALYSIS REVEALS THE ROLES OF ARGININES AND AROMATICS IN THE CORE OF THE $GABA_A$ RECEPTOR LIGAND-BINDING POCKET

by

Phu N. Tran, B.S.

A Dissertation submitted to the Faculty of the Graduate School,
Marquette University,
in Partial Fulfillment of the Requirements for
the Degree of Doctor of Philosophy

Milwaukee, Wisconsin

May 2011

ABSTRACT
MUTATIONAL-KINETIC ANALYSIS REVEALS THE ROLES OF ARGININES AND AROMATICS IN THE CORE OF THE $GABA_A$ RECEPTOR LIGAND-BINDING POCKET

Phu N. Tran, B.S.

Marquette University, 2011

The γ-aminobutyric acid type A (GABA) receptor is a member of the cys-loop family of ligand-gated ion channels that plays a crucial role in normal brain function by transducing the majority of inhibitory neurotransmission in the central nervous system. The studies documented in this dissertation were aimed at validating and refining the current best model for the interaction of GABA with the $GABA_A$ receptor via structure-function perturbation analysis. Mutational-kinetic data was used in conjunction with homology modeling knowledge to draw up architectural and functional roles of the arginines and aromatics in GABA-binding pocket. The results provide interesting new insights.

Two positively charged arginine residues, which have been implicated in ligand binding, were profiled through serial mutagenesis, to get at the specific side chain properties required for the roles they serve. The structural and functional contribution of four aromatic residues were examined through measuring the influence of their side chain on GABA binding rate with respect to changes caused by point mutations. An interaction between two aromatic residues critical for proper ligand binding was discovered through a screen for functional coupling between them and four neighboring arginines. These results were subsequently employed in an attempt to refine the current ligand-receptor interaction model, proposing specific roles for the amino acid residues studied.

In the current best model of the $GABA_A$ receptor's ligand-binding pocket, the amino moiety of GABA is coordinated by a cation-π interaction with β_2Y97 and the carboxyl moiety coordinated by an interaction with either β_2R207 or α_1R67 (or possibly both). Here, we incorporate the results of this dissertation to modify and add significant detail to this model. The model proposed here includes the following features: a hydrophobic interaction between β_2Y97 and β_2F200, an inter-subunit cation-π interaction between β_2Y97 and α_1R132, a cation-π interaction between the amino group of GABA and β_2F200, hydrogen bond(s) between the carboxyl end of GABA and the guanidinium group of α_1R67, and an interaction between the side chain of β_2R207 and the backbone carbonyl of β_2Y97.

ACKNOWLEDGEMENTS

Phu N. Tran, B.S.

I am extremely grateful for the guidance and support I have received over the past six years from everyone in my life. The faculty at Marquette University, especially those serving on my advising committee, was instrumental in my development as a scientist. My colleagues, Dr. David A. Wagner and Dr. Kurt T. Laha, have been an enormous help when struggling through experiments in the lab and have become great friends. I am also fortunate to have a family that continues to offer me encouragement and assurance that I have been doing the right thing.

TABLE OF CONTENTS

LIST OF TABLES

LIST OF FIGURES

CHAPTER I

CHAPTER II

CHAPTER III

CHAPTER IV

CHAPTER V

CHAPTER VI

APPENDIX

ABBREVIATIONS

5HT-3 receptor, serotonin type 3 receptor

AChBP, acetylcholine binding protein

EC_{50}, effective concentration evoking 50% of a maximal current response

eGFP, enhanced green fluorescent protein

GABA, γ-aminobutyric acid

$GABA_A$ receptor, γ-aminobutyric acid receptor type A

HEK-293, human embryonic kidney cells (lineage 293)

HEPES, 4-(2-hydroxyethyl)-1-piperazineethanesulfonic acid

I, current

IPSP, inhibitory postsynaptic potential

K_D, dissociation constant

k_{off}, microscopic unbinding rate

k_{on}, microscopic binding rate

SCAM, substituted cysteine accessibility method

LB, Luria-Bertani broth

LGIC, ligand-gated ion channel

MTS reagent, methane thiol sulfonate

nAChR, nicotinic acetylcholine receptor

PCR, polymerase chain reaction

SDS-PAGE, sodium dodecyl sulfate polyacrylamide gel electrophoresis

S.E.M., standard error of mean

I. INTRODUCTION

This dissertation documents experiments aimed to study the structure and function of the γ-aminobutyric acid type A ($GABA_A$) receptor. Specifically, the experiments presented here were designed to test, refine, and advance the current best model for how γ-aminobutyric acid (GABA) interacts with the ligand-binding site of the $GABA_A$ receptor. This process involved identification of an amino acid residue of interest, mutation of the residue, assessment of the functional effects of the mutation, incorporation of the results into the structural model of the receptor, and the inference of functional roles of the residue in question from the new structural model.

This approach was initially applied to two arginine residues implicated in GABA binding (Chapter III) and then extended to a cluster of four aromatic residues that are believed to be in the heart of the binding pocket (Chapter IV). Finally, double mutant cycle analysis was applied to identify functional interactions between, and within, the studied arginines and aromatics (Chapter V). This approach identified as well as ruled out a number of possible interactions among amino acid residues that line ligand-binding pocket of the $GABA_A$ receptor. The results of these studies are used to validate and refine the current best model for the interaction of GABA with the $GABA_A$ receptor and produce a model that contains novel and detailed information about the molecular architecture of the ligand-binding pocket.

The physiological and pharmacological relevance of $GABA_A$ receptor

Two amino acids, glutamate and GABA, are neurotransmitters responsible for most of the fast excitatory (glutamate) and fast inhibitory (GABA) communication between nerve cells in the brain. At a basic level, normal brain function may be thought of as a balance between excitation and inhibition mediated by glutamate and GABA

transmission, respectively. It is thought that all nerve cells in the brain have receptors for the neurotransmitters glutamate and GABA (Johnston, 2003). In addition, it is estimated that 40% of nerve cells release glutamate as an excitatory neurotransmitter, while a different 40% release GABA as an inhibitory neurotransmitter (Johnston, 2003; Bowery and Smart, 2006).

Therefore, the homeostatic balance between these two amino acid transmitters is vital to normal brain function. An excess of excitation over inhibition, for instance, results in an overexcited brain that can be manifested as anxiety, agitation, exhilaration, convulsions and even death. On the other hand, an excess of inhibition over excitation can be manifested as depression, sedation, coma and death. In fact, mutations that alter the proper function of the $GABA_A$ receptors, for example, have been implicated in Angelman's syndrome (Dan and Boyd, 2003) and epilepsy (Baulac et al., 2001; Bowser et al., 2002).

Additionally, there are many substances that can tip such a balance, if not used properly. When improper usage of substances occurs, such as sleeping aid and anesthetic overdose, proper intervention may dictate whether the victim will survive. Proper intervention often means administering some type of pharmacological agents to counteract the effects. It is, therefore, particularly important to understand the mechanism of how these transmitters activate their target and how various substances modulate this activation process. Such understanding will be of clinical relevance in terms of enabling more effective therapeutic interventions.

Interestingly, the contribution of $GABA_A$ receptors to clinical medicine was established long before the role of GABA as a neurotransmitter had even been suggested.

As early as the 19th century, barbiturates were first used as anxiolytic hypnotics and anticonvulsants, and eventually as intravenous anaesthetics; however, it was not until the mid 20th century that their molecular targets, $GABA_A$ receptors, started to emerge. In 1967, evidence for GABA as an inhibitory transmitter in the CNS was finally achieved when Krnjevic and Schwartz demonstrated that application of GABA to cat cortical neurons caused activity that resembled inhibitory postsynaptic potential (IPSP). The association of various modulators' action with GABA receptors only became clear, when Haefely et al. (1975) first described the effects of an important class of modulators, the benzodiazepines. It was discovered that benzodiazepines produce their effects by potentiating the response to GABA stimulation, and part of this potentiation is underlied by an increase in the mean open time of the intrinsic chloride channel, enabling more current to flow (Bianchi et al., 2009). The advent of the benzodiazepines, in a way, opened the "door" for the discovery of more pharmacological agents that are known to modulate $GABA_A$ receptor function. For instance, besides barbiturates and benzodiazepines, $GABA_A$ receptors are also modulated by an array of other compounds such as neurosteroids, flavonoids, and ethanol (see review by Johnston, 2005).

Despite the vast amount of information about the function of $GABA_A$ receptors, and the compounds that interact with them, there are still many unknowns regarding the details of their structure and function and their interactions with modulators. Therefore, it is important to continue $GABA_A$ receptor structure-function studies. Knowledge gained from studying $GABA_A$ receptors will not only allow for more intelligent drug design targeting $GABA_A$ receptors but also contribute to better understanding of the general mechanisms of ligand-gated ion channels' function and regulation.

Diversity of the $GABA_A$ receptors

In mammals, 19 different $GABA_A$ receptor subunit genes have been cloned and grouped into seven families (α_1-α_6, β_1-β_3, γ_1-γ_3, δ, ε, θ, π, and ρ_1-ρ_3) by sequence similarity (Simon et al., 2004; Sieghart and Ernst, 2005). Some members of α, β, and γ families (i.e. α_5, β_2, β_3 and γ_2) also exist in alternatively spliced forms, giving rise to even greater subunit diversity (Simon et al., 2004). Such subunit diversity, however, may not result in a very large number of pentameric combinations because receptor assembly and distribution appears to follow some basic stoichiometric patterns (Luscher and Keller, 2004). During the folding and oligomerization processes, each subunit must recognize its neighbors via specific high-affinity interactions. This recognition between a given subunit and its adjacent neighbor subunits is necessary for achieving the correct stoichiometry and order of subunits around the pore. The stoichiometry and ordered arrangement of $GABA_A$ receptor subunits has been explored using biochemical, immunohistochemical, and electrophysiological methods.

In early expression studies, it was recognized that combinations of α and β subunits are sufficient to form functional $GABA_A$ receptors (i.e. 2 α subunits and 3 β subunits to form a receptor). However, the majority of native receptors contain a third subunit type. For example, using western blots where the relative reactivity of the antibodies had been determined, Tretter et al., (1997) found that the ratio of subunits in recombinant receptors $\alpha_1\beta_3$ and $\alpha_1\beta_3\gamma_2$ are $2\alpha_1$:$3\beta_3$ and $2\alpha_1$:$2\beta_3$:$1\gamma_2$, respectively. In a different quantitative study, which compared the maximal fluorescent signal from c-myc-labeled subunits expressed as α_1(c-myc)$\beta_2\gamma_2$, $\alpha_1\beta_2$(c-myc)γ_2, and $\alpha_1\beta_2\gamma_2$(c-myc) receptors,

the measured fluorescent signal was found to be twice as intense in expression with labeled α_1(c-myc) or β_2(c-myc) than in expression with labeled γ_2(c-myc). This finding supported a 2:2:1 stoichiometry (Farrar et al., 1999). Another line of evidence for the 2:2:1 stoichiometry came from studies that employed the expression of α-β and β-α concatenated subunits. These concatenated complexes could not produce functional receptors when expressed alone or with α, but when β or γ was included functional expression resulted (Baumann et al., 2001). The use of a variety of concatenated subunit combinations also demonstrated that the only subunit arrangement of $\alpha_1\beta_2\gamma_2$ receptors' subunits that get trafficked to the cell surface was $\beta_2\alpha_1\beta_2\alpha_1\gamma_2$ in a counterclockwise order (Baumann et al., 2002). This subunit arrangement is consistent with the formation of the appropriate inter-subunit interfaces known to bind GABA (β/α interfaces) and benzodiazepines (α/γ interface) (Cromer et al., 2002). All in all, data accumulated from different studies using quantitative immunoprecipitation (Tretter et al., 1997), fluorescence resonance energy transfer between epitope-tagged subunits (Farrar et al., 1999) and electrophysiology of receptors with concatenated subunits (Baumann et al., 2002; Boileau et al., 2005; Baur et al., 2006) revealed a stoichiometry of two α, two β and one γ subunit, arranging in a counterclockwise order of βαβαγ, as the dominant assembly of $GABA_A$ receptor subunits. In addition, studies employing subunit-specific antibodies demonstrated that the most abundant $GABA_A$ receptor subtype in brain is formed from α_1, β_2 and γ_2 subunits (McKernan and Whiting, 1996; Sieghart and Sperk, 2002; Whiting, 2003; Benke et al., 2004).

Receptors composed of alternate subunit combinations have also been identified. For examples, $GABA_A$ receptors are also commonly formed from other α, β and γ

combinations such as $\alpha_2\beta_3\gamma_2$ and $\alpha_3\beta_3\gamma_2$. Less common, though no less functionally important, are receptors in which the third subunit is a δ subunit (e.g. $\alpha_4\beta_3\delta$ or $\alpha_6\beta_3\delta$) instead of a γ subunit. γ-containing receptors are thought to primarily localize at the synapse, while δ-containing receptors tend to localize extrasynaptically or perisynaptically (Sun et al., 2004). In other receptor subtypes, the γ subunit may be replaced by either ε or π, while π and θ subunits may be capable of co-assembling with α, β and γ subunits to form receptors containing representatives from four families (Bonnert et al., 1999; Neelands and Macdonald, 1999; Neelands et al., 1999; Sieghart and Sperk, 2002). Additional variability comes from the fact that individual receptors may contain two different α or β subunit isoforms (Benke et al., 2004; Minier and Sigel, 2004; Boulineau et al., 2005).

The diversity of pentameric combinations is also limited by the differential distribution of subunit types among brain regions and neuron groups (Fritschy and Mohler, 1995; Pirker et al., 2000). For example, while some subunits such as the α_1 and γ_2 are ubiquitous, others such as α_6, ε and π are much more restricted in their distribution. For example, α_6 has been shown to express primarily in granule cells of the cerebellum and inferior colliculus (Luddens et al., 1990). On the other hand, the ε and θ subunits are found mainly in modulatory regions or nuclei such as cholinergic, noradrenergic, serotonergic, dopaminergic, and histaminergic cell groups (Sinkkonen et al., 2000; Moragues et al., 2003; Sergeeva et al., 2005). The π subunit is present at low levels in brain, but is strongly expressed in various other organs, including uterus and breast (Hedblom and Kirkness, 1997; Zafrakas et al., 2006).

The diversity of $GABA_A$ receptors is further enhanced by another subtype known as $GABA_A$ ρ (formerly referred to as the $GABA_C$ receptor). This receptor subtype consists entirely of ρ subunits, which were first cloned from retina (Cutting et al., 1991). Unlike the majority of $GABA_A$ receptors, which are heteromeric pentamers, the ρ-containing family of $GABA_A$ receptors can form homomeric pentamers consisting of entirely ρ_1 subunits or from heteromeric receptors containing only combinations of ρ_1, ρ_2, and ρ_3 subunits (Enz and Cutting, 1999; Sieghart and Sperk 2002). Compared to other $GABA_A$ receptor subtypes, $GABA_A$ ρ receptors are known to have higher sensitivity for GABA, yet their currents are generally smaller (Enz and Cutting, 1999). Also, pharmacologically, they are insensitive to such modulators as barbiturates, benzodiazepines as well as to the classical $GABA_A$ receptor antagonist bicuculline (Feigenspan et al., 1993; Feigenspan and Bormann, 1994). It was this difference in substrate preference that initially caused them to be classified as $GABA_C$ receptors, However, the later characterization of their subunit composition and transduction mechanism revealed them to be a $GABA_A$ receptor subtype (Mohler, 2007).

The diversity in function among subtypes of $GABA_A$ receptors potentially gives rise to a great array of targets for pharmacologic agents. Presented with many similar targets, the one potential problem for drug design would be undesirable non-specific effects. Therefore, to target a specific population of $GABA_A$ receptors effectively, it is crucial to first understand the functional parameters that set them apart. Often, such functional parameters include the nature of ligand binding, the kinetics elicited, and the physiologically relevant effects. While the kinetics and effects of activating certain

subpopulation of receptors can be readily measured, it is much more difficult to detect the nature of ligand-receptor interaction.

$GABA_A$ receptor as a member of the cys-loop ligand gated ion channels family

The $GABA_A$ receptor is a member of the cys-loop superfamily of ligand-gated ion channels (cl-LGICs), which includes nicotinic acetylcholine (nACh) and 5-hydroxytryptamine type 3 (5-HT_3) receptors (cation channels) and anionic GABA and glycine receptors (anion channels). The members of this superfamily are characterized by a conserved motif in the extracellular amino-terminal domain in which two cysteine residues form a disulphide bridge (Simon et al., 2004). The cl-LGICs are pentameric, often arising from the assembly of heterologous subunits that form a central ion channel, are activated by the binding of a small neurotransmitter molecule to the extracellular inter-subunit interfaces (Lester et al., 2004; Peters et al., 2005; Sine and Engel, 2006). Besides an extracellular amino terminal domain responsible for ligand binding, each subunit also has a carboxyl terminal part containing four trans-membrane domains (M1–M4) that form the ion-selective channel (Figure 1.1).

The binding of GABA molecules to the receptor's extracellular domains must somehow be rapidly translated into movement of the appropriate parts of the pentameric complex to lead to opening of the channel. It is known that binding of two GABA molecules at the extracellular interfaces between α and β subunits is necessary to fully activate the receptor (Figure 1.2). The lack of a crystal structure for $GABA_A$ receptor has made it difficult to dissect the binding and gating processes involved in normal $GABA_A$ receptor function. However, in recent years, models of receptor structure such as those arising from combining the atomic-scale model of the nicotinic acetylcholine receptor

(nAChR) from electric organ of electric ray, *Torpedo marmorata*, (Unwin, 2005) and the crystal structure of the soluble acetylcholine binding protein (AChBP) from snail, *Lymnaea stagnalis*, (Brejc et al., 2001; Celie et al., 2004) have helped advance our understanding for the molecular basis of $GABA_A$ receptor function.

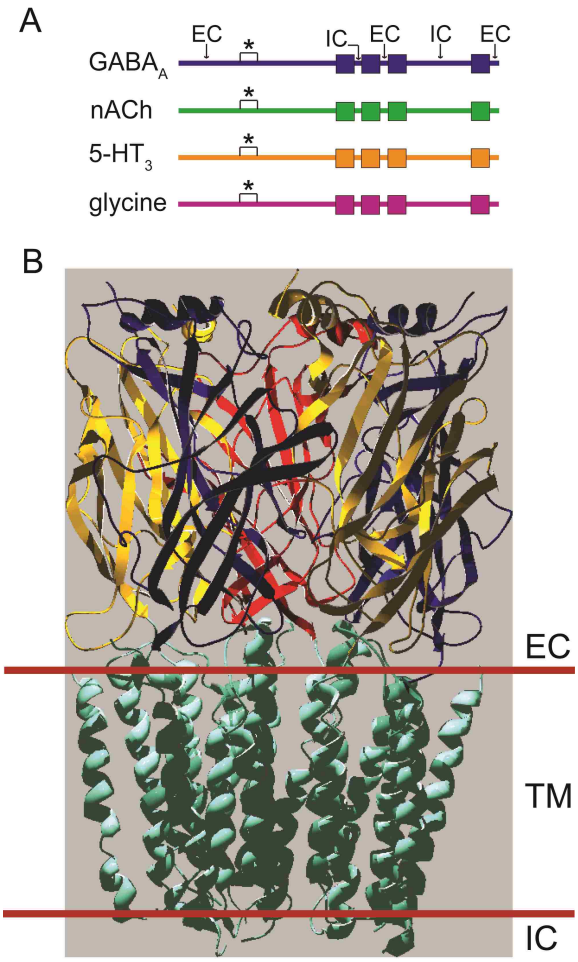

Figure 1.1 Characteristics structural domains of a cl-LGIC subunit. A) Linear illustration of the cl-LGICs subunit. Each subunit possesses a large extracellular N-terminal domain containing the disulfide bond (cys-loop) charateristic of the superfamily (*) and ligand-binding regions, followed by four transmembrane domains (squares). Arrows indicate the extracellular (EC) and the intracellular (IC) domains. B) Receptors are constructed as pentameric ion channels from the assembly of five subunits in a ring structure, creating an ion pore within. This image shows ribbon presentation of the receptor viewed from the side, based on a homology model. Only a small part of the intracellular domain is shown.

General description of the cl-LGICs' ligand-interacting domain

The structure of the nAChR, by far, is the best understood among cl-LGICs. The nAChRs are found in the CNS and in neuromuscular junctions. A major subtype of nAChRs, with a heteropentameric stoichiometry of $(\alpha_1)2\beta_1\delta\gamma$ is found at the neuromuscular junction in vertebrates and in the electric organs of fish (i.e. electric ray,

Torpedo californica). In the CNS, nAChRs exist in many different subtypes; the most common of which is made up of two α_4, one β_2 and two other subunits. It is also known that α_7-α_9 can form homopentamers (McGehee, 1999).

Early studies involving immunoelectron microscopy provided limited structural information of the receptor complex (Klymkowsky and Stroud, 1979; Kistler and Stroud, 1981). However, more recent data coming from electron microscopy (EM) studies of *Torpedo* receptors (Unwin, 1995; Miyazawa et al., 1999), which were refined and compared (Unwin, 2005) with the AChBP crystal structure (Brejc et al., 2001), have allowed for a more detailed model of the nAChR's extracellular domain. This model was verified by Dellisanti et al. (2007) when they solved the crystal structure of the extracellular domain of nACh receptor α_1 in complex with the α-bungarotoxin at 1.94 Å.

In 2001, Brejc and colleagues reported the discovery of an acetylcholine binding protein from snails. This protein was thought to act as a buffer for ACh in the synapse. It is homologous to the extracellular region of the nAChR α subunit and is also a pentamer. This AChBP, which is water soluble, was crystallized and its structure was resolved to 2.7Å. The sequence of AChBP aligns with the N-terminal extracellular ligand-binding domains of all cl-LGICs (Brejc et al., 2001). AChBP has sequence identities between 15 – 25% with respect to $GABA_A$, glycine, 5-HT_3, and nAChR subunits (Sixma and Smit, 2003). Although this level of identity in primary sequence is relatively low, the secondary structures are much more conserved. Thus, the current homology models of the extracellular domain of receptors such as nACh and $GABA_A$ receptors are based on the known structure of AChBP.

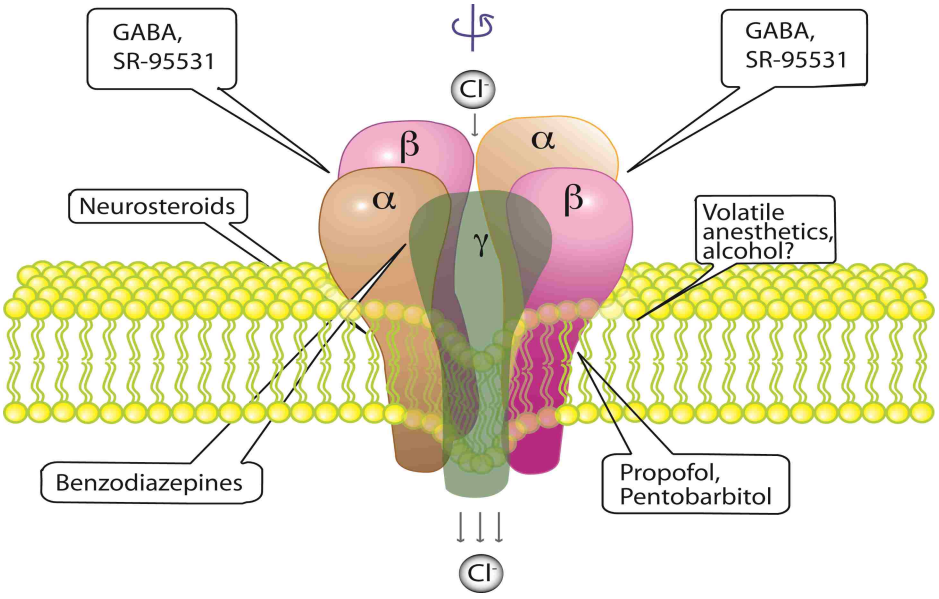

Figure 1.2 $GABA_A$ receptor – subunits stoichiometry, arrangement, ligand binding sites, and modulator sites. Depicted is the most common subunit stoichiometry of $GABA_A$ receptor, consisting of 2α, 2β, and one γ subunit. These subunits have been shown to assemble in a counterclockwise order of βαβαγ (top arrow). The endogenous agonist, GABA, binds at the two β/α interfaces, leading to channel opening and conduction of chloride. This schematic representation of a $GABA_A$ receptor also illustrates the different sites of action for different classes of molecules that interact with $GABA_A$ receptor. The agonist, GABA, and the antagonist, SR-95531, bind at both β/α inter-subunit interfaces. Benzodiazepines bind at the α/γ inter-subunit interface (Sigel and Buhr, 1997; Boileau et al., 1998). Propofol binds near the extracellular end of the third transmembrane domain on the β subunit (Bali and Akabas, 2004). Pentobarbitol interacts with parts of the first three transmembrane domains of β subunits (Amin, 1999; Serafini et al., 2000). Neurosteroids interact with the transmembrane domains at β/α inter-subunit interfaces and within a cavity of the α subunit (Hosie et al., 2006; Akk et al., 2008). Volatile anesthetics and alcohols interact with the receptor at sites in the transmembrane domains (Mihic et al., 1997).

A common theme, between the structure of AChBP's and all cl-LGICs' ligand-binding sites, is an inter-subunit "pocket" lined with six characteristic discontinuous loops termed A-F. Loops A through C are contributed by the one subunit and loops D through F are contributed by an adjacent subunit. For example, in nACh receptors, photoaffinity studies have identified that the α-subunit contributes what has been termed the principal binding face (+), which consists of residues clustered in loops A, B, and C (Galzi et al., 1990; Dennis et al., 1988; Sine et al., 1994) and the neighboring subunit (γ or δ) contributes loops D, E, and F on what has been termed the complementary binding

face (-) (Chiara et al., 1999; Czajkowski and Karlin, 1995; Sine, 1997). Across the cl-LGICs, amino acid residues from these loops have consistently been identified to hold critical roles in ligand binding.

Photoaffinity labeling experiments have also provided evidence for the location of the GABA-binding site, which is located at the interface of β and α subunits (Figure 1.2). Two separate studies labeled $GABA_A$ receptor subunits isolated from the brain with a tritiated homologue of GABA, [^{3}H] muscimol (Casalotti et al., 1986; Deng et al., 1986). [^{3}H] muscimol was found to incorporate into a band of 57 kD, corresponding to the β subunit and was also found to label a 52 kD band corresponding to the complementary α subunit when higher concentrations of purified receptor protein were analyzed.

Mutagenic-based examinations of the GABA-binding pocket

Mutagenesis studies of the $GABA_A$ receptor have identified several amino acid residues that may be involved in GABA binding. Consistently, almost all of these binding-related residues are found on the six discontinuous loops at the β/α inter-subunit interface. A rather useful application of mutagenesis, for the initial screen of an amino acid residue's involvement in receptor function, is the substituted-cysteine accessibility method (SCAM). This method provides an approach for identifying the amino acid residues that line channels, transporters, or binding-site pockets in membrane-spanning proteins (Akabas et al., 1992; Chen et al., 1997; Karlin and Akabas, 1998). Briefly, SCAM works on the premise that amino acid residues involved in ligand binding, for example, would face into the aqueous environment and therefore be more accessible than those not participating in ligand binding. As such, residues are mutated to cysteine and subsequently tested for accessibility by measuring reaction with a sulfhydryl reactive

reagent. The measured reactivity would indicate whether the residue is found on the aqueous surface within or near the ligand-binding site. Generally, residues found to be accessible to the sulfhydryl reactive reagent would be said to potentially face the binding pocket. On the other hand, the lack of reactivity may arise if the mutated residue is not accessible and does not react with the reagent.

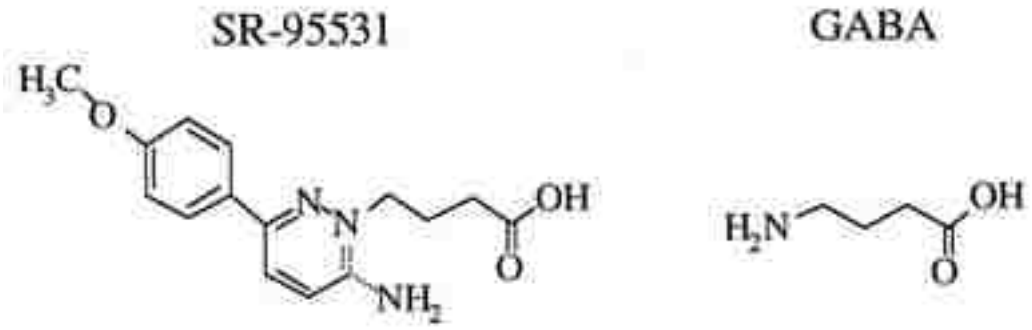

Figure 1.3 Chemical structures of the competitive antagonist (SR-95531) and the agonist (GABA)

While the measured reactivity only indicates whether an amino acid residue is exposed to the aqueous environment, a further test involving the measured rate of reaction in the presence of agonist or antagonist would indicate whether a given residue lies near the ligand-binding site. As such, several studies employing SCAM have identified a number of amino acid residues that line the binding pocket of $GABA_A$ receptors (Boileau et al., 1999; Boileau et al., 2002; Newell and Czajkowski, 2003; Wagner and Czajkowski, 2001; Holden et al., 2002; Kloda and Czajkowski, 2007). GABA and SR-95531 share a structural motif – a carboxyl group and an amino group separated by a length of a three-carbon chain (Figure 1.3). This SCAM approach identified 20 residues for which the rate of reaction with sulfhydryl reagents was reduced in the presence of GABA (**loop A**: β_2Y97C and β_2L99C; **loop B**: β_2T160C and β_2D163C; **loop C**: β_2S204C, β_2Y205C, β_2R207, and β_2S209; **loop D**: α_1F65C, α_1R67C, and α_1S69C;

loop E: α_1K117C, α_1L118C, α_1E123C, α_1L128C, α_1T130C, and α_1R132; **loop F**: α_1V178C, α_1V180C, and α_1D183C). Two residues, α_1D63C (Loop D) and α_1R120C (Loop E), were only protected by SR-95531. Since SR-95531 is larger than GABA, these residues are considered less proximal to the actual GABA-binding site.

One way to further assess the involvement of a residue in agonist-receptor interaction is by measuring the changes in a receptor's function caused by its mutation. This approach can be referred to as the structure-function perturbation method (Ackers and Smith, 1986). Typically, if a mutation results in a large rightward shift of the GABA concentration-response curve, the residue has a possible role in binding. Although in this mutational-electrophysiological approach, a variety of expression systems, subunit isoforms, and side-chain substitutions have been utilized in different studies, the basic interpretation that a residue has a role in binding process if its mutation leads to a large significant change in $EC_{50\text{-}GABA}$ remains the norm.

However, EC_{50} value is actually a macroscopic manifestation that is influenced by the integration of multiple microscopic processes such as ligand binding and unbinding, channel opening and closing, and desensitization and resensitization; therefore, concentration-response curves do not directly reveal information about these individual microscopic processes (Colquhuon, 1998). As such, a finer analysis is needed to determine if a residue is directly involved in binding. Wagner et al. (2004) provided the first detailed dissection of the biophysical role of a binding-pocket residue, applying the biophysical tools described by Jones et al., (1998), Jones et al., (2001), Sigworth, (1980), and Colquhoun and Hawkes, (1995). They examined the effects caused by cysteine substitution of β_2R207 using rapid-ligand application, single-channel recording, and

kinetic modeling. It was found that β_2R207C caused a 20-fold increase in the unbinding rate of GABA, an eight-fold decrease in the binding rate of GABA, and had no effect on any of the rates associated with gating. They concluded that β_2R207 is important for stabilizing the ligand-receptor complex, and suggested a possible direct interaction between the GABA molecule and β_2R207.

Additionally, given that cation-π interactions, which occur between a cation and the negative electrostatic potential on the face of an aromatic ring, are common at protein-protein interfaces (Gallivan and Dougherty, 1999; Crowley and Golovin, 2005) and especially protein-ligand interfaces (Zacharias and Dougherty, 2005), aromatic amino acid residues (π orbital donors), too, have emerged as central structure-function determinants at these interfaces. The use of unnatural aromatic amino acid substitution has been used extensively to test for cation-π involvement of aromatic residues at the ligand-binding site of cl-LGICs. Briefly, *in vivo* nonsense suppression methods allow synthetic amino acids (i.e. via engineered t-RNAs) to be incorporated during translation of a protein, allowing point mutation with an unnatural amino acid (Beene et al., 2002). This approach provides a powerful tool to get at the specific chemical properties of a side-chain. The technique has been successfully applied in LGICs to explore cation-π interactions.

Amino acid residues implicated in GABA-receptor interaction

As mentioned above, aromatic residues are known to cluster at or near the binding pockets of cl-LGICs. In nAChR this cluster of aromatic residues is referred to as the "aromatic box". These aromatic residues are associated with the six discontinuous binding pocket loops (Akabas, 2004). The resulting "aromatic box", which consists of

tyrosines and tryptophans from loops A, B, C, and D, may provide a hydrophobic barrier that excludes water from the binding pocket and, at the same time, serve as potential sites for direct docking of ligand. At least one aromatic residue in nACh receptors (Zhong et al., 1998), 5-HT_3 receptors (Beene et al., 2002), $GABA_A$ receptors (Padgett, et al., 2007) and $GABA_A$ ρ receptors (Lummis et al., 2005), and glycine receptors (Pless et al., 2008), has been shown to participate in cation-π interaction at the binding pocket.

On the $GABA_A$ receptor, several aromatic residues have been shown to be at the binding pocket, including β_2Y97, β_2Y157, β_2F200, β_2Y205, and α_1F65. Padgett et al. (2007) explored whether β_2Y97, $\beta_2$157, and β_2Y205 participate in cation-π interactions, using unnatural amino acid mutagenesis in which fluorinated aromatic side chains were substituted for the natural tyrosine side chains. This technique takes advantage of the fact that fluorine is electron-withdrawing, and each fluorine added to the aromatic ring serves to further reduce the negative electrostatic potential on the face of the aromatic ring. They found that only β_2Y97 demonstrated a direct relationship between the number of fluorines added and $EC_{50\text{-}GABA}$. Due to the strong correlation observed between cation-π ability at position 97 of β_2 and $EC_{50\text{-}GABA}$, they proposed that β_2Y97 directly interacts with the primary amine of GABA via a cation-π bond. From the lack of evidence for cation-π interaction at β_2Y157 and β_2Y205 they suggested that these residues require the electronegative groups at their C4 positions to function, perhaps via hydrogen bonds with neighboring side chains. This proposal is consistent with an earlier study, which suggested that β_2Y157 and β_2Y205 are involved in GABA binding. When these residues were conservatively substituted by phenylalanine, the receptors had a much-reduced sensitivity to GABA; $EC_{50\text{-}GABA}$ was increased by 50-fold compared to normal (Amin and

Weiss, 1993). The same study also reported that an even further reduction in GABA sensitivity resulted when either tyrosine residues were mutated to such non-aromatic amino acids as serine and asparagines, hinting that these tyrosine side chains may be bifunctional.

While these aromatic tyrosine residues may have significant contribution to GABA binding, the data reported by Padgett et al. (2007) was incomplete. For instance, it emphasized only on what type of interaction may occur between aromatic residues with the amino end of the GABA molecule. The interaction at GABA's carboxyl end is still unaccounted for. There is as high a chance for the carboxyl end of GABA to interact with surrounding residues as the amino end. Therefore, it is expected that some non-aromatic elements at the binding pocket may serve to secure the carboxyl end of GABA.

A study by Wagner and Czajkowski (2001), using SCAM and patch clamping techniques, identified one arginine residue and two aromatic residues critical in GABA as well as SR-95531 (competitive antagonist) binding. This study showed that β_2R207C, β_2Y205C, and β_2F200C caused 70, 18,000, and 300 fold increases in $EC_{50\text{-}GABA}$ respectively. However, no reaction was detected between biotin-tagged methanethiosulfonate, a thiol-reactive reagent used for cysteine residue labeling, and β_2F200C. They subsequently proposed that β_2Y205 and β_2R207 but not β_2F200 line the GABA-binding pocket. Wagner and colleagues (2004) provided evidence that β_2R207 directly influence the binding rate of GABA by measuring the changes in the GABA binding rate ($k_{on\text{-}GABA}$) caused by mutating β_2R207. They proposed that β_2R207 may help coordinate the carboxyl end of GABA.

Other arginines have been suggested to play a role in GABA binding. SCAM was used to demonstrate that α_1R67 lines the GABA-binding pocket and influences GABA affinity (Boileau et al., 1999). α_1R67 is also suggested to be a likely partner of the carboxyl end of GABA, through homology modeling (Cromer et al., 2002). Additionally, Westh-Hansen et al. (1999) found that a lysine substitution at α_1R120 (α_1R120K) resulted in a 180-fold increase in $EC_{50\text{-}GABA}$. The critical roles of these arginines were demonstrated by a study involving their counterparts on the α_5 subunit (α_5R70 and α_5R123). In this study, mutation of α_5R70 and α_5R123 to lysines caused 650- and 148-fold increases in $EC_{50\text{-}GABA}$, respectively (Hartvig et al., 2000).

Structural motifs crucial for GABA binding are conserved in other cl-LGICs

A convenient way to assess functional conservation of key motifs among cl-LGICs is to consider them in the context of the discontinuous loops that line each ligand-binding pocket (Figure 1.4). For reference, when considering a ligand-binding pocket formed at the interface of two adjacent subunits (i.e. β/α interface), loops A through C are located on the "principal" face (i.e. β subunit side) and loops D through F are located on the "complementary" face (i.e. α subunit side) (Figure 1.4). In $GABA_A$ receptors, several aromatic and positively charged residues found on these loops have been both directly shown and indirectly implicated in ligand binding. These residues are listed in Table 1.1. Residues playing similar roles in ligand binding have also been identified in other cl-LGICs (Figure 1.5, Table 1.1).

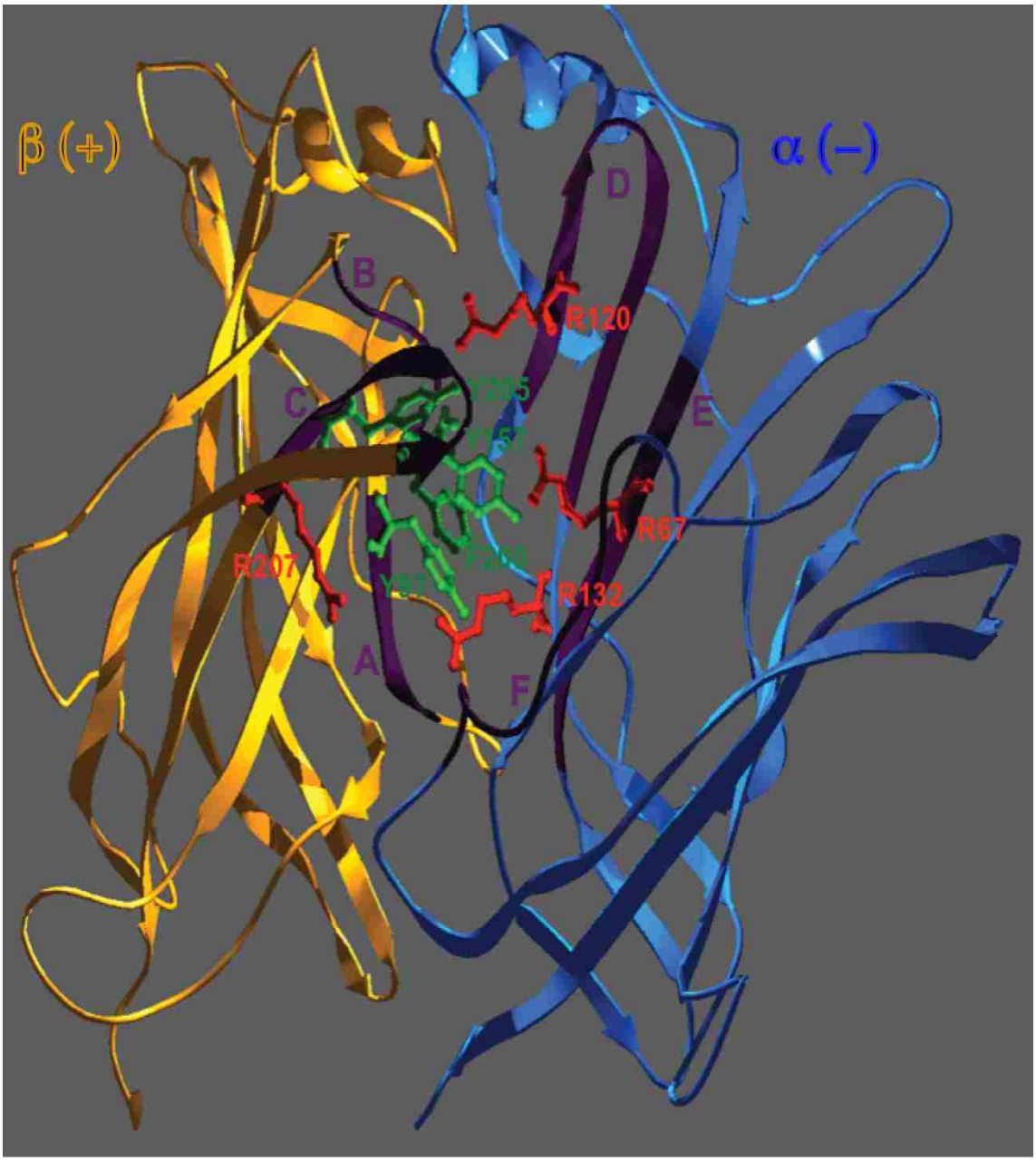

Figure 1.4 Important elements at the GABA-binding pocket. Side view of the extracellular domain of the β/α inter-subunit interface. In purple are six discontinuous loops that line the inter-subunit interface where GABA binds. By orientation, loops A through C are contributed by β subunit (primary face, +) and loops D through F are contributed by α subunit (complementary face, –). The aromatic residues (green) and the arginine residues (red) shown are explored in the studies documented here. Note each subunit is asymmetric and therefore opposite sides of the α subunit and β subunit are involved in GABA binding. The classic binding site loop nomenclature is used (Kash et al., 2004).

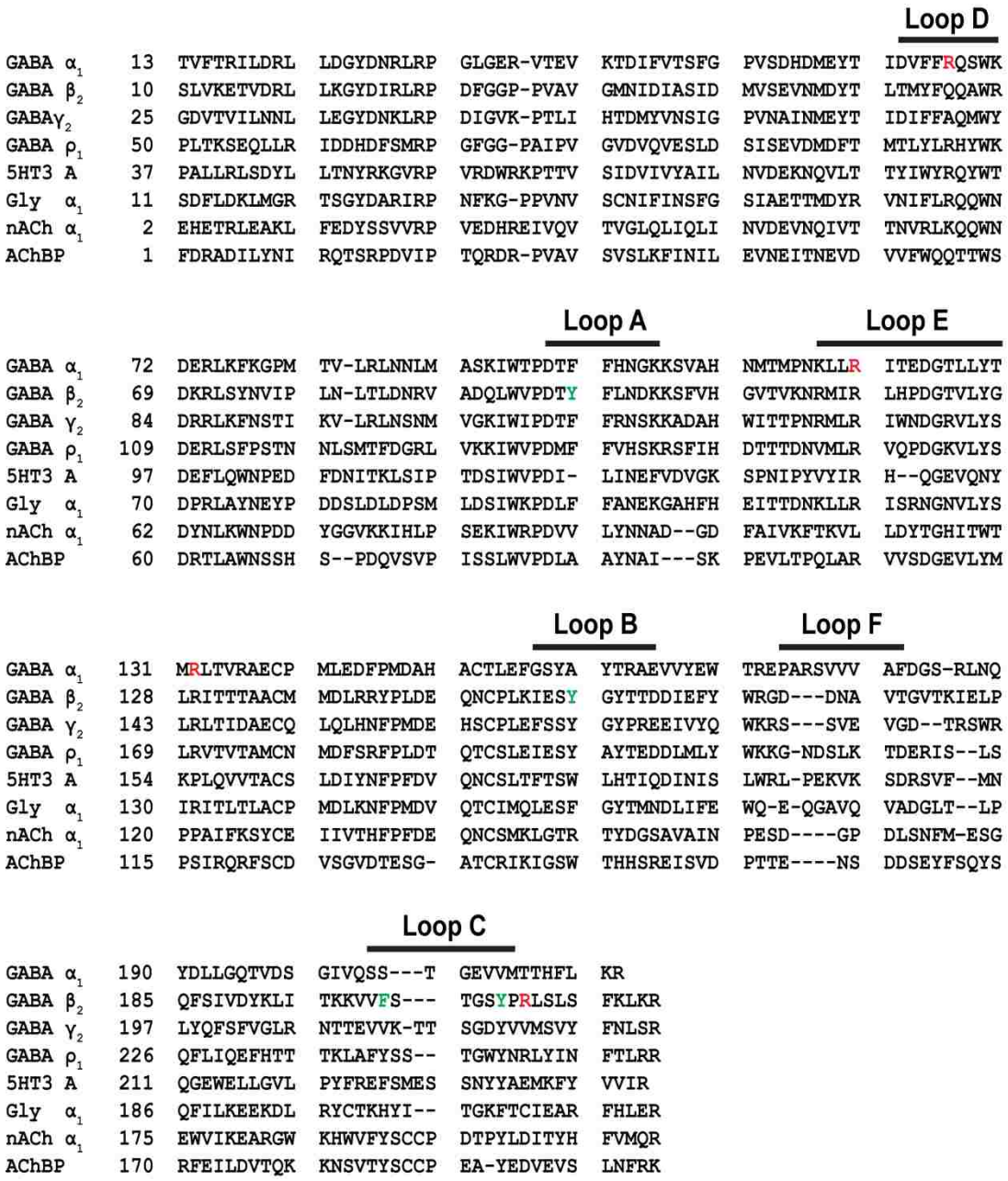

Figure 1.5 Sequence alignments of the extracellular domains of cl-LGICs and AChBP. Presented here is the alignment of the extracellular N-terminal domains of the α_1, β_2, γ_2, and ρ_1 subunits of the human $GABA_A$ receptor, a mouse serotonin type 3A receptor subunit, the α_1 subunit of the human glycine receptor, the α_1 subunit of the mouse nicotinic acetylcholine receptor, and the *Lymnaea stagnalis* acetylcholine binding protein (Brejc et al., 2001; O'Mara et al., 2005; Dellisanti et al., 2007). Identity between these primary sequences ranges from 15-25%; however, the secondary structures align very well. The six putative binding site loops are labeled A-F (Kash et al., 2004). Located on the discontinuous loops are a number of aromatic (green) and charged (red) residues implicated in GABA binding, which are also the focus of the studies presented in this dissertation.

Table 1.1 Discontinuous loop residues that play important roles in ligand binding, investigated here, and in other cl-LGICs.

Loop	$GABA_A$	$GABA_A$ ρ	Gly	AChBP	nACh	5-HT_{3A}
A	**β_2Y97**	F138	F99	Y89	α_1Y93	
B	β_2Y157	**Y198**	**F159**	**W143**	**α_1W149**	**W183**
C	β_2F200 β_2Y205 β_2R207	Y241 Y247 R249	Y202 F207	Y185 Y192	α_1Y190 α_1Y198	F226 Y234
D	α_1R67	R104	R65	W53	γW55	W90
E	α_1R120 α_1R132	R158 R170	R119 R131	R104	γL109	Y153
F	--	--	--	--	--	--

Bold = participates in cation-π bond that influence ligand binding. Residues from homomeric receptors are not preceded by subunit name.

In the original crystallization of AChBP, a HEPES (N-2-hydroxyethylpiperazine-N9-2-ethanesulphonic acid) buffer molecule was found in the ligand-binding site (Brejc et al., 2001). HEPES contains a positively charged quaternary ammonium group and this group stacks on W143 (loop B). The other four aromatic residues, Y89 (loop A), Y185 (loop C), Y192 (loop C), and W53 (loop D), form the remainder of the binding cavity, often referred to as the "aromatic box", directing their π electrons or hydroxyl groups towards the agonist (Brejc et al., 2001). The interactions between ligand and receptor were further revealed by the crystal structures of the AChBP in complex with nicotine

and carbamylcholine (both exogenous nAChR agonists) solved by Celie et al. (2004). These structures identified a number of amino acids that interact with the ligand.

The principal face of the binding pocket makes the most contacts with the ligand. W143, which aligns with β_2Y157 of the $GABA_A$ receptor, forms a cation-π interaction with both agonists. Other residues that make aromatic contacts with the ligand include Y192 ($GABA_AR$ β_2Y205) and Y185 ($GABA_AR$ β_2F200). No aromatic contact with the ligand was identified for Y89 (loop A), which roughly aligns with $GABA_AR$ β_2Y97. However, Y89's hydroxyl group has a close contact with the ligand.

On the complementary side, W53 ($GABA_AR$ α_1F65) makes limited aromatic contacts to nicotine. L112 ($GABA_AR$ α_1L128) and M114 ($GABA_AR$ T130) contribute hydrophobic contacts to the binding of both nicotine and carbamylcholine. R104 ($GABA_AR$ α_1R120) was found to only make contacts carbamylcholine. This loop E arginine was recently shown to participate in an inter-subunit state-dependent salt bridge, in $GABA_A$ receptor (Laha and Wagner, 2011).

Additionally, Celie et al. (2004) noted that AChBP's Y185 (loop C), which aligns with β_2F200 of the $GABA_A$ receptor, forms hydrogen bond with K139 (adjacent to Loop B), upon ligand binding. This ligand-dependent interaction may influence ligand affinity, either by reorienting the Y185 side chain or by stabilizing the loop C in its binding conformation. Also, this intra-subunit interaction may help transduce ligand binding into channel gating (Celie et al., 2004). This proposed role is based on observations of Y185's equivalent in the nAChR (α_1Y190).

Nicotinic AChR α_1Y190 has been demonstrated to be critical for acetylcholine binding affinity and desensitization (Sine et al., 1994). By individually mutating α_1Y190

as well as two other tyrosines (α_1Y93 and α_1Y198) to cysteine, histidine, isoleucine, phenylalanine, serine, threonine, and tryptophan, Sine et al. (1994) found that the hydroxyl group of the aromatic side chain is essential for functional contribution of α_1Y93 and α_1Y190, while the aromatic ring of the side chain is essential for α_1Y198 ($GABA_AR$ β_2Y205). It should be noted here that if the homology model of the $GABA_A$ receptor (Cromer et al., 2002) is accurate, it is expected that the side chain function would not be conserved for β_2F200 of $GABA_A$ receptor because it lacks a hydroxyl group. Another nAChR aromatic residue (α_1W149, loop B) is known for the importance of the aromatic ring of its side chain. This residue was shown to possess a cation-π interaction important for ligand interaction (Zhong et al., 1998), like W143 in AChBP.

As seen in AChBP and nAChR, a tryptophan in the 5-HT_3 receptor (W183 from the type A subunit) contributes a cation-π interaction that facilitates ligand binding (Beene et al., 2002). 5-HT_3 receptors exist in two forms, either as homopentameric 5-HT_3A or as a heteropentameric combination of type A subunits with either B, C, D, or E subunits. (Sixma and Smit, 2003). The homology model developed for the 5-HT_3 receptor (Reeves et al., 2003; Thompson et al., 2005) describes a ligand-binding pocket lined by many aromatic residues. Besides the tryptophan (W183) that forms a cation-π interaction with the agonist, the 5-HT_3 receptor's binding site also contains one additional tryptophan (W90), a phenylalanine (F226) and several tyrosines (Y143, Y153, Y234) that contribute to the characteristic "aromatic box" of this receptor (Beene et al., 2002). Beene et al., 2004 also showed, through unnatural amino acid substitution, that Y143 forms a hydrogen bond that is essential for receptor gating but does not affect binding, and that Y153 forms a hydrogen bond involved in both binding and gating of the

receptor. The same study also demonstrated that the aromatic, not the hydroxyl, group of Y234 is essential for proper function of the 5-HT3 receptor. This Y234 residue is conserved among cl-LGICs (i.e. aligns with $\beta_2$205 of $GABA_A$ and α_1Y198 of nACh receptors). The model they derived suggests that Y143 is likely to hydrogen bond with the backbone carbonyl of W183, an interaction proposed elsewhere (Maksay et al. 2003). These different effects of various tyrosine side chains at the ligand-binding pocket will provide useful references for the investigation of $GABA_A$ receptor tyrosines (chapter IV).

A cation-π interaction that mediates ligand binding has also been identified at GlyR binding site. The GlyR cation-π aromatic is a phenylalanine (F159, loop B) that aligns with the cation-π aromatics identified in nACh (α_1W149), 5-HT_3 (W183), and $GABA_A$ ρ (Y198) receptors (Pless et al., 2008; Pless et al., 2011). The exception is the $GABA_A$ receptor in which the aligned aromatic (β_2Y157) does not appear to be involved in a relevant cation-π bond while a tyrosine on loop A (β_2Y97) does (Padgett et al., 2007).

The way that $GABA_A$ receptor interacts with its ligand is not entirely different from those found in other cl-LGICs. For example, similarities between $GABA_A$Rs and GlyRs are found with the critical roles played, in ligand affinity, by various charged amino acid side chains. Using site-directed mutagenesis combined with AChBP-base homology modeling, Grudzinska et al. (2005) identified key ligand-binding residues of recombinant homopentameric α_1 and heteropentameric $\alpha_1\beta$ GlyRs. They located the major determinants of the ligand-binding site to two highly conserved, oppositely charged residues (α_1R65 and α_1E157) positioned on adjacent interfaces of the α and β subunits. Interestingly, GlyR α_1R65 aligns with $GABA_A$R α_1R67, a residue whose

contribution to structure and function at the GABA-binding site was explored and documented in chapter III. GlyR α_1E157 aligns with $GABA_AR$ β_2E155, mutation of which was suggested to affect both binding and gating processes (Newell et al. 2004).

Also, aligned with GlyR α_1R65 and $GABA_AR$ α_1R67 is an arginine (R104) from homopentameric $GABA_A$ ρ receptor. Harrison and Lummis (2006) showed that mutating R104 to either alanine or glutamate causes at least a 10,000-fold increase in $EC_{50\text{-}GABA}$. The same study found that mutating residue R158 of $GABA_A$ ρ (which aligns with $GABA_AR$ β_2R120) to alanine, glutamate, or lysine resulted in nonfunctional receptors, and mutating $GABA_A$ ρ R170 (which aligns with $GABA_AR$ α_1R132) caused either total loss of function (R170D, R170A) or 10-fold increase in $EC_{50\text{-}GABA}$ (R170K). Additionally, Harrison and Lummis (2006) found that mutating R249 of $GABA_A$ ρ receptor caused relatively milder effects on $EC_{50\text{-}GABA}$ (R249A: 15-fold increase, R249D: 4-fold increase, and R249K: 289-fold increase). The homopentameric $GABA_A$ ρ receptor also resembles other $GABA_A$ receptors (heteropentamers) in terms of the aromatic residues responsible for cation-π interaction at the ligand-binding pocket. Lummis et al. (2005) demonstrated that Y198 (loop B) of ρ $GABA_A$ receptor participates in a cation-π interaction critical for GABA binding.

Table 1.1 is by no means an exhaustive list of residues that play important roles at the ligand-binding pocket of $GABA_A$ receptor and other cl-LGICs. The list, however, reflects the relevance of studying the contributions of these residues in the $GABA_A$ receptor. The major aim of this dissertation is to refine and add to the current best model of the $GABA_AR$ ligand-binding pocket. To this end, three studies, presented in the following chapters, aim to: (i) examine the roles of arginine residues in GABA binding

via serial mutagenesis and kinetic analysis; (ii) examine the roles of aromatic side chains in GABA binding via serial mutagenesis and kinetic analysis; (iii) identify possible interactions between aromatic and arginine residues using double mutant cycle analysis. This work has resulted in the creation of a refined model for the $GABA_A$ receptor ligand-binding pocket in which specific interaction and roles are proposed for β_2F200, β_2Y97, β_2R207, α_1R67, and α_1R132. Notably, we propose a tight structural and functional interaction between β_2F200 and β_2Y97, a novel coordination of the amino group of GABA via a cation-π interaction with β_2F200, and provide the most comprehensive evidence yet for an interaction between α_1R67 and the carboxyl group of GABA.

II. MATERIALS AND METHODS

Engineering $GABA_A$ receptor mutant using site-directed mutagenesis

In order to effectively drive the expression of the desired $GABA_A$ receptor subtype, the gene of each subunit was cloned into pcDNA3.1 vectors (Invitrogen, Carlsbad, CA) under the control of a high level expression human cytomegalovirus (CMV) promoter. The resulting plasmids were used in combinations to achieve expression of heterologous $GABA_A$ receptors. For example, to express receptors containing α_1, β_2, and γ_{2S} subunits, plasmids containing the sequences encoding each subunit were introduced to expression vessels (i.e. HEK293 cells).

PCR-based site-directed mutagenesis (QuikChange, Stratagene, La Jolla, CA) was utilized to introduce point mutations we wanted to investigate. Briefly, for each mutation, we designed two complementary oligonucleotides, typically 40 to 50 bp. These oligonucleotides covered the codon of interest and incorporated a specific mismatch that changed the codon. The QuikChange method utilizes an ultra-high fidelity polymerase (Pfu-Ultra). In one reaction, with both primers, the polymerase amplified the entire plasmid. Following the PCR reaction, DpnI, which digests methylated DNA, was added in order to eliminate the original template, leaving only the mutant products. After DpnI digestion, 2 µl of the mixture was used for transformation into competent *E. coli* cells. These cells were plated onto a LB-ampicillin (50 µg/ml) agar plate. The ampicillin selected for cells that took up the pcDNA3.1 vector, which contains an ampicillin resistance gene. After 18 hours of incubation several colonies were picked and used to inoculate 3 mL LB cultures with ampicillin (50 µg/ml). Plasmid DNA from these cultures was then isolated using Wizard Plus SV mini-preps (Promega, Madison, WI). Minipreps often yielded 100 µl of pure plasmid at a concentration between 80 ng/µl to

250 ng/μl. The coding region of each mutant plasmid was sequenced with forward and reverse primers to ensure the intended mutation was achieved and no additional undesireable changes occurred.

Transient expression of $GABA_A$ receptors in HEK-293 cells

Human embryonic kidney (HEK-293) was used for heterologous expression of $GABA_A$ receptors. These cells were maintained in Minimum Essential Medium Eagle with Earle's salts (Mediatech, Manassas, VA) supplemented with 10% newborn calf serum (Thermo Scientific, Waltham, MA) and Penicillin-Streptomycin-Glutamine (Mediatech) in a 37^o C incubator under a 5% CO_2 atmosphere. They generally remained in optimal condition up to 50 passages. For experiments, cells were plated onto 35 mm dishes coated with poly-L-lysine and were transfected 18 to 24 hours later using Lipofectamine 2000 (Invitrogen, Carlsbad, CA).

Lipofectamine consists of cationic lipids, which interact with the phosphate backbone of the nucleic acid. This interaction is via the cationic head groups of the lipids and does not result in the formation of micelles or liposomes surrounding the nucleic acid. The cationic lipids also mediate the interaction of the nucleic acid with the negatively charged cell membrane. The complex enters the cell through endocytosis.

Receptors consisting of α_1 and β_2 subunits, or α_1, β_2, and γ_2 subunits were used throughout this study. For $\alpha_1\beta_2$ receptors, the following amounts of cDNA were transfected: 500ng enhanced green fluorescent protein (eGFP), 1.5 μg of α_1, 1.5 μg β_2. For $\alpha_1\beta_2\gamma_2$ receptors the following amounts of cDNA were transfected: 500ng eGFP, 1 μg of α_1, 1 μg of β_2, and 3 μg of γ_{2S}. eGFP serves as a marker for identifying cells that are transfected. A generally high correlation exists between expression of eGFP and

expression of $GABA_A$ receptors (unpublished); the exact mechanism is not understood. Cells were recorded from 48-72 hours post-transfection.

Electrophysiology

All recordings for this study were collected from outside-out patches excised from HEK-293 cells. Patches were held at -60 mV. Experiments were conducted at room temperature. The outside-out configuration is achieved by obtaining a tight seal with a cell, followed by break-in using negative pressure, and then slowly drawing back the pipette, stretching the membrane until a portion re-seals over the tip as it separates from the cell. Recordings were made using borosilicate glass pipettes filled with (in mM): 140 KCl, 10 EGTA, 2 MgATP, 20 phosphocreatine and 10 HEPES, pH 7.3. $GABA_A$ receptor agonists and antagonists were dissolved in the perfusion solution, which contained (in mM): 145 NaCl, 2.5 KCl, 2 CaCl2, 1 MgCl2, 10 HEPES, 4 mM Glucose, pH 7.4. For extracellular solutions that contained >30 mM GABA, the concentration of NaCl was reduced to 95 mM, and a combination of sucrose and GABA was added to compensate for the reduced osmolarity. Final volume was carefully maintained to accurately obtain the desired concentration of GABA. The pipette solution was adjusted in conjunction, reducing the KCl concentration to 90mM, and adding 50mM K-gluconate to maintain a constant Cl^- driving force. GABA, propofol and SR-95531 were obtained from Sigma-Aldrich Chemicals, St Louis, Mo. Data were collected at 10-20 kHz using an Axopatch 200B amplifier (Axon Instruments, Foster City, CA) and an ITC-1600 digitizer (InstruTech, Port Washington, NY), controlled by Axograph X software (Axograph Scientific, Sydney, AUS). Currents were low-pass filtered at 2-5 kHz with a four-pole Bessel filter, and digitized at a rate no less than twice the filter frequency.

In vivo, GABA mediated synaptic transmission normally takes place in less than a millisecond and the post-synaptic current decays in tens of milliseconds. In order to study the receptor kinetics during such an event, it is necessary to apply and remove agonist on a similar time scale. Rapid-solution exchange was accomplished by using a four-barreled flowpipe array (Vitrodynamics, Rockaway, NJ) mounted on a piezoelectric bimorph (Vernitron, Bedford, OH) (Figure 2.1).

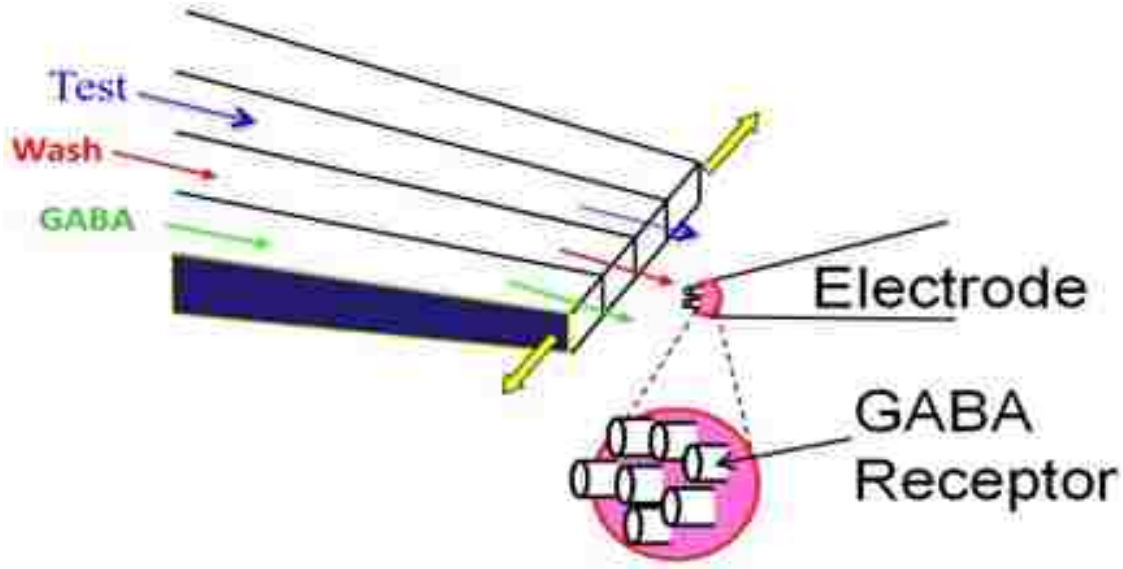

Figure 2.1 Rapid-ligand application protocol. After pulling an outside-out patch, the electrode is lifted up to the flow-pipes, which are already positioned in the bath solution. While the electrode remains stationary, the flow-pipes can be rapidly shifted from side to side, exposing the patch at the tip of the electrode to the solution flowing out of any one of the four barrels. In a typical three-pipe protocol, the sequence of exposure is GABA (saturating concentration), wash, test (subsaturating GABA or saturating GABA plus SR), and back to wash.

The four pipes are fused in a linear arrangement and manually pulled down to 100 to 200 μm openings separated by septa of less than 10 μm. A computer-controlled current source stimulates the bimorph to shift the position of the flowpipes with high precision, and causes enough displacement to expose a patch to solutions from all four pipes without moving the electrode. The exchange time (the time it takes to completely clear the liquid junction interface between two pipes) is measured by examining open tip

potentials during a shift. Open tip potentials are the result of differences in the mobility of sodium and potassium ions, which are at different concentrations in the internal pipette solution compared to the external solution. In order to distinguish the agonist solution from the wash solution, a small amount of NaCl is added to the agonist solution, raising the Na^+ concentration 5 mM. This difference gives rise to the open tip potential. The 10-90% exchange time less than 200 μs would be considered good exchange time. Good exchange is routinely checked between patches.

Concentration-response experiments

To obtain concentration-response curves, current responses evoked by a series of GABA concentrations are compared to the current response evoked by a saturating concentration of GABA. The protocol begins with the electrode and patch in wash solution, then the pipes shift, exposing the electrode to the solution containing a saturating concentration of GABA. After 500 ms the pipes shift back and the electrode is in wash solution for 12 to 15 seconds in order to recover from desensitization. Next, the flowpipes shift the opposite direction, exposing the electrode to a solution containing a sub-saturating concentration of GABA. After 500 ms the pipes shift back and the electrode is in the wash solution for 12 to 15 seconds. This protocol is repeated 5 to 15 times and an ensemble average for the two solutions is taken. During a stable patch the sub-saturating solution can be changed by switching the solution with open flow directed through a 4:1 (inflow:outflow) manifold preceding the flowpipe. Although three or four concentrations can sometimes be tested on a single patch, only one concentration was tested on the majority of patches due to difficulty in maintaining patch stability. Therefore, each concentration-response curve relies on data from several patches.

For each concentration, the peak current was measured in Axograph X and normalized to the peak current for the saturating concentration on the same patch. For a given concentration the normalized values for each patch were averaged and were plotted against the log of the concentration of GABA using Prism 4 software (GraphPad Software, Inc., San Diego, CA). Non-linear regression of the plot was performed using a variable slope sigmoidal curve (Y = Ymin + (Ymax – Ymin) / (1+10^((LogEC_{50} - X)*HillSlope))). This identified the concentration that gives a half-maximal response, termed EC_{50}.

Analysis of macroscopic kinetics: Desensitization and Deactivation

During rapid-ligand application distinct desensitization and deactivation phases of the current response are observed. The desensitization phase of current responses during a 500 ms application of a saturating concentration of GABA was used for analysis (Figure 2.2 A). The ensemble average of such responses was taken for a given patch and was used for analysis. The ensemble average was fit using Axograph X. The time of onset of desensitization was set to zero, and the region of desensitization was fit with a bi-exponential equation ($Y= A_1 \times e^{-t/\tau 1} + A_{2\,x}\, e^{-t/\tau 2} + C$), where t is time, Y is the total current amplitude at a given time, $\tau 1$ is the time constant of the fast component of decay, A1 is the relative amplitude of the fast component, $\tau 2$ is the time constant of the slow component of decay, A2 is the relative amplitude of the slow component, and C is a constant that accounts for the amplitude of current that remains.

The deactivation phase following a 2-4 ms application of a saturating concentration of GABA was analyzed (Figure 2.2 B). Ensemble averages were used. The time of GABA removal was set to zero, and the region of deactivation was fit with a

bi-exponential equation ($Y= A_1 \times e^{-t/\tau 1} + A_2 \times e^{-t/\tau 2}$). Since deactivation decays back to baseline, no constant was added.

For both deactivation and desensitization, a weighted time constant (τ_w) was also calculated for each analysis. $\tau_w = (A_1/(A_1 + A_2)) \times \tau_1 + (A_2/(A_1+A_2)) \times \tau_2$. This value allows for a simplified comparison of major changes that may occur in macroscopic rates of either phase. For desensitization, the extent of desensitization is also taken into consideration. This value is represented by the percent remaining.

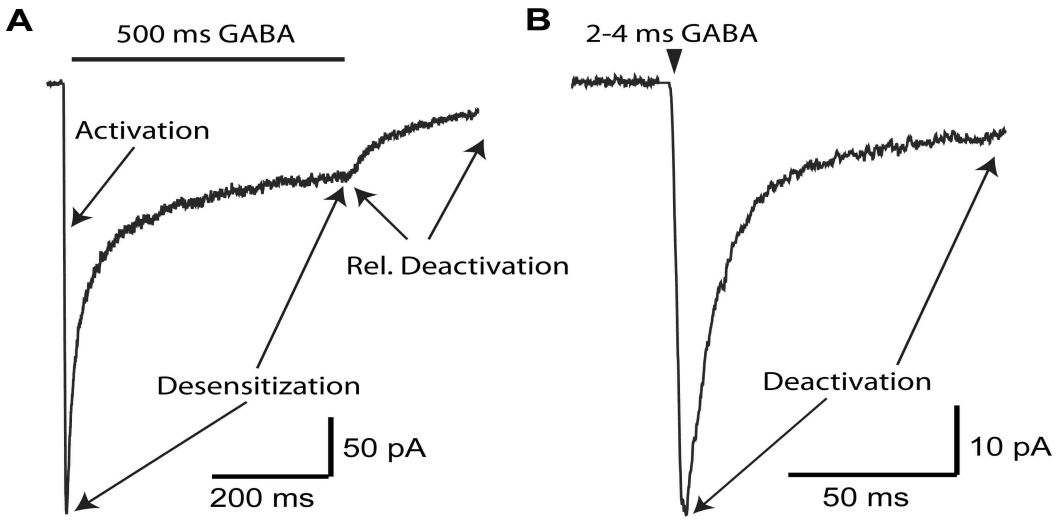

Figure 2.2 Example of a recording from wild-type receptors using a saturating GABA application for 500 ms and 2-4 ms. A) Current evoked by long (500 ms) pulse of saturating GABA has three distinct phases. First, when the patch has GABA solution applied, there is rapid activation as chloride ions flow across the membrane through the open channels. Activation is determined both by binding ($k_{on\text{-}GABA}$) and gating. The next phase is macroscopic desensitization, which is influenced by multiple microscopic transition states. While still in GABA, receptors begin to close even though GABA is bound. When the GABA solution is removed, the last phase, deactivation, occurs. Current dissipates as channels close and GABA unbinds. This is a complex process, which is determined by transitions in and out of desensitization and gating until unbinding is completed. B) Typically, a purer deactivation is obtained following a brief (2-4 ms) pulse of GABA. This brief application closely resembles the synaptic release of GABA.

Antagonist unbinding experiments

During antagonist unbinding experiments, the current that is evoked by GABA following a pre-equilibration in SR-95531 (a competitive antagonist) is measured.

Outside-out patches containing $GABA_A$ receptors were first exposed to a saturating concentration of GABA in order to establish a control response. After returning to the wash solution for 12 to 15 seconds, SR-95531 was applied for 750 ms, and then rapidly switched to a solution containing saturating GABA. This procedure was repeated 5 to 15 times (for each patch), and ensemble averages were used for analysis. The entire experiment was repeated several times, pre-equilibrating in the same concentration of SR-95531, to obtain a statistical n patches. The whole process is repeated for different concentrations of SR to obtain a concentration response.

The evoked current following pre-equilibration in SR-95531 (I_{ant}) is shaped by the convolution of the time course of antagonist unbinding and the waveform of the control current, I_{ctrl} (evoked with no pre-equilibration in antagonist) (Figure 2.3 A). Mathematically I_{ant} is the convolution of I_{ctrl} and the function (a(t)) that describes the rate at which receptors become available due to the unbinding of SR-95531 (Jones et al., 1998). Therefore, a(t) can be obtained by deconvolving I_{ctrl} from I_{ant}. The following relationship expresses this operation, where F(f(x)) is the Fourier transform of f(x):

$$A(t) = F^{-1}(F(I_{ant})/F(I_{ctrl}))$$

Integration of a(t) then gives A(t), the fraction of receptors available for binding GABA as a function of time. This is the deconvolved curve and reflects the time course of antagonist unbinding. This curve was fit in Axograph X with the function:

$$A(t) = [P_\infty - (P_\infty - P_0)\exp(-t/\tau_u)]^N,$$

where P_0 and P_∞ are the probabilities of being available initially (at t=0) and at steady state (as $t \rightarrow \infty$), N is the number of antagonist binding sites per receptor, and τ_u is the

time constant of antagonist unbinding (Jones et al., 1998). $k_{off\text{-}SR}$ was obtained by taking the reciprocal of τ_u.

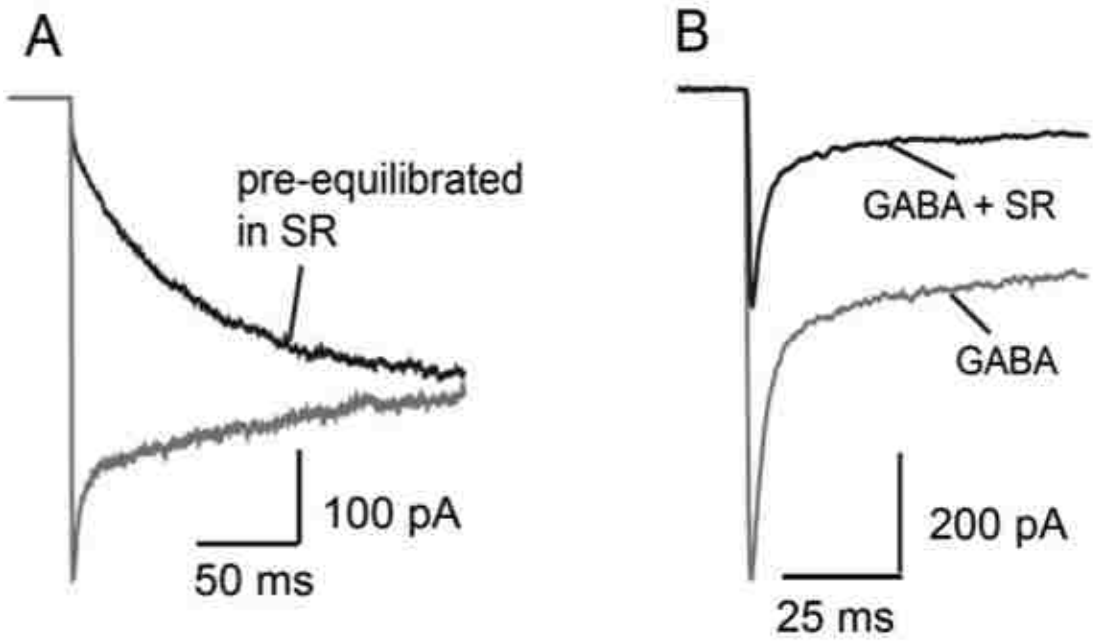

Figure 2.3 Antagonist unbinding and race experiments. A) Current evoked by a control pulse of GABA alone is overlayed with current evoked by GABA following pre-equilibration in SR-95531. B) Current resulted from simultaneous application of GABA and SR-95531 is compared to current evoked GABA alone.

The experiment was repeated several times, pre-equilibrating in different concentrations of SR-95531. The fraction of receptors available at t = 0 was plotted against the log of the concentration of SR-95531 (Prism 4). This plot was fit with the normalized Hill equation for an antagonist:

$$B_\infty = 1/(K_{D\text{-}SR}/[\text{SR-95531}]^N + 1).$$

The best curve fits were always achieved with N=1, indicating that one SR-95531 compound is bound. This provided an accurate estimate of $K_{D\text{-}SR}$. After directly measuring $k_{off\text{-}SR}$ and $K_{D\text{-}SR}$, the $k_{on\text{-}SR}$ was calculated.

$$k_{on\text{-}SR} = K_{D\text{-}SR} / k_{off\text{-}SR}$$

Measuring the microscopic binding rate of GABA

The microscopic binding rate of GABA ($k_{on\text{-}GABA}$) was measured using an established method, the race experiment, involving competition of GABA with an antagonist of known kinetics. GABA was co-applied with the competitive antagonist SR-95531. SR-95531 binds in the GABA binding pocket but does not induce any activation. The ratio of channels that bind antagonist to those that bind GABA depends on the concentrations and relative binding rates of each. The resulting activation is dependent on the percent of channels that bind GABA and are hence open. The GABA binding rate was determined using the ratio of the peak current generated in the presence and absence of antagonist. This ratio is termed I_{race}, and has the following relationship to $k_{on\text{-}GABA}$:

$$k_{on\text{-}GABA} = ([\text{SR-95531}]k_{on\text{-}SR})/([\text{GABA}](1/I_{race} - 1)).$$

Alternating pulses of a solution containing only GABA with a solution containing GABA and SR-95531 were applied in order to observe I_{race} (Figure 2.3 B). Incubation in wash solution (12 to 15 seconds) separated each application. The only uncontrolled parameters were I_{race} (measured here), and the binding rate of SR-95531 ($k_{on\text{-}ant}$), which was measured separately.

Double-mutant cycle analysis

Double mutant cycle analysis was performed on EC_{50} values, deactivation rates, and binding rates. $\Delta\Delta G'^{o}$ was calculated as RT ln ($k_{mutant}/k_{wild\text{-}type}$), where R is the ideal gas constant (1.987 calories/mole) and T is the absolute temperature (296 K). Although EC_{50} and deactivation rates do not provide true kinetic rate constants, comparison of macroscopic parameters have been previously utilized to support side-chain interactions

and establish coupling coefficients (Kash et al., 2003; Price et al., 2007; Gleitsman et al., 2008). If two mutations have independent effects $\Delta\Delta G'^{o}_{(1,2)} = \Delta\Delta G'^{o}_{(1)} + \Delta\Delta G'^{o}_{(2)}$. Any value of the coupling energy [$\Delta\Delta G'^{o}_{coupling} = (\Delta\Delta G'^{o}_{(1)} + \Delta\Delta G'^{o}_{(2)}) - \Delta\Delta G'^{o}_{(1,2)}$)] that deviates from zero could indicate a dependence between two residues. Due to the methodological inability to determine a true standard deviation in the sample population for several of our measured parameters (i.e. EC_{50} or K_D), we consider a coupling energy of |0.5| kcal/mol or greater sufficiently indicates two residues are dependent. This value is consistent with confirmed interaction energies between two side-chains (Hidalgo and MacKinnon, 1995; Ranganathan et al., 1996; Horovitz, 1996). A significant coupling energy may not exclusively result from a direct interaction between two residues, but could result from secondary interactions through a third side-chain, or could be the result both residues contributing to the same structural element.

III. SERIAL MUTAGENESIS OF α_1R67 AND β_2R207

Introduction

In earlier site-directed mutagenesis studies, two arginine residues, α_1R67 and β_2R207, have been implicated in GABA binding (Boileau et al., 1999; Holden and Czajkowski, 2002; Wagner and Czajkowski, 2004). Work from our lab further showed that these two arginine residues, when individually mutated to alanine, caused 142 and 25 fold increases in $EC_{50\text{-}GABA}$, respectively. However, no specific information about their interactions with either GABA or other binding pocket structures has been identified.

Here, we sought to understand how these arginines contribute to the structure and operation of the $GABA_A$ receptor's binding pocket. We addressed this question by mutating each arginine to a series of amino acid residues (Figure 3.1) and measuring changes in the function of $GABA_A$ receptor. We quantified the effects of a mutation on receptor function by measuring the alterations in concentration response (i.e. affinity for GABA) and macroscopic kinetic parameters, such as desensitization and deactivation, from which we may draw binding and gating implications.

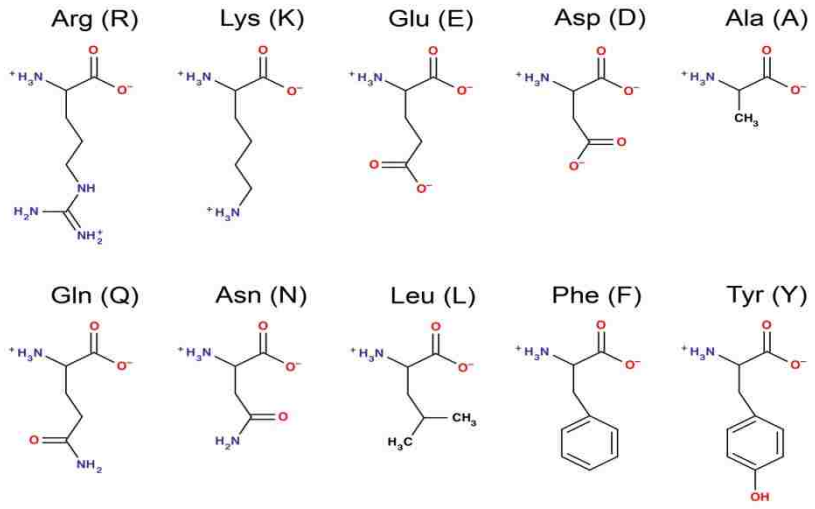

Figure 3.1 A selection of amino acids mutagenically introduced at α_1R67 and β_2R207.

Results

In order to achieve consistent expression, all of the mutations were initially expressed in the background of $\alpha_1\beta_{2\text{-GKER}}$, which also served as our control construct (Laha and Wagner, 2011; Bollan et al., 2003); this receptor shows no difference in its macrokinetic profile compared to $\alpha_1\beta_2$ receptor (Table 3.1). For readability, the mutant constructs α_1R67A$\beta_{2\text{-GKER}}$ and $\alpha_1\beta_{2\text{-GKER}}$R207A, for example, will be referred to as R67A and R207A; this same nomenclature will also be used with other mutant constructs. In later experiments in which γ_2-containing receptors were expressed, the full labels, such as α_1R67A$\beta_{2\text{-GKER}}\gamma_2$ and $\alpha_1\beta_{2\text{-GKER}}$R207A$\gamma_2$, will be used.

Each construct studied was transiently expressed in HEK-293 cells, in order to record GABA-evoked currents from outside-out patches. Initial evaluation typically involved determination of $EC_{50\text{-GABA}}$, characterization of macroscopic desensitization (current decay during a 500ms pulse of saturating GABA), and characterization of macroscopic deactivation (current decay after a 2-4 ms pulse of saturating GABA). $EC_{50\text{-GABA}}$ was determined by fitting concentration-response plots with a form of the Hill equation. Desensitization and deactivation waveforms were fit with a bi-exponential decay function, from which a weighted time constant (τ_w) was calculated (see methods). Data from multiple patches were averaged for statistical relevance.

Effects of serial point mutations at α_1R67 on the apparent affinity of GABA

α_1R67 was systematically mutated into polar charged (R67K, R67E, R67D), polar uncharged (R67N, R67Q), and hydrophobic (R67L, R67F, R67Y) residues. Compared to R67A, which causes a 154-fold reduction in GABA affinity ($EC_{50\text{-GABA}}$ = 926 μM), all

other mutations cause even greater alterations in receptor function (Figure 3.2 A); these effects range from a 2173-fold reduction in GABA affinity to complete abolishment of $GABA_A$ receptor function. At closer examination, a pattern can be detected between the side chain property of each amino acid substitution and its effect on $GABA_A$ receptor's function.

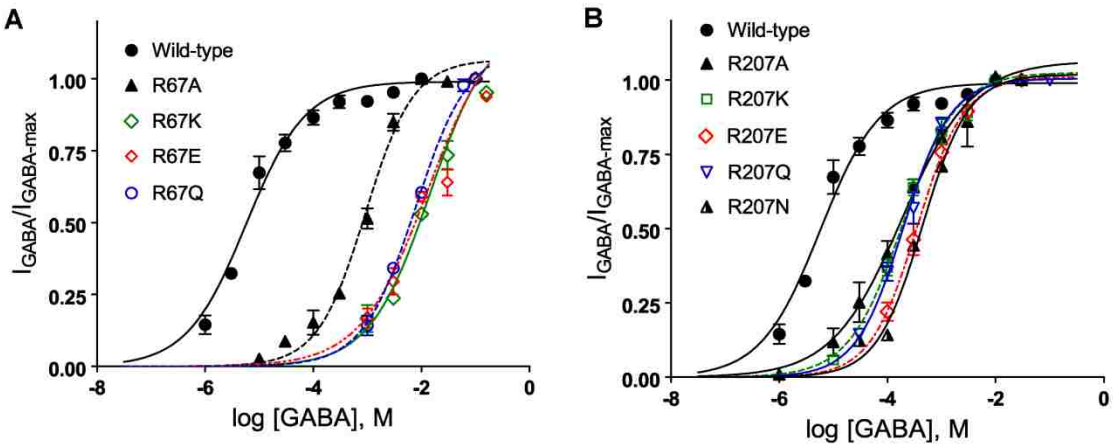

Construct	$EC_{50\text{-}GABA}$ (μM)	$I_{Propofol}$?
Wild-type	6	Yes
R67A	926	
R67K	14,270	
R67D	ND	Yes
R67E	13,040	
R67N	ND	Yes
R67Q	7,855	
R67F	ND	
R67Y	ND	
R67L	ND	Yes

Construct	$EC_{50\text{-}GABA}$ (μM)
Wild-type	6
R207A	185
R207K	190
R207E	355
R207N	444
R207Q	196
R207F	ND
R207Y	ND

Figure 3.2 Mutations at α_1R67 and β_2R207 shift the concentration response curve of GABA to the right. A) Concentration-response curves of α_1R67 mutants are right-shifted with respect to wild-type. R67D and R67N mutations yield GABA-insensitive receptors. Concentration-response curves for R67F, R67L, and R67Y mutations could not be completed because a saturating concentration could not be experimentally reached. B) Concentration-response curves of β_2R207 mutants are right-shifted with respect to wild-type. Saturating concentrations could not be reach for R207F and R207Y. ND indicates that a concentration-response curve could not be obtained.

Regarding the polar charged mutations, R67E and R67K cause quantitatively similar reduction in GABA affinity (2173-fold and 2378-fold respectively). Compared to these mutations, R67D causes much more severe alteration in GABA affinity, resulting in complete disruption of GABA-evoked current. This loss of GABA-evoked current could have arisen from either a complete local disruption of the GABA binding pocket or a global disruption in which the mutant receptor fails to assemble properly. A good test to determine which type of disruption actually takes place is to measure propofol-evoked current. Since propofol binds at a site distinct from GABA binding site (Bali and Akabas, 2004), it would generally be expected to evoke current independent of the local disruption of the GABA binding pocket. If propofol fails to evoke current, it would be likely that the disruption is more global. It turns out, R67D shows propofol-evoked current, indicating that the disruption caused by the mutation is localized at the GABA-binding pocket.

The two polar uncharged mutations, R67N and R67Q, cause very different magnitudes of effect on GABA-evoked response. R67Q causes a 1309-fold increase in $EC_{50\text{-}GABA}$, while R67N yields no GABA-evoked current. Propofol test of R67N showed robust current (Figure 3.3 C). As with R67D, the effect seen with R67N appears to result from local disruption of the GABA-binding pocket rather than global disruption of receptor assembly.

The hydrophobic mutations (R67F, R67L, R67Y) collectively caused the most severe alterations in GABA-evoked response. R67F and R67Y greatly reduce the size of GABA-evoked current, with the average current size much less than that of wild-type (mean peak current: wild-type = -113.0 ± 12.3 pA, n = 46; R67F = -6.6 ± 1.3 pA, n =4;

R67Y = -3.9 ± 0.6 pA, n = 8). In fact, the peak currents elicited were so small for R67F and R67Y that a concentration response curve could not be completed. Similarly, R67L appears to severely disrupt GABA-evoked current; it was subsequently tested positive for propofol-evoked current that was more robust than the current elicited by GABA (Figure 3.3 C).

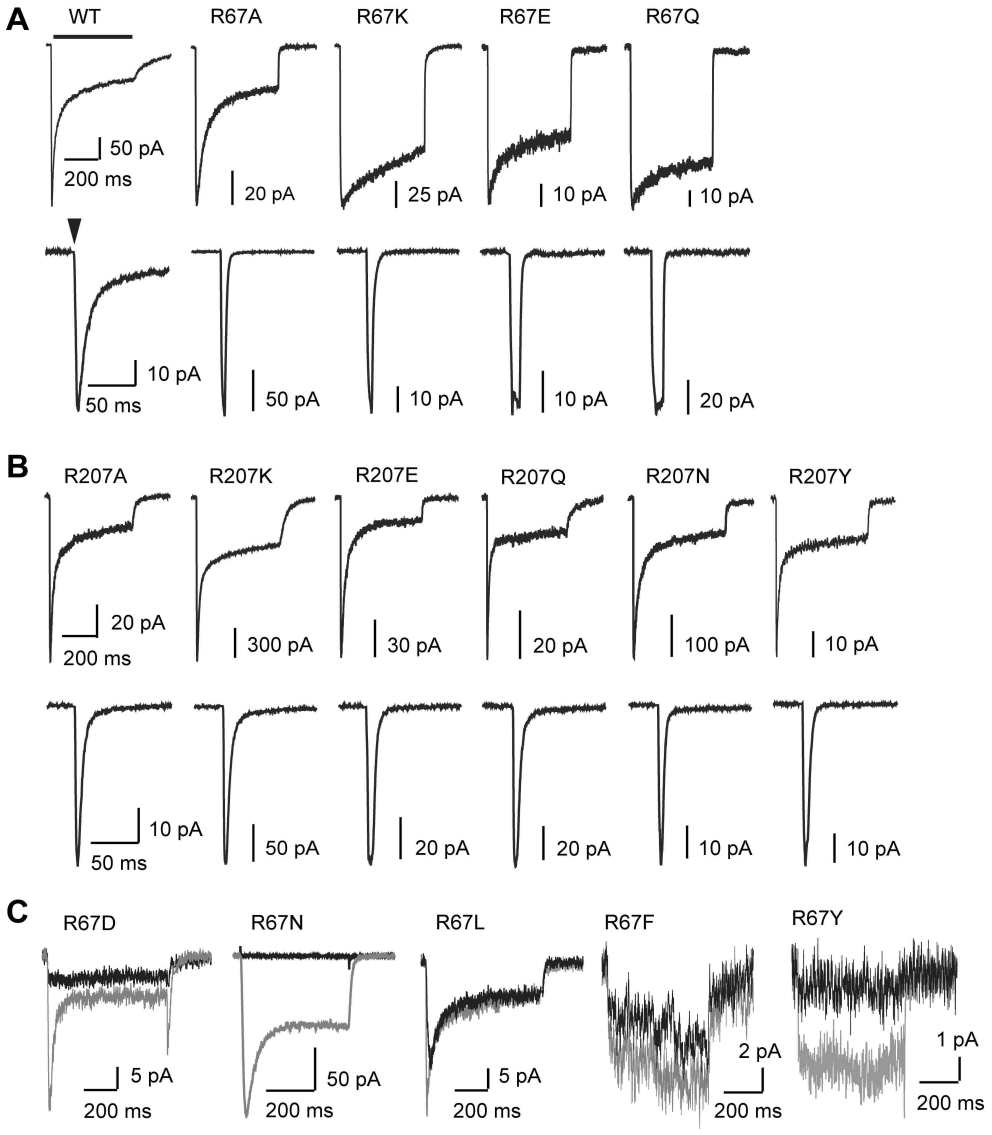

Figure 3.3 Point mutations at β_2R207 accelerates macroscopic deactivation, while point mutations at α_1R67 accelerates macroscopic deactivation and slowed macroscopic desensitization. A) Wild-type and α_1R67 mutant currents induced by long (500 ms, top row) and short (2-4 ms, bottom row) pulses of saturating GABA. B) β_2R207 mutant currents induced by

long (500 ms, top row) and short (2-4 ms, bottom row) pulses of saturating GABA. C) α_1R67 mutants that did not respond robustly to GABA. R67D, and R67N exhibit peak response to propofol (gray trace, 300 μM) but not GABA (black trace, 100 mM). R67F and R67Y exhibit GABA-evoked current but with drastically reduced current size, making it impossible to obtain an accurate concentration-response curve (black trace and gray trace represents response to 300 μM and 100 mM GABA respectively). R67L results in much reduced sensitivity to GABA (black, 160 mM) but peak response for propofol (gray, 100 μM).

Correlation between properties of side chain and severity of functional defect

Interestingly, when each group of mutations (i.e. polar charged and polar uncharged) is considered in isolation, it appears that the amino acid substitutions possessing a longer side chain tend to cause less severe disruption in $GABA_A$ receptor function. For examples, R67E has a longer (one extra carbon) side chain and causes less disruption than R67D. Similarly, R67Q is longer and less disruptive than R67N. In comparing similar side chains, it is not entirely accurate to assume that possessing one extra carbon would mean that a side chain could always reach a longer distance. Rather, it is perhaps more accurate to consider the difference that one extra carbon adds to the total volume of the side chain. Table 3.1 lists the volume of some selected amino acid residues.

Also, it appears that amino acid substitutions with high relative hydrophobicity (R67L, R67F, R67Y) collectively cause the most severe disruption of $GABA_A$ receptor function. However, though less hydrophobic aspartate (R67D) causes more severe reduction of GABA affinity compared to glutamate (R67E), which has higher relative hydrophobicity. The same is seen between asparagine (R67N) and glutamine (R67Q); glutamine has higher relative hydrophobicity but causes less alteration on GABA affinity. This observation is not surprising because the two pairs of residues compared here are not hydrophobic. Rather, they are categorized as neutral or hydrophilic residues. Therefore,

the relative degree of alteration may have more to do with the physical dimension of a side chain at position 67 of the α_1 subunit. It appears that a large polar side chain is preferred at position 67 of the α_1 subunit.

Effects of serial point mutations on the macroscopic kinetics of GABA-evoked current

The $EC_{50\text{-}GABA}$ or apparent affinity GABA was obtained from concentration response curve looking at peak current amplitude. Therefore, in order to understand how the physical and chemical properties of the amino acid side chain at position 67 of the α_1 subunit contribute to $GABA_A$ receptor function, we looked more closely at the macroscopic phases (i.e. activation, desensitization and deactivation) of the GABA-evoked current. It was observed that most α_1R67 mutants (R67A, R67K, R67E, and R67Q) cause significantly faster deactivation (Figure 3.3 A, Table 3.1). At the same time, these mutations also slowed the rate of desensitization as well as the extent of desensitization. The weighted time constant (τ_W) of desensitization is significantly increased for R67A, R67K, R67E, and R67Q, and the percent desensitized (100 - % remaining) is reduced for R67K, R67E, and R67Q (Table 3.1).

Additionally, it was observed that activation rate is significantly decreased for all α_1R67 mutations that show robust GABA-evoked current (Figure 3.4 A, B). Activation rate is a macroscopic parameter that represents the initial response to ligand application. In a simple 3-state kinetic model (Figure 3.4 C), this parameter is influenced by binding, gating, and desensitization events. However, in the presence of high GABA concentration, gating and desensitization become the dominant forces driving this activation rate; therefore, a decrease in either gating or desensitization rate can slow

activation. Apparently, the slowed activation rate observed here is consistent with the reduction in desensitization and gating.

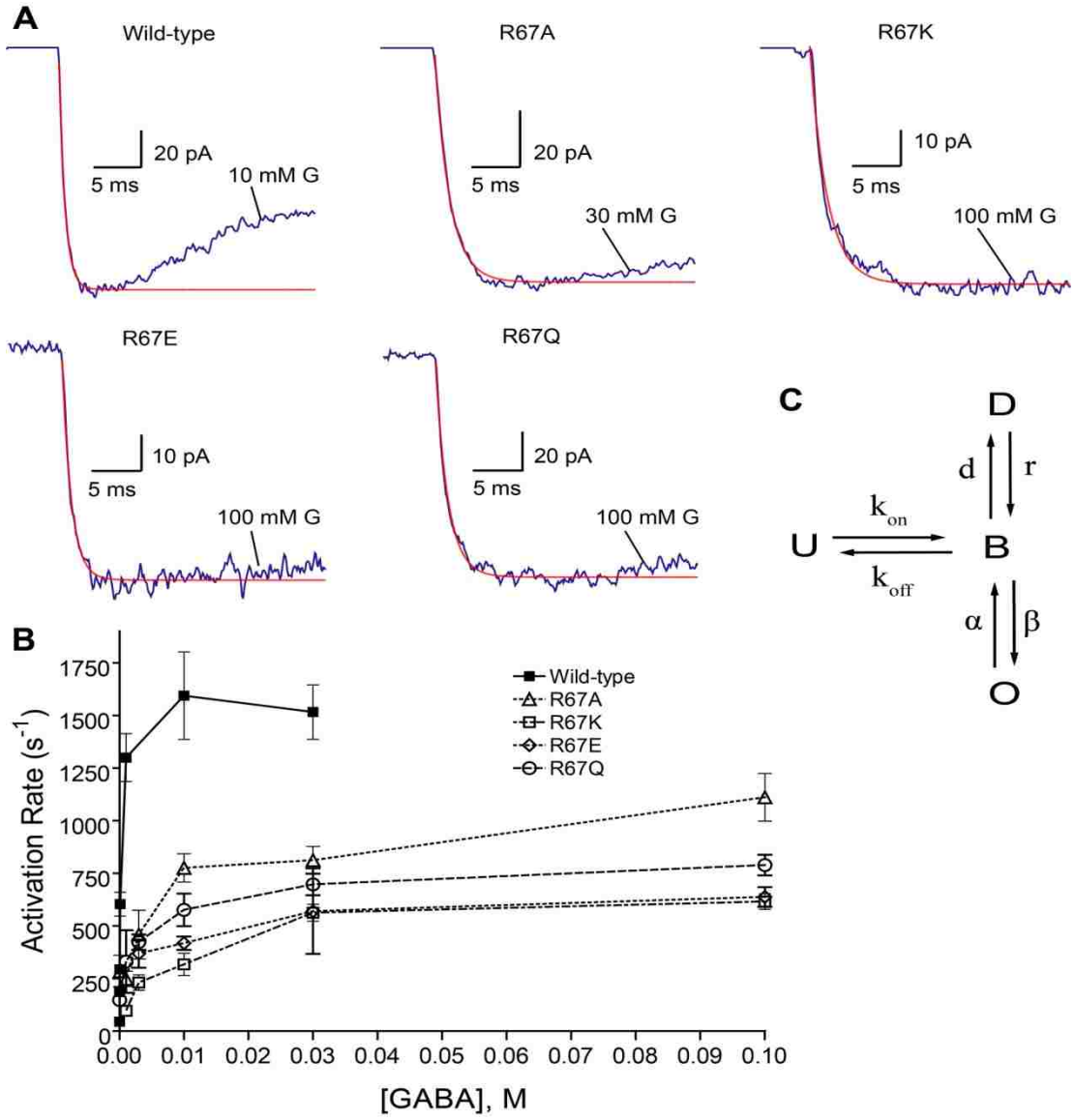

Figure 3.4 Mutations at α_1R67 decrease the GABA-induced activation rate. A) Raw traces of currents induced by saturating GABA, showing the activation phase and part of early (fast) desensitization phase. Red trace represents the single-exponential fit of the activation phase. Compared to wild-type, α_1R67 mutants (R67A, R67K, R67E, R67Q) exhibit slower activation rate and the absence of early desensitization. B) Plots of activation rate with respect to GABA concentration indicate that saturation was reached for wild-type and mutants. A quality fit to the equation ($Y = (Rmax * [GABA]) / (K_D + [GABA])$, where Rmax is the maximum activation rate) could not be achieved for the mutants. C) A simple kinetic scheme used to illustrate parameters that influence the time course of activation and macroscopic desensitization.

Table 3.1 Summary of the effects on macroscopic deactivation and desensitization caused by serial mutations to α_1R67 and β_2R207.

	Deactivation			Desensitization			Activation	
	τ_w (ms)	n	Vol ($Å^3$)	τ_w (ms)	% Remain	n	$\tau_{Activation}$ (ms)	n
$\alpha_1\beta_2$	92 ± 7	19	173.4	66 ± 15	30 ± 13	20	na	na
$\alpha_1\beta_{2\text{-GKER}}$	92 ± 8	15	173.4	88 ± 11	28 ± 2	25	0.65 ± .09	13
R67A	3.7 ± 0.7*&	7	88.6	180 ± 26*&	31 ± 3	34	1.14 ± .24	18
R67E	1.4 *&	2	138.4	251 ± 35*&	57 ± 4	10	1.63 ± .27	10
R67Q	2.3 ± 0.1*&	6	143.8	256 ± 31*&	54 ± 4	20	1.71 ± .71	12
R67K	3.3 ± 0.1*&	11	168.6	253 ± 26*&	56 ± 2	15	1.76 ± .36	14
R207A	7.9 ± 0.6*&	3	88.6	58 ± 14	37 ± 15	7	na	na
R207N	3.5 ± 0.6*&	6	114.1	79 ± 9	18 ± 2	8	0.61 ± .13	12
R207E	4.3 ± 0.5*&	7	138.4	50 ± 4	13 ± 1	12	0.72 ± .06	12
R207Q	8.8 ± 0.7*&	8	143.8	76 ± 24	26 ± 3	10	0.60 ± .11	10
R207K	9.2 ± 1.2*&	11	168.6	49 ± 7	16 ± 1	15	0.81 ± .28	13
R207Y	3.8 ± 0.5*&	8	193.6	76 ± 11	30 ± 3	8	0.69 ± .13	7

***** different from $\alpha_1\beta_2$ ($P < 0.01$); **&** different from $\alpha_1\beta_{2\text{-GKER}}$ ($P < 0.01$); ANOVA with Dunnets post-test; V represents volume of corresponding amino acid residue (Zamyatin, 1972).

Serial mutagenesis of β_2R207 reveals relative tolerance but with subtle correlation to side chain properties' influence on $GABA_A$ receptor function

As with studying α_1R67, β_2R207 was systematically mutated into polar charged (R207K, R207E), polar uncharged (R207N, R207Q), and hydrophobic (R207F, R207Y) residues. However, the pattern of effects seen here is different from that seen with α_1R67 mutations. Generally, for most of the mutations made to β_2R207, the effects on $GABA_A$ receptor function are not as severe as those observed for the same mutations to α_1R67.

However, as seen with the α_1R67 mutations, there is a similar trend, though subtle, which correlates to the extent of alteration in GABA-evoked response and the side chain property of the substituting amino acid residue. Particularly, regarding the amino acid substitutions that are polar, those with larger side chains tend to cause less disruption (i.e. smaller increase in $EC_{50\text{-}GABA}$). For example, R207Q causes a 33-fold increase in $EC_{50\text{-}GABA}$ as compared to a 74-fold increase caused by R207N (Figure 3.2 B).

More interesting, perhaps, are the hydrophobic substitutions, R207F and R207Y. These mutations yield different extents of effects on $GABA_A$ receptor function. R207F yields smaller peak GABA-evoked current (Mean Ipeak = -17 ± 2.6 pA, n = 12), while R207Y yield more robust current (Mean Ipeak = -47 ± 6.8 pA, n = 9). It should also be noted that 12 out 44 patches (27%) pulled for R207F gave currents, while 13 out of 15 patches (87%) pulled for R207Y yielded currents. This difference is consistent with the above trend that amino acid substitution with larger side chain causes less disruption. The fact that larger polar side chains are closer to wild-type in size may help explain for their lesser disruption.

Mutations at β_2R207 alter macroscopic deactivation but not desensitization

Closer examination of how mutations at β_2R207 change $GABA_A$ receptor function reveals that the deactivation phase of a GABA-evoked current (500 ms pulse) is accelerated (Figure 3.3 B, Table 3.1). Unlike α_1R67 mutations, however, β_2R207 mutations cause no change in the desensitization phase of GABA-evoked current (Table 3.1). Also, no change in activation rate was recorded for β_2R207 mutants. From these results, it is clear that β_2R207 plays a different role compared to α_1R67.

A

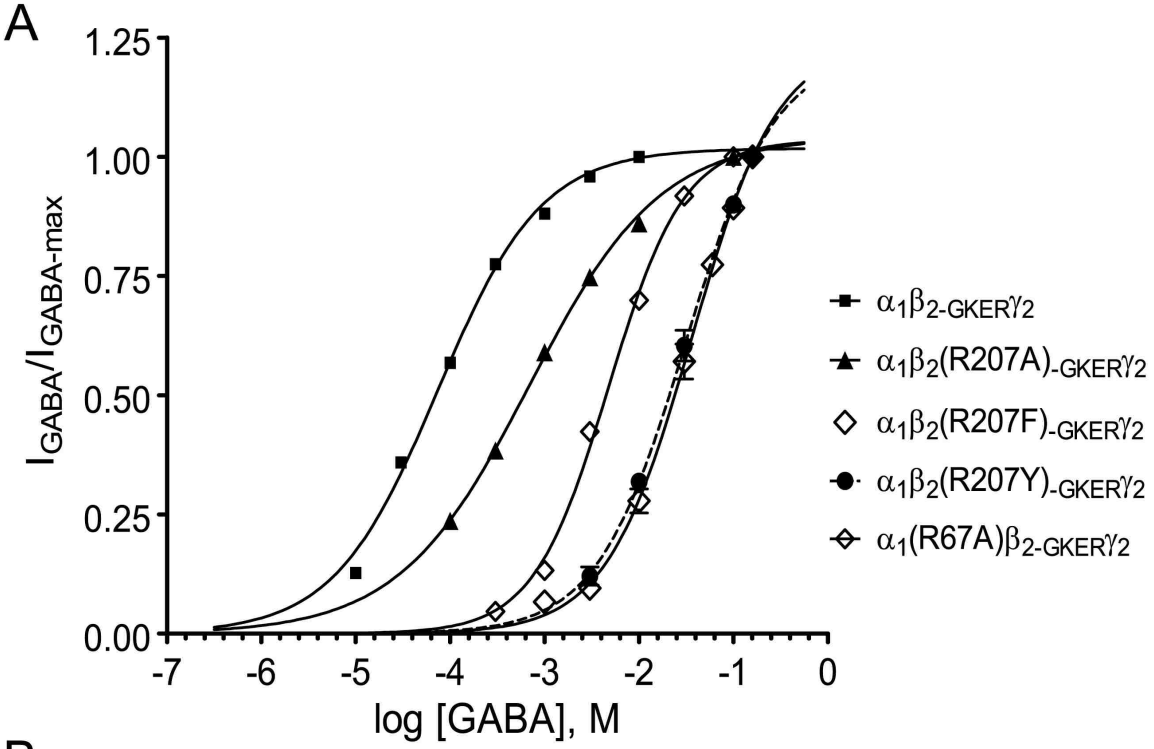

B

Receptor	Mean I_{Peak} (pA)	n	$EC_{50\text{-}GABA}$	ΔAffinity (fold)
$\alpha_1\beta_{2\text{-}GKER}$	114 ± 12	47	6 μM	--
$\alpha_1\beta_{2\text{-}GKER}\gamma_2$	443 ± 80	26	73 μM	--
R67A	91 ± 20	31	926 μM	154
R67A-γ_2	312 ± 67	24	4.78 mM	65
R207A	117 ± 38	43	185 μM	31
R207A-γ_2	418 ± 88	22	696 μM	10
R207F	17 ± 2.6	12	ND	--
R207F-γ_2	280 ± 65	10	> 36.3 mM	--
R207Y	47 ± 6.8	9	ND	--
R207Y-γ_2	562 ± 134	13	> 31 mM	--

Figure 3.5 γ_2-containing receptors yield more robust currents for both wild-type and mutants. A) Concentration-response curves of γ_2-containing wild-type ($\alpha_1\beta_{2\text{-}GKER}\gamma_2$) and mutants (see graph). α_1R67 and β_2R207 mutations co-expressed with γ_2 consistently exhibit right-shifted concentration response compared to wild-type. B) Summary of the effects of co-expressing with γ_2 subunit: co-expression with γ_2 increases average current size and decreases a mutation's effect of GABA affinity.

Co-expression with γ_2 subunit yields more robust currents

Up until this point, the $GABA_A$ receptors studied were expressed in the form of $\beta_2\alpha_1\beta_2\alpha_1\beta_2$ pentameric assembly. In this arrangement, a mutation introduced to the β_2R207 position would end up at three different inter-subunit interfaces, instead of two. Therefore, an attempt was made to limit the mutation to only two inter-subunit interfaces by introducing third kind of subunit, γ_2. In the presence of γ_2 subunits, the $GABA_A$ receptor will be arranged as $\beta_2\alpha_1\beta_2\alpha_1\gamma_2$.

It was observed that $\alpha_1\beta_2\gamma_2$ receptors yield larger GABA-evoked current compared to $\alpha_1\beta_2$ receptors (Figure 3.5 B). However, $\alpha_1\beta_2\gamma_2$ receptors have higher $EC_{50\text{-}GABA}$ (Figure 3.5 A). Additionally, mutations introduced to γ_2-containing receptors cause less shift in $GABA_A$ receptor function.

Discussion

As a whole, the mutants R67D, R67E, R67K, R67F, R67L, R67N, R67Q, and R67Y yield greater disruption of $GABA_A$ receptor's function compared to R67A mutation. The severe effects seen here lead to a logical conclusion that the existence of an arginine at position 67 of the α_1 subunit is specific and critical, if not absolutely necessary, for proper function of the $GABA_A$ receptor. In fact, primary sequence homology indicates that this arginine residue is conserved between all six isoforms of α subunits and this conservation extends to other receptors from the cl-LGIC family.

On the other hand, β_2R207 mutations tend to cause less debilitating effects on $GABA_A$ receptor function. This difference in effects could result from either the tolerant nature of the local environment where the side chain of β_2R207 is located or the degree of contribution that β_2R207 has to the overall function of $GABA_A$ receptor. For example, β_2R207 mutations only affected the deactivation phase of GABA-evoked current, while α_1R67 mutations altered both deactivation and desensitization phases.

Apparently, α_1R67 influences, if not participates in, more processes that underlie proper function of $GABA_A$ receptor, as compared to β_2R207. Both α_1R67 and β_2R207 contribute to the binding of GABA to the receptor, a role inferred from the fact that their mutations accelerated deactivation. Deactivation is a macroscopic kinetic parameter that is influenced mainly by how fast GABA binds and unbinds. On top of that, α_1R67 mutations also slowed the desensitization phase. Macroscopic desensitization involves the integration of multiple microscopic kinetics such as ligand binding and unbinding, channel gating, desensitization and resensitization (Colquhoun, 1998). Therefore, it follows that α_1R67 is involved in more processes than just GABA binding.

IV. DISSECTING THE STRUCTURAL AND FUNCTIONAL CONTRIBUTION OF BINDING POCKET TYROSINES: β_2Y97, β_2Y157, and β_2Y205

Introduction

In cl-LGICs, ligand binds at inter-subunit interfaces, and among the residues lining the walls of these interfaces is a group of aromatics. These aromatic residues are shown to cluster together at the ligand-binding site in the crystal structure of the AChBP (Brejc et al., 2001). Acetylcholine binding protein (AChBP) is homologous to the extracellular domain of the cl-LGICs, including glycine receptor, serotonin receptor (5-HT3), acetylcholine receptor, and $GABA_A$ receptor (Brejc et al., 2001). As a result, the model structure of the extracellular domain of these cl-LGICs has been constructed based on the known characteristics of AChBP and various details derived from mutational-electrophysiological studies of each receptor type (Cromer et al., 2002; Grudzinska et al., 2005; Harrison and Lummis, 2006; Dellisanti et al., 2007; Padgett et al., 2007; Pless et al., 2008). In AChBP, the characteristic aromatic amino acid residues have collectively been referred to as the "aromatic box". These aromatic residues are associated with six discontinuous loops, termed A to F (Akabas, 2004). This "aromatic box" is thought to acts as a hydrophobic barrier that facilitates the access of a charged ligand by minimizing the interference of water. Since these aromatic residues are highly conserved between AChBP and all cl-LGICs, the obvious question is whether they also play similar roles in ligand binding. As reviewed previously (chapter I), accumulated experimental data suggest that the general influence of these aromatics on ligand binding is well conserved; mutating these aromatics results in altered receptor function.

One prominent way for ligand to interact with binding site residues is through cation-π interaction, a type of interaction involving the cationic group of the ligand and the π orbitals of an aromatic side chain. Currently, one aromatic residue in each cl-LGIC

has been identified to be involved in cation-π interaction. For examples, such cation-π interaction has been suggested for the positively charged amino group of the ligand and an aromatic on loop B of the nACh receptor (α_1W149), the 5-HT3 receptor (W183), $GABA_A$ ρ receptor (ρY198), Gly receptor (F159) (Zhong et al., 1998; Beene et al., 2002; Lummis et al., 2005; Pless et al., 2008), and on loop A of $GABA_A$ receptor (β_2Y97) (Padgett et al., 2007).

These "aromatic box" residues include several tyrosines that have been demonstrated to not participate in cation-π bond. For example, β_2Y157 and β_2Y205 of the $GABA_A$ receptor do not participate in cation-π interaction. Tyrosines are different from other aromatics (tryptophan and phenylalanine) in that their side chain possesses a hydroxyl group. This hydroxyl group can participate in hydrogen bonds. In the $GABA_A$ receptor, β_2Y157 and β_2Y205 do not participate in cation-π interaction critical for ligand binding (Padgett et al., 2007). While unnatural aromatic amino acid substitution has been used to test the importance of the aromatic component of each tyrosine in ligand binding, the functional contribution of the hydroxyl group has been assessed by simply making a phenylalanine substitution and measuring changes in receptor function (Amin and Weiss, 1993). It was found that the mutant receptors, $\alpha_1\beta_2$Y157Fγ_2 and $\alpha_1\beta_2$Y157Fγ_2, exhibited a 50- and 56-fold increases in $EC_{50\text{-}GABA}$, respectively.

Accumulated data from the above study and later studies (Boileau et al., 2002; Padgett et al., 2007) have implicated β_2Y157, β_2Y205, and β_2Y97 of $GABA_A$ receptor in ligand binding. However, "direct" evidence for their involvement is still lacking. For example, Padgett et al. (2007) demonstrated that one of these, β_2Y97, participates in a cation-π bond that mediates ligand binding and that β_2Y157 and β_2Y205 do not

participate in functionally important cation-π interactions. Padgett et al. (2007) proposed that β_2Y97 directly interacts with the primary amine of GABA. Due to the lack of evidence for cation-π interaction, they suggested that β_2Y157 and β_2Y205 require the electronegative groups at their C4 positions to function, perhaps via hydrogen bonds with neighboring side chains. This suggestion is consistent with an earlier study, which demonstrated decreased sensitivity to GABA when β_2Y157 and β_2Y205 were conservatively substituted by phenylalanine (Amin and Weiss, 1993). The same study also reported that an even further reduction in GABA sensitivity resulted when either tyrosine residues were mutated to such non-aromatic amino acids as serine and asparagine, hinting that these tyrosine side chains may be bifunctional. In other words, both the hydroxyl and the aromatic elements of these tyrosine side chains contribute to proper function of the $GABA_A$ receptor. Generally, the participation of a given amino acid residue in ligand binding can often be inferred from the effect on ligand affinity caused by its mutation. However, such inferred evidence would not be as accurate and conclusive as the directly measured change in GABA binding rate. As such, the present study seeks to directly measure the contribution of each tyrosine's aromatic and hydroxyl elements to ligand binding, by quantifying the changes in measured GABA binding rate resulting from mutating each tyrosine.

Results

In the present study, β_2Y97, β_2Y157, and β_2Y205 were first individually mutated to alanine and co-expressed with wild-type α_1 and γ_2 subunits for functional assessment, since the mutations were all on the β_2 subunit. $\alpha_1\beta_{2\text{-GKER}}\gamma_2$ was used as wild-type reference; this receptor showed no difference in its macrokinetic profile compared to $\alpha_1\beta_2\gamma_2$. β_2Y97, β_2Y157, and β_2Y205 were subsequently mutated to phenylalanines. For readability, the mutant receptors will be referred to as Y97A, Y97F, Y157A, Y157F, Y205A, and Y205F, corresponding to the point mutation they contain.

Effects of mutating binding pocket tyrosines on $EC_{50\text{-}GABA}$ and receptor macrokinetics

Functional significance of β_2Y97, β_2Y157, and β_2Y205 was verified by assessing the effects of Y97A, Y157A, and Y205A on GABA affinity and macroscopic desensitization and deactivation. While Y97A only causes a 13-fold increase in $EC_{50\text{-}GABA}$, Y157A causes more than a 400-fold increase, and Y205A completely disrupts $GABA_A$ receptor function (Figure 4.1). To assess the functional contribution of the hydroxyl group on each tyrosine's side chain, phenylalanine substitutions were introduced, allowing only the benzene ring component to be maintained. It was observed that each phenylalanine substitution causes less disruption (i.e. less increase in $EC_{50\text{-}GABA}$) than an alanine mutation at the same residue. It was also observed that mutating β_2Y97 causes relatively less severe effects than mutating either β_2Y157 or β_2Y205. Y97F only increases $EC_{50\text{-}GABA}$ by 4-fold, while Y157F and Y205F increase $EC_{50\text{-}GABA}$ by 21 and 22-fold, respectively (Figure 4.1).

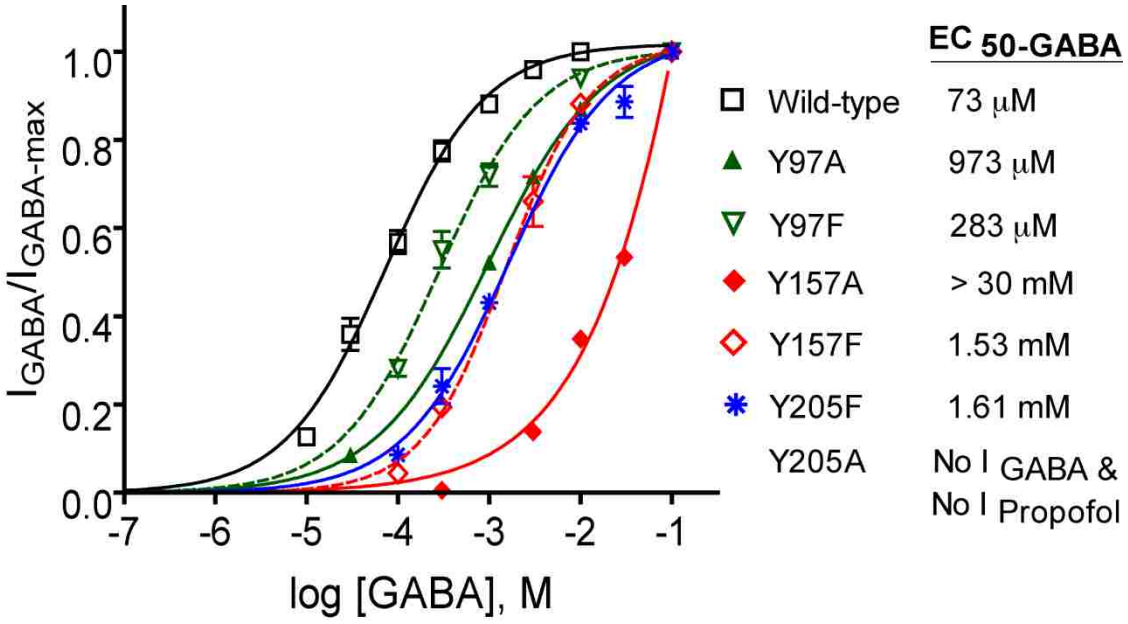

Figure 4.1 Peak concentration-response curves of tyrosine mutants are right-shifted with respect to wild-type. Y97A causes a 13-fold increase, while Y97F only causes a 4-fold increase in $EC_{50\text{-}GABA}$. Y157A causes more than 400-fold increase, while Y157F causes 21-fold increase in $EC_{50\text{-}GABA}$. Y205F causes a 22-fold increase in $EC_{50\text{-}GABA}$, while Y205A completely disrupts both GABA-evoked and propofol-evoked current.

When macroscopic desensitization and deactivation were examined, it was found that mutations made to the three tyrosine residues all result in an increased rate of deactivation but no significant changes in either the rate or extent of desensitization (Figure 4.2, Table 4.1). Mutating β_2Y97 causes less alteration in macroscopic deactivation compared to either mutating β_2Y157 or β_2Y205 (Table 4.1). Since a full GABA-evoked response could not be achieved for Y157A and Y205A, only the macrokinetic effects of Y157F and Y205F were assessed. Y97F causes less increase in deactivation rate (i.e. less decrease in τ_w of deactivation) than Y157F and Y205F (Table 4.1). Regarding macroscopic desensitization, Y97F, Y157F, and Y205F cause no significant changes in τ_W.

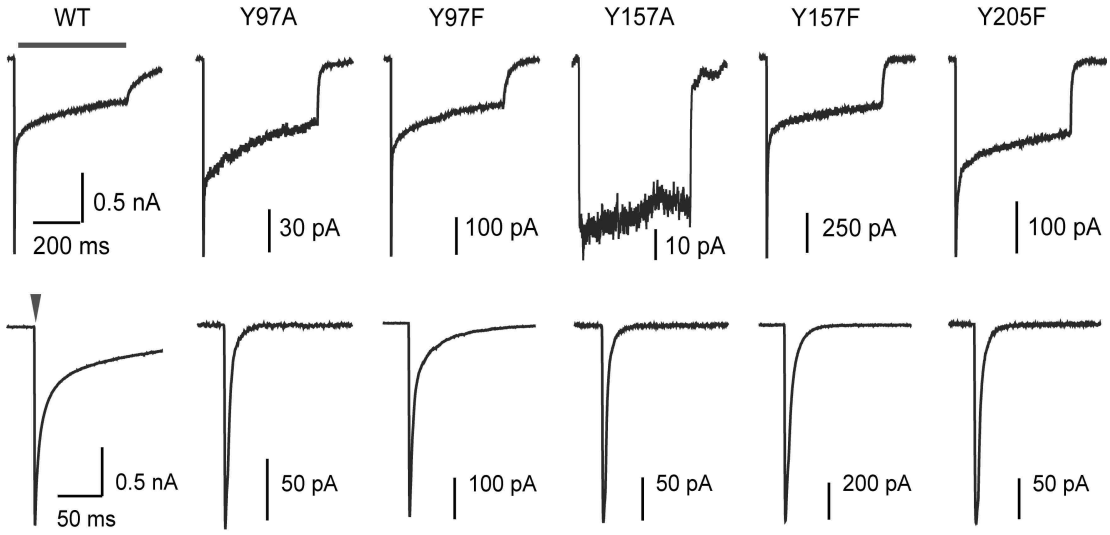

Figure 4.2 Mutating β_2Y97, β_2Y157, and β_2Y205 to either alanine or phenylalanine results in more rapid macroscopic deactivation. In upper row are representative currents evoked by long (500 ms, bar) and lower row are representative currents evoked by short (4 ms, arrow head) pulses of saturating GABA. Macroscopic desensitization and deactivation are quantified by fitting each phase with an exponential decay function. Results are summarized in table 4.1.

Table 4.1 Point mutations at β_2Y97, β_2Y157, and β_2Y205 increase rate of deactivation

	Deactivation (2-4 ms pulse)		Desensitization (500 ms pulse)		
	τ_w (ms)	n	τ_w (ms)	% Remaining	n
WT	37.4 ± 5.4	14	130 ± 11	39 ± 2%	39
Y97A	11.8 ± 2.7*	7	136 ± 20	33 ± 22%	12
Y97F	14.7 ± 1.6*	5	58 ± 9	19 ± 2%	10
Y157A	ND		ND	ND	
Y157F	8.5 ± 2.1*	5	96 ± 10	33 ± 1.4%	17
Y205A	ND		ND	ND	ND
Y205F	5.2 ± 0.4*	8	160 ± 18	41 ± 2%	11

* different from WT ($\alpha_1\beta_{2\text{-GKER}}\gamma_2$) ($P < 0.01$); ANOVA with Dunnets post-test; ND = could not be determined.

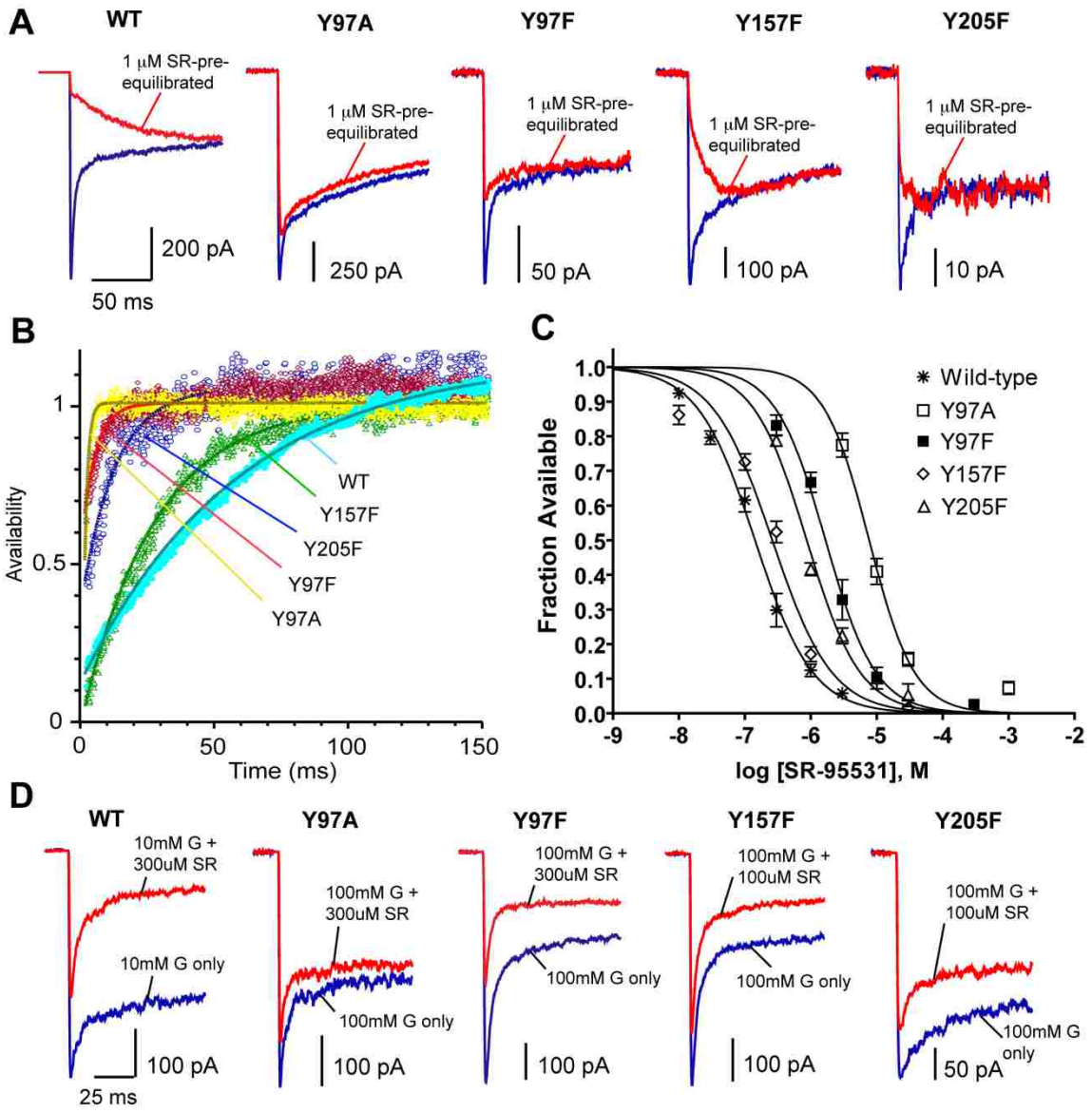

Figure 4.3 Antagonist unbinding and race experiments. A) Sample raw traces recorded from antagonist unbinding experiments. Solution exchange protocol was designed to go in the sequence of 500 ms in saturating GABA solution, 15 seconds in wash, then 500 ms in a test concentration of SR-95531 followed immediately by 500 ms in saturating GABA solution, back to wash for 15 seconds, and the cycle repeats. The resulting raw data was analyzed to determine the microscopic kinetics, K_D, k_{off}, and k_{on}, for SR-95531. The sample raw traces show current resulted from control GABA (blue) and pre-equilibration (red). B) Deconvolution of GABA-evoked currents after SR-95531pre-equilibration from control currents (no pre-equilibration) reveals the time course of SR-95531 unbinding. Deconvolved signals were fit to the equation $A(t) = [P_\infty - (P_\infty - P_0)\exp(-t/\tau_u)]^N$, where A(t) is the fraction of available receptors (antagonist not bound at any site), P_0 and P_∞ are the probabilities that a single binding site is available initially at t = 0 and at steady state as $t \rightarrow \infty$, τ_u is the time constant of antagonist unbinding from each site ($k_{off\text{-}SR} = 1/\tau_u$), and N is the number of binding sites (Jones et al., 2001). C) Concentration response curves, for the equilibrium antagonist occupancy in the absence of GABA A(t = 0), were fit to the normalized hill equation $I/I_{max} = 1 - 1/[(K_{D\text{-}SR}/[SR\text{-}95531])^N + 1]$. D) Sample raw

traces recorded from race experiments. Solution exchange protocol was designed to alternate between control (only GABA, 500ms, blue) and test (GABA and SR-95531 simultaneously, 500ms, red) every 15 seconds. The known concentrations of GABA and SR and the ratio of GABA+SR : GABA only (I_{Race}) were used to calculate $k_{on\text{-}GABA}$ (see methods).

Effects on GABA binding rate

While changes in $EC_{50\text{-}GABA}$ and macroscopic deactivation provide good indications that the tyrosine residues are involved in GABA binding, they do not qualify as "direct" evidence. Basically, EC50 value encompasses both binding and gating parameters (Colquhoun, 1998), and at a lower level of complexity, macroscopic deactivation and desensitization are influence by multiple microscopic transition states. Fortunately, one microkinetic parameter we can readily measure is the binding rate of GABA ($k_{on\text{-}GABA}$), which can serve as the "direct" evidence for a residue's participation in GABA binding.

Table 4.2 Summary of results from antagonist unbinding and race experiments

	$K_{D\text{-}SR}$ (μM)	$k_{off\text{-}SR}$ (s^{-1})	$k_{on\text{-}SR}$ ($M^{-1}s^{-1}$)	$k_{on\text{-}GABA}$ ($M^{-1}s^{-1}$)	n
Wild-type	0.14	15.9 ± 0.8	(1.14 ± 0.10) x 10^8	(7.40 ± 0.40) x 10^6	6
Y97A	7.68	832.1 ± 91.5	(1.08 ± 0.12) x 10^8	(2.17 ± 0.11) x 10^6	4
Y97F	1.67	188.91 ± 9.66	(1.13 ± 0.06) x 10^8	(5.66 ± 0.62) x 10^6	5
Y157F	0.26	44.43 ± 1.62	(1.71 ± 0.06) x 10^8	(1.60 ± 0.31) x 10^6	4
Y205F	0.87	121.01 ± 7.94	(1.39 ± 0.09) x 10^8	(6.0 ± 0.44) x 10^5	4

$k_{on\text{-}GABA}$ was measured as previously described in chapter II. Briefly, this process first involves determining the binding rate for a competitive antagonist, in this case SR-95531. Once the binding rate for SR-95531 ($k_{on\text{-}SR}$) is obtained, the binding rate of GABA can be determined by performing an experiment in which GABA and SR-95531

are co-applied, known as race experiment. The resulting co-application current is compared to the current evoked by application of GABA alone. The extent to which the peak current is reduced by the presence of antagonist depends on the relative binding rates of the two compounds and the relative concentrations available. Since $k_{on\text{-}SR}$ has been determined by antagonist unbinding experiment, $k_{on\text{-}GABA}$ can be calculated as $k_{on\text{-}GABA}$ = [SR-95531] $k_{on\text{-}SR}$/([GABA](1/I_{race} -1)) (Jones et al., 1998). I_{race} is the ratio of the peak response of co-application to the peak response of GABA alone. Data from the present study are summarized in figure 4.3.

It was observed that Y97A reduces binding rate GABA ($k_{on\text{-}GABA}$) about 3.4-fold and Y97F only reduces $k_{on\text{-}GABA}$ about 1.3-fold (Table 4.2). Y157F decreases $k_{on\text{-}GABA}$ by about 4.6-fold. Y205F decreases $k_{on\text{-}GABA}$ by 12-fold. Comparing these changes in $k_{on\text{-}GABA}$, it is clear that eliminating the hydroxyl group on β_2Y205 causes the most reduction in $k_{on\text{-}GABA}$. Therefore, the inferred result is that the hydroxyl group of β_2Y205 plays a relatively more significant role in GABA binding than that of β_2Y97 and β_2Y157.

Discussion

As mentioned, cation-π interactions at ligand-binding site play a prominent role in facilitating ligand-receptor interaction. Such cation-π interactions have been suggested for the positively charged amino group of the ligand and an aromatic on loop B of the nACh receptor (Zhong et al., 1998), the 5-HT3 receptor (Beene et al., 2002), $GABA_A$ ρ receptor (Lummis et al., 2005), but on loop A of $GABA_A$ receptor (Padgett et al., 2007). Cation-π interactions have been demonstrated for at least one tyrosine at the ligand-binding pocket of $GABA_A$ and $GABA_A$ ρ (formerly known as $GABA_C$) receptors (Padgett et al., 2007; Lummis et al., 2005). In addition to cation-π interaction capability, tyrosine residues also possess a hydroxyl group that can potentially participate in hydrogen bonding.

This study aimed to assess the relative significance of the hydroxyl group from each of the three tyrosines at the GABA-binding pocket by mutating each tyrosine to phenylalanine and measuring the direct effects on $k_{on\text{-}GABA}$. The results show that the hydroxyl group on β_2Y97 makes no significant contribution, while the hydroxyl groups on β_2Y157 and β_2Y205 greatly influence binding rate GABA. This difference is relevant on two counts. First, it is consistent with the observation that mutating β_2Y97 causes much less change in gross receptor function (i.e. $EC_{50\text{-}GABA}$). Second, the benzene ring of β_2Y97, not the hydroxyl group, has previously been demonstrated to participate in interaction critical for ligand binding (Padgett et al., 2007). Also, the benzene rings of β_2Y157 and β_2Y205 were previously tested negative for binding-determining cation-π interaction (Padgett et al., 2007).

Surprisingly, mutations at β_2Y97 do not result in very big changes in $k_{on\text{-}GABA}$. This small change on $k_{on\text{-}GABA}$ somewhat contradicts the proposed role of β_2Y97 in ligand binding shown by Padgett et al. (2007). They proposed a ligand-receptor interacting model in which the amino group of GABA forms a cation-π bond with the aromatic face of β_2Y97. If this model were entirely accurate, removing the aromatic at position 97 of β_2 (i.e. β_2Y97A) would have caused a greater shifted in $EC_{50\text{-}GABA}$ than demonstrated here. Consistent with the model proposed by Padgett et al. (2007), however, the hydroxyl group of β_2Y97 is not crucial for GABA binding.

V. A TIGHT INTERACTION BETWEEN β_2Y97 AND β_2F200 OF THE GABA$_A$ RECEPTOR THAT MEDIATES GABA BINDING

Introduction

A profusion of studies have contributed to our understanding of the interaction between $GABA_A$ receptors and their endogenous ligand, γ-aminobutyric acid (GABA). From these, it is clear that the GABA binding site is located at the interface of the α and β subunits (Cromer et al., 2002; Kash et al., 2004), and a multitude of amino acid residues that are located at this interface and mediate GABA affinity have been identified (Lummis, 2009). In addition, the general architecture of the binding site has been determined through homology modeling (Cromer et al., 2002). However, details of the molecular interactions that underlie the ligand-receptor interaction remain elusive.

A particularly intriguing possibility is that the positively charged amino group of GABA may interact with an aromatic residue in the GABA-binding pocket via a cation-π bond. Padgett et al. (2007) tested for this using unnatural amino acid substitution and found that a tyrosine in the binding pocket, β_2Y97**,** participates in a cation-π bond that is immediately involved in GABA affinity. As a result they, very reasonably, concluded that β_2Y97 directly interacts with the amino group of GABA. However, the possibility remains that β_2Y97's cation partner is, instead, one of the multiple arginine residues located in the GABA binding pocket. These include α_1R67, α_1R120, α_1R132, and β_2R207, all of which have been shown to mediate GABA binding (Westh-Hansen et al., 1999; Holden and Czajkowski, 2002; Laha and Wagner, 2011; Wagner et al., 2004). Therefore, we set out to test for this interaction.

Here, we utilized double-mutant cycle analysis to test for potential interactions between β_2Y97 and each of α_1R67, α_1R120, α_1R132, and β_2R207, by quantifying functional coupling in the context of changes in free energy resulting from mutating

amino acid residues in singles and in pairs (Figure 5.1). We also tested for functional coupling between each arginine and β_2F200, another aromatic residue located in the GABA-binding pocket that has been shown to influence GABA affinity (Wagner and Czajkowski, 2001). Our results identified functional coupling between two of the arginines (α_1R132, β_2R207) and both β_2Y97 and β_2F200. Furthermore, we demonstrate an even tighter coupling between β_2Y97 and β_2F200. We conclude that β_2Y97 and β_2F200 form a single functional unit that is critical for GABA binding. The Y97/F200 pair could interact with the ammonium moiety of GABA via a cation-π bond and its position may be fine tuned via secondary interactions with β_2R207 and/or α_1R132.

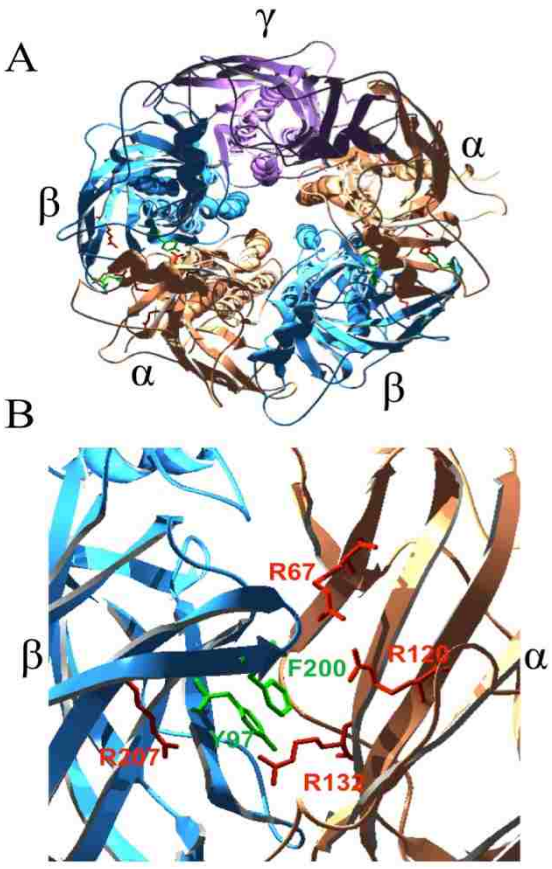

Figure 5.1 Homology models of the $GABA_A$ receptor show arginines located proximal to the aromatics. A) Top view looking in from the extracellular side through the channel pore. Structurally, $GABA_A$ receptor is pentameric, with the five subunits pseudo-symmetrically arranged around a central ion pore. The most abundant $GABA_A$ receptor subtype, found in the brain, has a stoichiometry of two α subunits, two β subunits, and one γ subunit arranged counter-clockwise as βαγβα (Benke et al., 1994; McKernan and Whiting; 1996; Baumann et al., 2002). Residues were mutated at both β/α interfaces (arrow heads). B) Side view of the extracellular domain at a single β/α interface. β_2Y97, β_2F200, β_2R207, α_1R67, α_1R120, and α_1R132 are thought to project their side chains toward the center of the β/α inter-subunit interface.

Results

The present study sought to employ double mutant cycle analysis to identify potential cation-π interactions between arginines (α_1R67, α_1R120, α_1R132, and β_2R207) and aromatics (β_2Y97 and β_2F200) located in the $GABA_A$ receptor ligand-binding pocket. The targeted amino acid residues were mutated singly and in pairs. In order to achieve consistent expression, all of the mutations were expressed in a background of $\alpha_1\beta_{2\text{-}GKER}\gamma_{2s,}$ which also served as our control construct (Bollan et al., 2003; Laha and Wagner, 2011). For readability, the mutant constructs will be referred to as R67A, R120A, R132A, R207A, Y97A, F200I, R120A-Y97A, R120A-F200I, R132A-Y97A, R132A-F200I, R207A-Y97A, R207A-F200I, Y97A-F200I, and Y97A-F200I-R207A to indicate the corresponding single, double, or triple mutant receptor.

Each mutation tested increases $EC_{50\text{-}GABA}$ and accelerates deactivation

Each of the arginines and aromatics of interest was mutated to alanine and transiently expressed in HEK-293 cells, in order to record GABA-evoked currents from outside-out patches. Initial evaluation included determination of $EC_{50\text{-}GABA}$, characterization of macroscopic desensitization (current decay during a 500ms pulse of saturating GABA), and characterization of macroscopic deactivation (current decay after a 2-4 ms pulse of saturating GABA). $EC_{50\text{-}GABA}$ was determined by fitting concentration-response plots with a form of the Hill equation. Desensitization and deactivation waveforms were fit with a bi-exponential decay function, from which a weighted time constant (τ_w) was calculated.

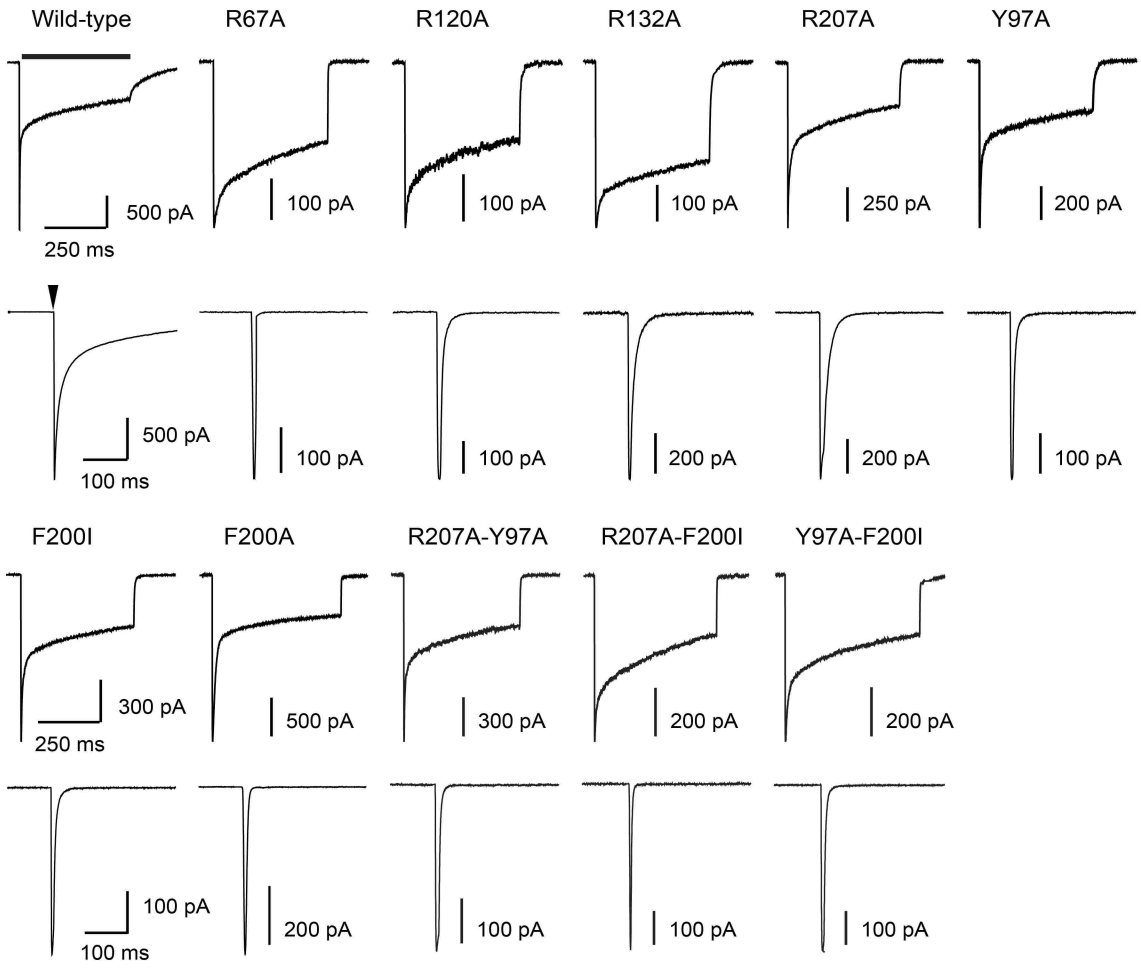

Figure 5.2 Effects of α_1R67 and β_2R207 mutations on macroscopic deactivation and desensitization. β_2Y97A, β_2F200A/I, and β_2R207A all accelerate deactivation, while α_1R67A, α_1R120, and α_1R132 cause both increased deactivation rate and decreased desensitization rate. Sample raw signals of long (ensemble average of 10 to 15 traces) and short (ensemble average of 20 to 30 traces) GABA-evoked currents are shown for wild-type, single mutants, and selected double mutants. While all mutants exhibit significantly accelerated rate of deactivation, only R67A, R120A, and R132A yield significantly slowed desensitization. Horizontal bar on wild-type long trace and arrowhead on wild-type short trace depict long (500 ms) and short (2-4 ms) pulses of GABA application respectively.

$EC_{50\text{-}GABA}$ for every mutant tested displayed a significant rightward shift ranging from 288 μM (4-fold, R132A) to 12.6 mM (173-fold, F200A) compared to control ($EC_{50\text{-}GABA}$ $\alpha_1\beta_{2\text{-}GKER}\gamma_{2s}$ = 73 μM) (Figure 5.3). Alanine substitution also significantly accelerated the time-course of deactivation for each of the mutants tested, with τ_w ranging from 10.3 ms (3.7-fold, R207A) to 1.7 ms (22-fold, R67A) (Table 5.1, Figure 5.2). These

effects on $EC_{50\text{-}GABA}$ and deactivation are entirely consistent with the previously published results that each of the residues tested mediates GABA binding.

Table 5.1: Effects of single and double mutants on GABA affinity, deactivation, and desensitization parameters.

		Deactivation		Desensitization	
	$EC_{50\text{-}GABA}$ (mM)	τ_W (ms)	n	τ_W (ms)	n
Wild-type	0.073	37.4 ± 5.4	14	130 ± 11	39
R67A	4.8	1.7 ± 0.1 *	9	262 ± 36 *	18
R120A	0.85	3.0 ± 0.3 *	7	274 ± 38 *	23
R132A	0.288	6.9 ± 0.4 *	9	283 ± 31 *	11
R207A	0.696	10.3 ± 1.2 *	10	177 ± 30	20
Y97A	1.06	3.9 ± 0.4 *	9	152 ± 24	16
F200A	12.6	2.1 ± 0.2 *	7	151 ± 24	11
F200I	6.5	3.0 ± 0.2 *	12	146 ± 20	19
R67A-Y97A	na	na	na	na	na
R67A-F200I	na	na	na	na	na
R120A-Y97A	17.89	1.4 ± 0.1*	8	337 ± 65 *	10
R120A-F200I	na	na	na	na	na
R132A-Y97A	2.31	3.1 ± 0.1*	7	299 ± 54*	8
R132A-F200I	12.93	1.6 ± 0.1*	7	244 ± 62*	7
R207A-Y97A	3.26	2.2 ± 0.2 *	7	131 ± 21	11
R207A-F200I	22.65	1.6 ± 0.1 *	8	188 ± 18	31
Y97A-F200I	5.04	2.1 ± 0.1 *	14	175 ± 17	15

One-way ANOVA with Dunnett's post-test was used to assess for significant difference between mutant and wild-type parameters (* indicates $p < 0.05$).

Effects on desensitization were less uniform. Alanine substitution at Y97, F200, and R207 had no effect on the desensitization time-course. However, R67A, R120A, and R132A all displayed significantly slower desensitization. The effect on desensitization for R120A has been previously reported (Laha and Wagner, 2011), and although we found it quite interesting that each of the other two arginines on the α_1 subunit showed a similar effect, we did not pursue this further.

In later experiments that depend on the competitive antagonist SR-95531, it was found that the β_2F200A mutation could not be used because it causes a debilitating reduction in SR-95531 affinity. Therefore, a milder mutation, β_2F200I, was tested. β_2F200I was found to adequately support SR-95531 binding and had less severe effects on $EC_{50\text{-}GABA}$ and deactivation than β_2F200A, making it very useful for the double-mutant cycle analysis studies that followed.

Double-mutant cycle analysis of $EC_{50\text{-}GABA}$ reveals little coupling between the arginines from the α_1 subunit and β_2Y97 or β_2F200

This study aimed to assess the relationships between residues using the method of double-mutant cycle analysis. Double-mutant cycle analysis quantifies the extent of coupling between two residues by comparing the changes in free energy ($\Delta\Delta G$) resulting from single mutations and the corresponding double mutation, to measure the likelihood of two residues interacting (Horovitz, 1996). One parameter that has been commonly used for double-mutant cycle analysis, in the study of proteins such as LGICs, is the apparent affinity for ligand, or EC_{50} (Kash et al., 2003; Price et al., 2007; Gleitsman et al., 2008). To this end, the effects of the above mutations were initially quantified by

conducting concentration-response experiments for the purpose of determining $EC_{50\text{-}GABA}$.

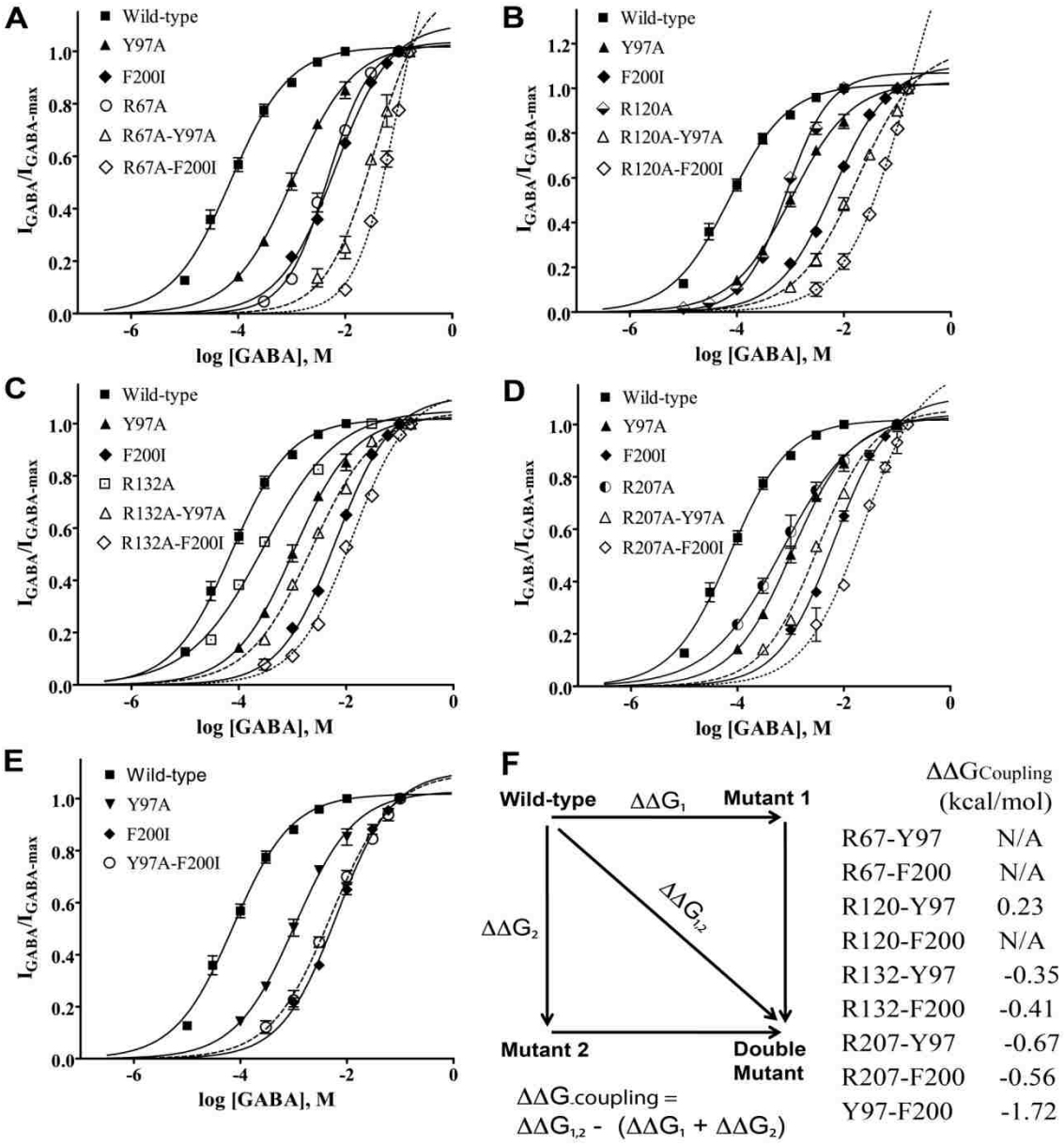

Figure 5.3 $EC_{50\text{-}GABA}$ double-mutant cycle analysis identified pairs of amino acid residues that are functionally coupled. $EC_{50\text{-}GABA}$ was obtained through concentration-response experiments in which the peak currents from a series of sub-saturating concentrations of GABA were compared to the peak currents at saturating GABA. The concentration-response plot was fit with a form of the Hill equation to obtain an EC_{50} value. A-D) Concentration response curves for wild-type ($EC_{50\text{-}GABA}$ = 73 μM), Y97A ($EC_{50\text{-}GABA}$ = 1.06 mM), and F200I ($EC_{50\text{-}GABA}$ = 6.50 mM); unique to each plot are the curves for specific arginine single mutant and the corresponding two double mutants containing that particular arginine ($EC_{50\text{-}GABA}$: R67A = 4.8 mM; R120A = 850 μM; R132A = 288 μM; R207A = 696 μM; R120A-Y97A = 17.89 mM; R132A-Y97A = 2.31

mM; R132A-F200I = 12.93 mM; R207A-Y97A = 3.26 mM; R207A-F200I = 22.65 mM). E) The double mutant Y97A-F200I concentration-response plot is identical to that of the single mutant F200I; both are right-shifted compared to wild-type. F) Double-mutant cycle analysis schematic and a summary of the coupling energies determined.

As a single mutation, R67A caused the largest shift in $EC_{50\text{-}GABA}$, and when combined with either Y97A or F200I even more severe shifts were observed (Figure 5.3 A). Curve fits to concentration-response data for either double mutant was not possible because the data never approached saturation. In addition, for either double mutant, propofol-evoked currents (1 mM) displayed peak amplitudes greater than twice those evoked by 160 mM GABA (the highest concentration tested, data not shown), suggesting that $EC_{50\text{-}GABA}$ for either of these constructs is greater than 160 mM. Because we were not able to accurately quantify $EC_{50\text{-}GABA}$ for these constructs we could not subject them to double-mutant cycle analysis. However, the fact that the double mutations are so debilitating is suggestive that no functional coupling exists between α_1R67 and either β_2Y97 or β_2F200, and it is unlikely that these residues share a cation-π interaction.

As was seen for R67A, when R120A was co-expressed with F200I, the effect on $EC_{50\text{-}GABA}$ was too severe to be quantified and the two residues are not likely to be functionally coupled. On the other hand, R120A-Y97A receptors displayed a measurable $EC_{50\text{-}GABA}$ (17.9 mM). This value, along with the $EC_{50\text{-}GABA}$ values for R120A (850 μM) and Y97A (1.06 mM), were used to drive double-mutant cycle analysis, which resulted in a coupling energy of 0.23 kcal/mol (Figure 5.3 B, F). It should be noted that, double-mutant cycle analysis works on the premise that if two residues are perfectly independent, we would expect the coupling energy to be 0 kcal/mol. As such, any value that deviates from zero may indicate coupling. The further a coupling energy deviates from 0 kcal/mol the less functionally independent the two residues are from one another. A coupling

energy of |0.5 kcal/mol| or greater would indicate possible interaction between two amino acid residues (Horovitz, 1996; Kash et al. 2003). Therefore, α_1R120 does not appear to be coupled to β_2Y97 and it is not likely to participate in a cation-π bond with either aromatic residue.

The double-mutant cycle analyses of R132A, with respect to the Y97A and F200I, yielded modest coupling energies of -0.35 kcal/mol and -0.41 kcal/mol for R132-Y97 and R132-F200 pairs respectively (Figure 5.3 C, F). These coupling energies are less than |0.5 kcal/mol| but are large enough that it should be considered a possibility for cation-π interactions. Interestingly, α_1R132 appears to be coupled to β_2Y97 and β_2F200 with same magnitude.

Double-mutant cycle analysis of $EC_{50\text{-}GABA}$ reveals a ternary functional interaction between β_2R207, β_2Y97, and β_2F200

When R207A was co-expressed with Y97A or F200I, the significant coupling energies resulted (-0.67 kcal/mol and -0.56 kcal/mol for the R207-Y97 and R207-F200 pairs respectively, Figure 5.3 D, F). These coupling energies indicate that β_2R207 is more tightly coupled to the aromatics, and it is possible that β_2R207 interacts with one or the other via a cation-π bond.

We find it interesting that, as was also seen for α_1R132, β_2R207 is coupled to both β_2Y97 and β_2F200 to the same degree. This result would be predicted if β_2Y97 and β_2F200 are tightly linked structurally, effectively acting as a single functional unit. If this is the case, then double-mutant cycle analysis of the two aromatics should give a strong coupling energy. Indeed, the Y97A-F200I double mutation revealed a highly significant coupling energy (-1.72 kcal/mol) between β_2Y97 and β_2F200 (Figure 5.3 E, F). Taken

together, the strong coupling energies of β_2R207/β_2Y97, β_2R207/β_2F200, and β_2Y97/β_2F200 suggest that these three residues act together as single functional ternary complex to mediate GABA binding.

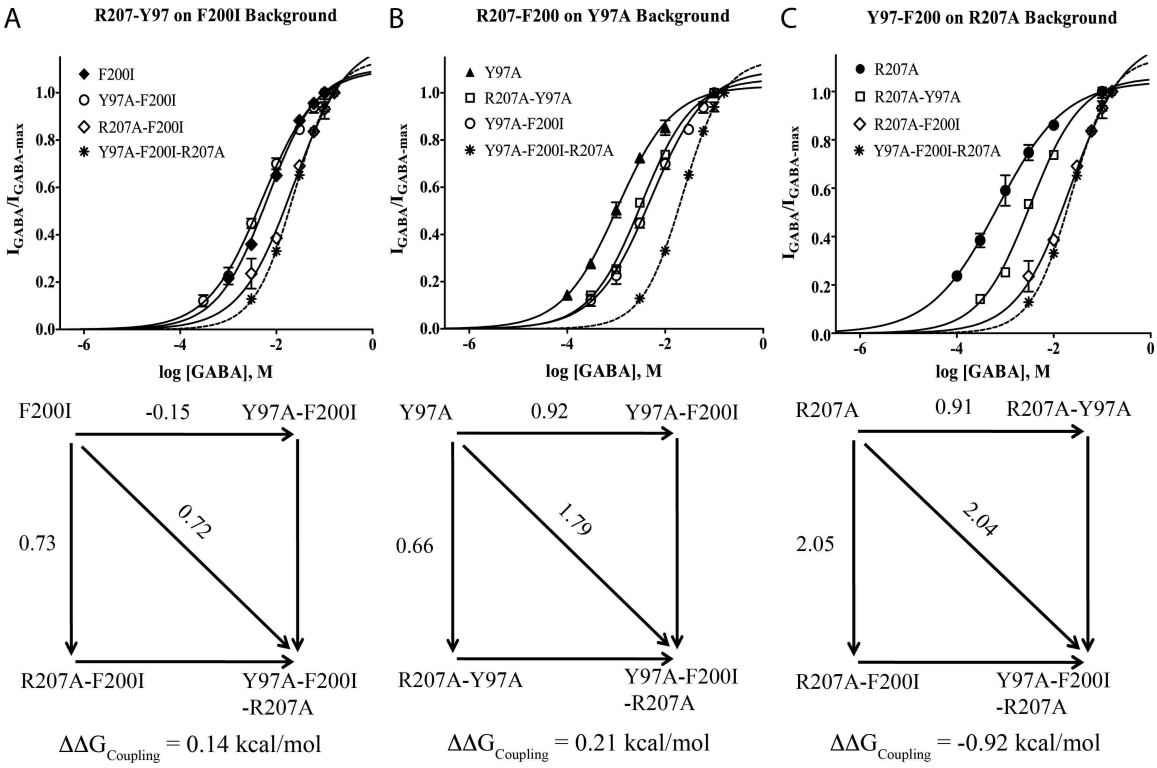

Figure 5.4. Functional coupling between β_2R207 and one of the two aromatic residues exists only in the presence of the other aromatic residue. Top row shows concentration response curves comparing the effects on GABA affinity caused by double mutants and triple mutant in the background of a single mutant control. Bottom row shows the double-mutant cycle analyses and the resulting coupling energies. A) β_2R207 is not functionally coupled to β_2Y97 when β_2F200 is mutated. B) β_2R207 is not functionally coupled to β_2F200 when β_2Y97 is mutated. C) β_2Y97 and β_2F200 remains coupled when β_2R207 is mutated.

Triple mutant cycle analyses revealed unequal partnerships among ternary complex members: β_2R207, β_2Y97, and β_2F200

To further dissect the relationship between members of the ternary complex, we performed triple mutant cycle analyses. In other words, we carried out double mutant cycle analysis measuring coupling of two residues on the background of a third mutant.

The only new data needed to perform this analysis was $EC_{50\text{-}GABA}$ for the triple mutant, Y97A-F200I-R207A. This construct displayed robust GABA-evoked current and caused a 305-fold decrease in GABA affinity, ($EC_{50\text{-}GABA}$ = 22.2 mM). When double-mutant cycle analysis was applied to β_2Y97 and β_2F200 in a R207A background, strong coupling was still observed ($\Delta\Delta G_{Coupling}$ = -0.92 kcal/mol, Fig. 5.4 C). However, coupling of β_2R207 with β_2Y97 disappeared when tested on the F200I background ($\Delta\Delta G_{Coupling}$ = 0.14 kcal/mol, Figure 5.4 A), as did coupling of β_2R207 with β_2F200 on Y97A background ($\Delta\Delta G_{Coupling}$ = 0.21kcal/mol, Figure 5.4 B). These coupling energies indicate that the presence of both β_2Y97 and β_2F200 is necessary for β_2R207's participation in the ternary complex. On the other hand, the presence of β_2R207 is not absolutely necessary for the interaction between β_2Y97 and β_2F200, despite a slight reduction in coupling energy.

Coupling between β_2R207, β_2F200, and β_2Y97 mediates GABA binding

While $EC_{50\text{-}GABA}$ is a useful parameter for driving double-mutant cycle analysis, it represents a complex interaction between several microscopic processes (i.e. ligand binding/unbinding, channel opening/closing, desensitization/resensitization) (Colquhoun, 1998; Gleitsman et al., 2008). Therefore, we thought it would be informative to directly measure the GABA binding rate ($k_{on\text{-}GABA}$) for each construct and repeat double-mutant cycle analysis using this microscopic parameter.

$k_{on\text{-}GABA}$ was measured as previously described by Jones et al. (2001). Briefly, this process first involves determining the binding rate for a competitive antagonist, in this case SR-95531. Once the binding rate for SR-95531 ($k_{on\text{-}SR}$) is obtained, the binding rate of GABA can be determined by performing an experiment in which GABA and SR-

95531 are co-applied, known as a race experiment. The resulting co-application current is compared to the current evoked by application of GABA alone. The extent to which the peak current is reduced by the presence of antagonist depends on the relative binding rates of the two compounds and the relative concentrations available. Since $k_{on\text{-}SR}$ has been determined by antagonist unbinding experiment, $k_{on\text{-}GABA}$ can be calculated as $k_{on\text{-}GABA}$ = [SR-95531] $k_{on\text{-}SR}$/([GABA](1/I_{race} -1)) (Jones et al., 1998). I_{race} is the ratio of the peak response of co-application to the peak response of GABA alone.

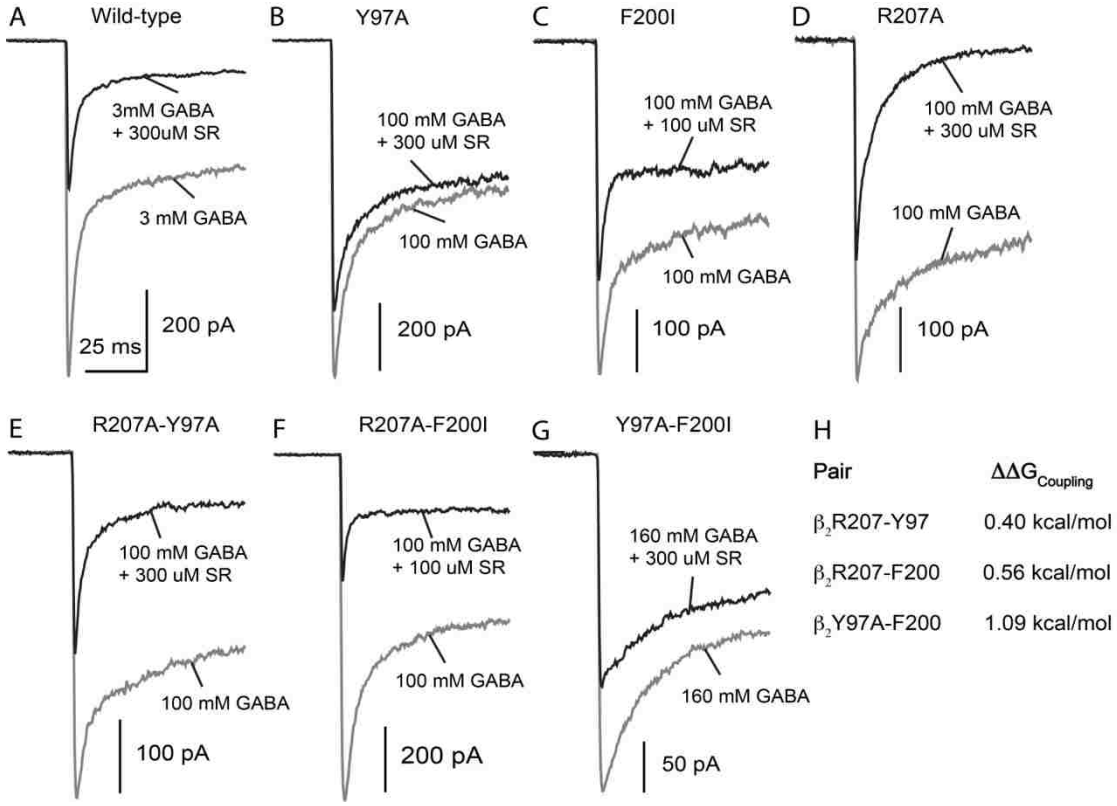

Figure 5.5. Functional coupling between β_2Y97, β_2F200, and β_2R207 at the microkinetic level ($k_{on\text{-}GABA}$). A-G) Sample raw traces recorded from race experiments. Solution exchange protocol was designed to alternate between control (only GABA, 500ms, gray) and test (GABA and SR-95531 simultaneously, 500ms, black) every 15 seconds. The known concentrations of GABA and SR and the ratio of GABA+SR : GABA only (I_{Race}) were used to calculate $k_{on\text{-}GABA}$ (see methods). H) Summary of the coupling energies determined from applying the $k_{on\text{-}GABA}$ values to double mutant cycle analysis.

The effects of each single mutant and double mutant receptor on the kinetics of SR-95531 and $k_{on\text{-}GABA}$ are summarized in Table 5.2. Alanine substitution at β_2R207 had no effect on $K_{D\text{-}SR}$. On the other hand, mutation of β_2F200 and β_2Y97 strongly affected SR-95531 affinity causing 55 and 20-fold increases in $K_{D\text{-}SR}$ respectively. This result supports the idea that β_2Y97 and β_2F200 are a tightly coupled functional group. Results from application of the $k_{on\text{-}GABA}$ values to double-mutant cycle analysis generally agreed with those seen from $EC_{50\text{-}GABA}$ (Figure 5.5). β_2Y97 and β_2F200 remain coupled ($\Delta\Delta G_{Coupling}$ = 1.09 kcal/mol), as do β_2R207 and β_2F200 ($\Delta\Delta G_{Coupling}$ = 0.56 kcal/mol). The coupling energy for β_2R207 and β_2Y97 dropped slightly below 0.5 kcal/mol ($\Delta\Delta G_{Coupling}$ = 0.40 kcal/mol) but is high enough that a potential interaction that mediates GABA binding remains possible. Because these results show that the identified ternary interaction mediates GABA binding, it is likely that the interaction exists in the unbound state of the receptor.

Table 5.2: Summary of results from antagonist unbinding and race experiments

	$K_{D\text{-}SR}$ (μM)	$k_{off\text{-}SR}$ (s^{-1})	$k_{on\text{-}SR}$ ($M^{-1}s^{-1}$)	$k_{on\text{-}GABA}$ ($M^{-1}s^{-1}$)	$\Delta\Delta G_{Coupling}$ (kcal/mol)
Wild-type	0.14	15.9 ± 0.8	$1.14 \pm 0.10 \times 10^8$	$7.40 \pm 0.40 \times 10^6$	--
Y97A	7.68	832.1 ± 91.5	$1.08 \pm 0.12 \times 10^8$	$2.17 \pm 0.11 \times 10^6$	--
F200I	2.79	331.0 ± 34.6	$1.19 \pm 0.12 \times 10^8$	$2.85 \pm 0.14 \times 10^5$	--
R207A	0.13	22.7 ± 3.6	$1.71 \pm 0.27 \times 10^8$	$9.16 \pm 0.35 \times 10^5$	--
Y97A-F200I	8.79	1159.5 ± 159	$1.32 \pm 0.18 \times 10^8$	$5.39 \pm 0.41 \times 10^5$	1.09
R207A-Y97A	0.97	151.7 ± 44.9	$1.57 \pm 0.46 \times 10^8$	$5.30 \pm 0.63 \times 10^5$	0.40
R207A-F200I	2.87	394.2 ± 56.2	$1.37 \pm 0.20 \times 10^8$	$9.28 \pm 0.46 \times 10^4$	0.56

Discussion

Cation-π bonding has been demonstrated to be a universal structural motif in proteins. In a cation-π bond the π orbital electrons from aromatic amino acid side chain (Trp, Tyr, Phe) interact with a cation. The cation may be provided by a basic residue (Arg, Lys, His) on the same subunit as the aromatic residue (Gallivan and Dougherty, 1999), a basic residue from a different subunit (Crowley and Golovin, 2005), or a positively charged exogenous ligand (Zacharias and Dougherty, 2002). Cation-π bonds have been demonstrated to be key players in ligand binding for many, if not all, members of the LGIC family (Zhong et al., 1998; Beene et al., 2002; Pless et al., 2008).

At least five aromatic residues from the $GABA_A$ receptor (α_1F65, β_2Y97, β_2Y157, β_2F200, and β_2Y205) have been implicated in ligand binding (Sigel et al., 1992; Boileau et al., 1999; Boileau et al., 2002; Amin and Weiss, 1993; Wagner and Czajkowski, 2001). Padgett et al. (2007) demonstrated that one of these, β_2Y97, participates in a cation-π bond that mediates ligand binding and that α_1F65, β_2Y157, and β_2Y205 do not participate in functionally important cation-π interactions. The remaining aromatic, β_2F200, remains untested for cation-π interaction.

In this study we employed double-mutant cycle analysis to screen for possible cation-π interactions between either β_2Y97 or β_2F200 and each of the arginines present in the GABA-binding pocket (α_1R67, α_1R120, α_1R132, and β_2R207). Our results identify α_1R132 and $\beta_2$207 as potential cation-π partners for each of the aromatics, and rule out α_1R67, and α_1R120. In addition, a strong and consistent coupling was identified between the two aromatics themselves, suggesting that β_2Y97 and β_2F200 directly interact.

β_2Y97 and β_2F200 as a tight aromatic pair

The clearest result from this study is that β_2Y97 and β_2F200 work together as a single functional unit. When double-mutant cycle analysis, using $EC_{50\text{-}GABA}$, was employed to test for coupling between β_2R207 and either β_2Y97 or β_2F200, the results were comparable ($\Delta\Delta G_{Coupling}$: R207/Y97 = -0.67 kcal/mol, R207/F200 = -0.56 kcal/mol). Similarly, α_1R132 was found to be equally coupled to each aromatic residue ($\Delta\Delta G_{Coupling}$: R132/Y97 = -0.35 kcal/mol, R132/F200 = -0.41 kcal/mol). These results strongly suggest that β_2Y97 and β_2F200 work in concert. This hypothesis is supported by the fact that the two residues are strongly coupled to each other when the mutational effects on $EC_{50\text{-}GABA}$ ($\Delta\Delta G_{Coupling}$ Y97/F200 = -1.72 kcal/mol), $k_{on\text{-}GABA}$ ($\Delta\Delta G_{Coupling}$ Y97/F200 = 1.09 kcal/mol) and $k_{off\text{-}SR}$ ($\Delta\Delta G_{Coupling}$ = -1.59 kcal/mol) are used to drive the double-mutant cycle analysis. Furthermore, mutation of either residue had qualitatively similar effects on every parameter we measured: $EC_{50\text{-}GABA}$, $k_{off\text{-}SR}$, $k_{on\text{-}SR}$, $k_{on\text{-}GABA}$, and the time courses of macroscopic deactivation and desensitization.

Another line of evidence supporting a tight interaction between β_2Y97 and β_2F200 comes from the fact that coupling between β_2R207 and each aromatic was completely abolished when tested in a background where the other aromatic residue had been mutated. In other words, whatever interaction β_2R207 might share with β_2Y97 disappears when β_2F200 is mutated, and whatever interaction β_2R207 shares with β_2F200 disappears when β_2Y97 is mutated. Conversely, the coupling energy between β_2Y97 and β_2F200 is only modestly reduced by mutation of β_2R207.

Taken altogether, these results suggest that β_2Y97 and β_2F200 form a single functional unit, that then interacts with β_2R207 and, possibly, α_1R132. It is possible that

these interactions between β_2R207 and α_1R132 and the Y97/F200 complex occur via a cation-π bond(s) with either aromatic, but it is also possible that the interaction of β_2Y97 and β_2F200 positions other elements (i.e. neighboring side chains or backbone carbonyls) for interactions with either of the arginines.

The role of arginines from the α_1 subunit

Of the arginines from the α_1 subunit that were tested, we found that α_1R132 can potentially interact with either β_2Y97 or β_2F200 but that neither α_1R67 nor α_1R120 is likely to participate in cation-π interactions with either of the two aromatics. When expressed as a single mutation, α_1R132A has relatively moderate effects on $EC_{50\text{-}GABA}$ (4-fold increase) and the weighted time constant of deactivation (5-fold decrease), suggesting that it might act to help position the more critical Y97/F200 pair. The lack of an interaction between α_1R120 and the aromatics is not particularly surprising. According to the homology model, α_1R120 is relatively distant from the aromatics and it has been proposed to participate in a state-dependent inter-subunit salt bridge with β_2D163 (Cromer et al., 2002; Laha and Wagner, 2011). The fact that α_1R67 does not interact with the aromatics examined here but is located nearby and, on its own, severely affects GABA affinity suggest that it plays a critical role in GABA binding that is independent of the Y97/F200 pair.

Another interesting result from this study is that there appears to be a general role for all arginines on the α_1 subunit in the process of macroscopic desensitization. R67A, R120A, and R132A receptors all display slowed desensitization with weighted time constants about twice as long as seen in wild-type receptors (Table 5.1). This effect has previously been reported for α_1R120A$\beta_2\gamma_2$ receptors (Laha and Wagner, 2011) but is

demonstrated for the first time here for α_1R132 and α_1R67. Desensitization of $GABA_A$ receptors is a macro-molecular phenomenon that depends on inter-subunit communications (Goldschen-Ohm et al., 2010). As arginine side chains are very long and charged, it is easy to envision them as providing communication links between subunits. In fact, an inter-subunit salt bridge has already been proposed for α_1R120 (Cromer et al 2002, Laha and Wagner, 2011) and here we demonstrate that α_1R132 may participate in an inter-subunit cation-π bond.

VI. DISCUSSION AND CONCLUSION

The studies documented in this dissertation were designed to further our understanding of the architecture of the GABA-binding site on the $GABA_A$ receptor. A refined blueprint of the GABA-binding pocket would involve identifying the various interactions (i.e. inter-subunit interactions, intra-subunit interactions, and interactions with GABA) that exist in the binding pocket. This refined understanding is necessary toward building a more complete biophysical model of the $GABA_A$ receptor. As such, the main approach used here involves reviewing the current best model of the GABA-binding pocket, verifying current elements and identifying new elements involved in $GABA_A$ receptor function, especially those involved in the ligand-receptor interaction, and incorporating new data to achieve a refined and more detailed model.

Implications of functional effects found upon mutation of binding pocket arginines

Due to the nature of their side chain, arginines have been found to play many important roles in protein structure and function. The arginine side chain contains a guanidinium group that makes it the most polar side chain in proteins. This guanidinium group allows the arginine side chain to participate in up to 5 hydrogen bonds. This positively charged side chain is also capable of participating in salt bridge and cation-π interactions. These various bonds enable the arginine side chain to interact with such elements as negatively charged substrates and cofactors, other neighboring side chains (i.e. aspartate, glutamate, and aromatics), and backbone carbonyls (Borders et al., 1994). Due to the diversity of various elements that can interact with an arginine side chain, it is not difficult to envision different arginines on the same protein play rather different roles or a single arginine being involved in multiple functionally diverse molecular interactions. For example, one arginine can form hydrogen bonds with the backbone

carbonyl to stabilize protein tertiary structure, while another arginine can form a salt bridge with a negatively charged substrate (i.e. substrate-enzyme interaction) or even a negatively charged ligand (i.e. ligand-receptor interaction). In cl-LGICs, the roles of arginines are, therefore, diverse and important.

Previous site-directed mutagenesis studies in which α_1R67 and β_2R207 were mutated to cysteines and alanines suggested that these two arginine residues are positioned at the GABA-binding pocket and play important roles in the binding of GABA (Boileau et al., 1999; Holden and Czajkowski, 2002; Wagner et al., 2004) but no specific information about their interactions with either GABA or other binding pocket structures have been identified. Here we sought to understand how these arginines contribute to the structure and operation of the $GABA_A$ receptor's binding pocket. We addressed this question by mutating each arginine to a series of amino acid residues and measuring changes in the function of the $GABA_A$ receptor. We quantified the effects of a mutation on receptor function by measuring the alterations in concentration response (i.e. affinity for GABA) and macroscopic kinetic parameters, such as desensitization and deactivation, from which we may draw binding and gating implications. In addition, when possible we also directly measured the effects on the GABA binding rate, $k_{on\text{-}GABA}$, to provide more precise quantification of how much a particular residue influences GABA binding.

As documented in Chapter III, each mutation made at α_1R67 significantly alters the GABA-elicited response of the $GABA_A$ receptor regardless of side chain chemistry. Every substitution that did not disrupt functional expression caused measurable severe and similar rightward shifts in $EC_{50\text{-}GABA}$, acceleration of the rate of deactivation, and slowing of desensitization. These observations led to a logical conclusion that the

existence of an arginine at position 67 of α_1 subunit is specifically critical for proper function of $GABA_A$ receptor.

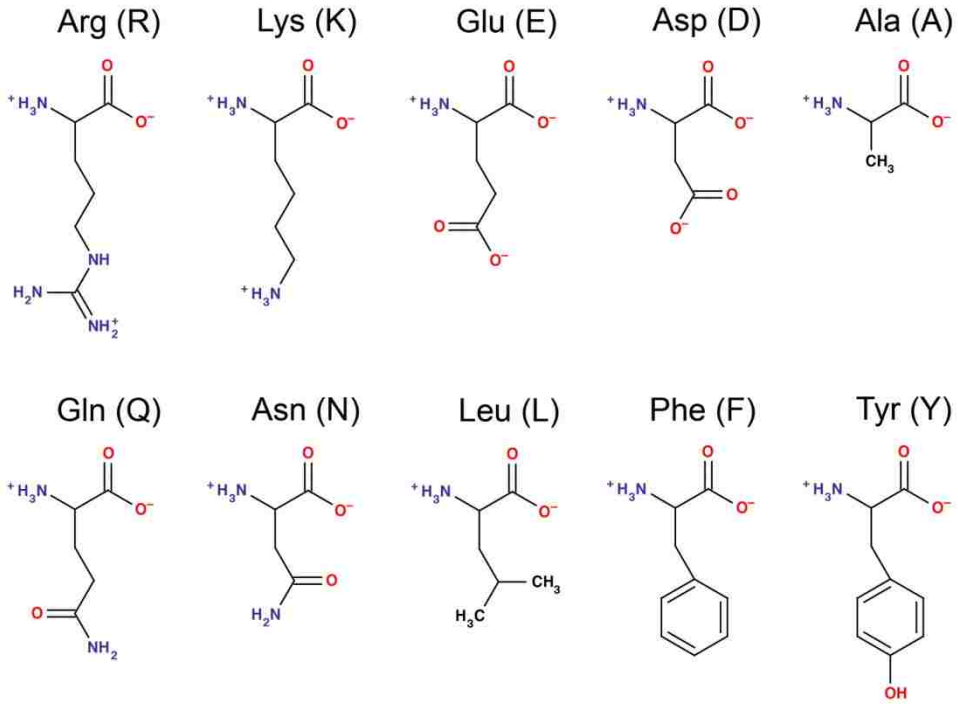

Figure 6.1 A selection of amino acids mutagenically introduced at α_1R67 and β_2R207.

Comparing the effects of mutating α_1R67 to different residues revealed the specific criteria or properties a residue must possess in order to facilitate proper receptor function at position 67 of the α_1 subunit. Individually, the mutations to K, E, D, Q, N, L, F, Y, and A (Figure 6.1) all significantly disrupted receptor function with the small non-polar alanine having the relatively mildest effects, the larger polar residues (lysine, glutamate, glutamine) having greater effects, and smaller polar residues (aspartate and asparagine) and larger hydrophobic residues (leucine, phenylalanine, and tyrosine) almost completely eradicating GABA-evoked current. It is notable that the long polar side chains (K, E, Q) had similar effects on function regardless of charge, with even the "conservative" lysine substitution having a greater effect on function than alanine

substitution did. There is something very specific about the nature of the arginine side chain (and perhaps it's ability to form multiple hydrogen bonds) that is required for GABA binding such that virtual removal of the side chain (alanine substitution) is less disruptive than any other substitution made. It is also possible that alanine substitution introduces a void that may allow a neighboring side chain to swing in and compensate.

Additionally, double mutant cycle analysis (Chapter V) identified no binding pocket residue that is functionally coupled to α_1R67. Though the number of amino acid pairs tested in chapter V was by no mean exhaustive, every double mutant containing α_1R67 tested caused near-ablation of $GABA_A$ receptor function. Such severe double mutant effect and the strong effect of mutating α_1R67 alone (Chapter III) on both GABA binding, desensitization, and even expression signifies multiple important roles of α_1R67 in GABA-receptor interaction. With the given results, it is tempting to propose that α_1R67 coordinates the carboxyl group of GABA. Indeed we will argue for this interpretation. However, it should be noted that α_1R67 is not the only arginine at the binding pocket. Other arginines must also be considered. It is nevertheless clear that α_1R67 plays a singularly important role in the function of the $GABA_A$ receptor.

Interestingly, this arginine residue is conserved between all six isoforms of $GABA_A$ α subunit and this conservation extends to other receptors from the cl-LGIC family (Chapter I). For example, mutating the arginine at this position in the homopentameric $GABA_A$ ρ receptor (R104) to alanine or glutamate results in a more than 10,000-fold increase in $EC_{50\text{-}GABA}$ (Harrison and Lummis, 2006). Also, in the homopentameric α_1 glycine receptor, mutating the equivalent arginine (R65) to lysine or alanine causes a 215-fold or a >1,300-fold increase in EC_{50} of glycine respectively

(Grudzinska et al., 2005). R104 and R65 have both been proposed to be involved in proper docking of the carboxyl end of GABA and glycine to $GABA_A$ ρ receptor and glycine receptor respectively.

Relative to the α_1R67 mutations, the β_2R207 mutations have smaller effects on $EC_{50\text{-}GABA}$ and the rate of deactivation, and do not affect desensitization or activation rates at all. In other words, β_2R207 is likely to have little or no effect on GABA receptor gating and plays a less primary role in GABA binding than α_1R67. Additionally, unlike α_1R67, β_2R207 (loop C) is not as conserved among cl-LGICs, being present only in the $GABA_A$ receptor β and ρ subunits. When R249, the aligned residue in $GABA_A$ ρ receptor, is mutated to alanine or lysine the $EC_{50\text{-}GABA}$ was increased by 15- or 28-fold respectively (Harrison and Lummis, 2006). These values are comparable to changes seen when mutating β_2R207 of the $\alpha_1\beta_2$ $GABA_A$ receptor.

Combining the difference in conservation and the variety of interactions that an arginine side chain possesses, one can argue that the different effects seen in mutating α_1R67 and β_2R207 reflect the dissimilar interactions they partake in. This notion is consistent with current understanding of two other $GABA_A$ receptor arginines (α_1R120, α_1R132). Laha and Wagner (2011) reported that α_1R120 participates in a state-dependent inter-subunit salt bridge with β_2D163 of the $GABA_A$ receptor (i.e. energetically coupled during GABA unbinding). Like α_1R67, when α_1R120 was mutated to alanine and co-expressed with $\beta_{2\text{-}GKER}$ (Laha and Wagner, 2011) or with both $\beta_{2\text{-}GKER}$ and γ_2, a significant increase in macroscopic deactivation rate and decrease in macroscopic desensitization rate were observed (Table 5.1). As with α_1R67, α_1R120 is conserved across most of the cl-LGIC family. Functionally, however, its contribution diverges

between different receptors. This arginine in $GABA_A$ ρ receptor (R158) is thought to be critical for GABA binding but not as important in glycine receptor (R119) (Harrison and Lummis, 2006; Grudzinska et al., 2005).

As seen with α_1R67 and α_1R120, mutation of α_1R132 to alanine slowed desensitization effects and accelerated deactivation (Table 5.1). The effect on desensitization was identical to that seen for α_1R67, α_1R120 but the effect on deactivation was noticeably less severe. It is possible that the increase in deactivation rate of α_1R132 mutation is mainly due to reduced desensitization (Jones and Westbrook, 1995) whereas the greater speeding of deactivation seen for α_1R67, α_1R120 is may be due to both a reduced rate of desensitization and an increased rate of unbinding. Again, multiple functional roles for these particular arginines seem apparent.

To put it all in perspective, point mutations made to the four binding pocket arginines (α_1R67, α_1R120, α_1R132, β_2R207) cause different degrees of increment in $EC_{50\text{-}GABA}$ of the $GABA_A$ receptor. Many of these changes in EC_{50} value have also been recorded in other anionic cl-LGICs (homopentameric $GABA_A$ ρ and glycine receptors). Positionally, α_1R67, α_1R120, and α_1R132 are conserved among anionic cl-LGICs with α_1R67 also being relatively conserved in cationic cl-LGICs (i.e. an arginine in 5-HT_3A receptors and a lysine in nACh receptors), while β_2R207 is not conserved in non-GABA receptors. Here, we also looked at the mutational effects of these arginines on macroscopic kinetics parameters of $GABA_A$ receptor. While β_2R207 mutations only cause significant increase in the rate of macroscopic deactivation, α_1R67, α_1R120, and α_1R132 mutations cause both significant increase in macroscopic deactivation rate and significant decrease in macroscopic desensitization rate. Desensitization effects indicate

that the α_1 arginines, which line the complementary (-) face of the binding pocket, contribute not only to binding but also to other mechanistic steps (i.e. microscopic transitions) that underlie $GABA_A$ receptor's response to GABA.

The ligands that bind anionic cl-LGICs, GABA and glycine are similar in that they are zwitterions, containing a positively charged amino end and a negatively charged carboxyl end. The presence of a carboxyl group sets GABA and glycine apart from other endogenous cl-LGIC ligands (acetylcholine, serotonin). This difference in ligand structure may be a source for the differences in the specific details of ligand-receptor interactions among cl-LGICs.

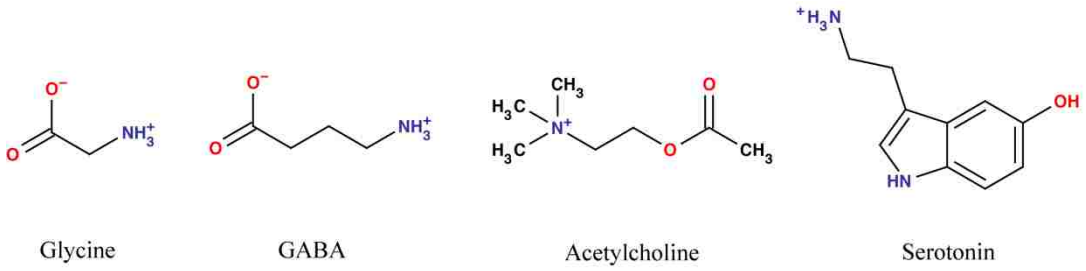

Figure 6.2 Endogenous ligands of cl-LGICs

However, one feature shared by the endogenous ligands (acetylcholine, GABA, glycine, and serotonin) of all members of the cl-LGIC family is a positively charged nitrogen (Figure 6.2). In early studies, the localization of several negatively charged amino acid side chains at the binding pocket led to the reasonable prediction that the positive charge of the ligand would be stabilized by an acidic amino acid residue (aspartate or glutamate). However, data have accumulated to indicate that this is not the likely scenario. Particularly, the idea of acidic residues anchoring the positive end of ligand was initially challenged when the three-dimensional structure of acetylcholinesterase, an enzyme that binds and hydrolyzes acetylcholine, was resolved at

2.8 Å (Sussman et al., 1991). This structure showed that the quaternary ammonium moiety of acetylcholine was bound, not to a negatively charged site, but to a pocket consisting of aromatic residues. Later crystallography studies showed similar results in AChBP and nAChR (Brejc et al., 2001; Celie et al., 2004; Dellisanti et al., 2007). Since then, evidence has been accumulating to show that aromatic residues are involved in the agonist binding process of the cl-LGICs. Thus, as arginine residues clearly play important roles in proper function of $GABA_A$ receptor, especially with respect to GABA-receptor interaction, aromatic residues, too, play no less important roles.

Implications of functional effects found upon mutation of binding pocket aromatic residues

It has been demonstrated, in many previous studies, that the "aromatic box" amino acid residues play important roles in ligand binding. These aromatic residues are known to cluster at or near the binding pockets of cl-LGICs, and it is hypothesized that they provide a hydrophobic barrier that excludes water from the binding pocket to facilitate docking of ligand (Padgett et al., 2007). For example, in AChBP and all cl-LGICs, at least one of these aromatic residues has been identified to participate in a cation-π interaction that directly correlates to ligand affinity (Zhong et al., 1998; Beene et al., 2004; Lummis et al., 2005; Padgett et al., 2007; Pless et al., 2008). In the $GABA_A$ receptor, cation-π bonding has been established for β_2Y97, whose cation partner is suggested to be the amino end of the GABA (Padgett et al., 2007). For the remaining aromatic box residues of the $GABA_A$ receptor that were demonstrated not to participate in a cation-π bond mediating binding (α_1F65, β_2Y157, β_2Y205) or not tested (β_2F200), relevant interactions in which they participate remain to be explored. Therefore, the

experiments, documented in chapter IV and chapter V, were designed to home in on the potential partners of these aromatics residues.

One of the goals of the experiments presented in chapters IV and V was to assess the relative significance of the hydroxyl group from each of the three tyrosines at the GABA-binding pocket by mutating each tyrosine to a phenylalanine and measuring the direct effects on $k_{on\text{-}GABA}$. This approach provided direct quantification for the contribution of these hydroxylated aromatics in GABA binding. At the same time, mutating these tyrosines to alanines confirmed the importance of their aromaticity in maintaining the integrity of the hydrophobic barrier. Then, the double mutant cycle analyses (Chapter V) were used to subsequently screen the binding-pocket arginines for possible cation partner of β_2Y97, a tyrosine whose hydroxyl group plays no significant role. Binding pocket arginines were also tested for possible interactions with β_2F200, a loop C aromatic whose significance might have been overlooked.

The results from chapter IV show that the hydroxyl group on β_2Y97 makes no significant contribution, while the hydroxyl groups on β_2Y157 and β_2Y205 greatly influence binding rate of GABA. This difference is relevant on two counts. First, it is consistent with the observation that mutating β_2Y97 has a quantitatively smaller effect on $EC_{50\text{-}GABA}$. Second, the benzene ring of β_2Y97, not the hydroxyl group, has previously been demonstrated to participate in interaction critical for ligand binding (Padgett et al., 2007). On top of that, the benzene rings of β_2Y157 and β_2Y205 were previously tested negative for binding-determining cation-π interactions (Padgett et al. 2007).

It is interesting that the mutations of β_2Y97 (β_2Y97A, β_2Y97F) do not result in very big changes in $k_{on\text{-}GABA}$ (Table 4.2). This small change on $k_{on\text{-}GABA}$ contradicts the

role of β_2Y97 in ligand binding, if previous proposal were entirely true. Padgett et al. (2007) proposed a ligand-receptor interacting model in which the amino group of GABA forms cation-π bond with the aromatic face of β_2Y97. If this model were entirely accurate, removing the aromatic at position 97 of β_2 (i.e. β_2Y97A) would be expected to have a more severe impairment in receptor's ability to bind GABA. Our results are consistent with this prediction in that mutating β_2Y97 to alanine reduces $k_{on\text{-}GABA}$ by 3-fold and that β_2Y97F causes no significant change in $k_{on\text{-}GABA}$. It is clear that the aromatic component of β_2Y97 is important for GABA binding. It is possible that the consequence of Y97A has more to do with the GABA unbinding rate ($k_{off\text{-}GABA}$) than $k_{on\text{-}GABA}$. Perhaps, the role played by β_2Y97 in GABA binding is less direct than previously thought.

Severe impairment in the receptor's ability to bind GABA was recorded for a previously overlooked aromatic residue (β_2F200) on the principle face of the binding pocket. We found that mutating β_2F200 to a non-aromatic hydrophobic residue (β_2F200I) causes a 26-fold decrease in $k_{on\text{-}GABA}$. Also, through utilizing $k_{on\text{-}GABA}$-based double mutant cycle analysis, we discovered that the effects of mutating β_2Y97 and β_2F200 on $k_{on\text{-}GABA}$, though different, are not independent (i.e. their simultaneous mutation does not cause an additive effect). Significant energetic coupling indicates that they are tightly linked in function. We, therefore, propose that they are structurally linked.

Double mutant cycle analysis also identified that β_2Y97 and β_2F200 are individually coupled to β_2R207 to the same degree. β_2Y97 and β_2F200 are also weakly coupled (i.e. low coupling energy) to β_2R132. Two other binding pocket arginines (α_1R67, α_1R120) were found not coupled to either β_2Y97 or β_2F200. Thus far, there are two distinct groups of binding pocket arginines – those functionally coupled to β_2Y97

and β_2F200 (α_1R132 and β_2R207) and those functionally independent from β_2Y97 and β_2F200 (α_1R67 and α_1R120). As functional coupling may reflect interaction (Kash et al., 2003), these findings deserve careful considerations in refining the model of GABA-receptor interaction.

The effects of mutating β_2Y157 and β_2Y205 are consistent with those seen in an earlier study, which suggested that β_2Y157 and β_2Y205 are involved in GABA binding. When these residues were conservatively substituted by a phenylalanine, the receptors had a much-reduced response to GABA; $EC_{50\text{-}GABA}$ was increased by 50-fold, compared to normal (Amin and Weiss, 1993). The same study also reported that an even further reduction in GABA sensitivity resulted when either tyrosine residues were mutated to such non-aromatic amino acids as serine and asparagines, hinting that these tyrosine side chains may be bifunctional. In other words, both the aromatic ring and the hydroxyl group of β_2Y157 and β_2Y205 hold relevant roles in GABA-receptor relationship. For example, it is possible that while the aromaticity of their side chain helps maintain the integrity of the hydrophobic barrier, the hydroxyl group forms a hydrogen bond that facilitates GABA binding. The logical undertaking that follows would be to identify hydrogen bond partners for these tyrosines. Though this would have been a logical endeavor, it was not the most efficient, for the scope of this dissertation. Particularly, the pool of potential hydrogen bond partners of β_2Y157 and β_2Y205 is larger and less defined than the pool of potential cation partners of β_2Y97 and β_2F200 to be explored effectively during the duration of this dissertation.

Nevertheless, having determined that the hydroxyl groups of β_2Y157 and β_2Y205 participate in GABA binding, we would now be more confident in assigning potential

interactions for them. Also, useful insights can be drawn from previous models of $GABA_A$ receptor and other cl-LGICs' binding pocket. In the $GABA_A$ receptor binding pocket model synthesized by Padgett et al. (2007), β_2Y157 was suggested to interact via hydrogen bond with backbone -NH of α_1T130, an interaction that was also suggested by the previous homology model generated by Cromer et al. (2002). In both models, however, the orientation of β_2Y205 was not clear; Cromer et al. (2002) only generally stated that β_2Y205 and two other residues, β_2T160 and β_2T202, could participate in some sort of hydrogen bond network.

Attempts were made to study one other aromatic box residue, α_1F65. When this residue was mutated to alanine, GABA-induced response of the receptor was not sufficiently robust for meaningful analysis; mostly, GABA-induced response was near-ablated. When mutated to a different hydrophobic residue (α_1F65C), by Boileau et al. (1999), a 70-fold increase in $EC_{50\text{-}GABA}$ was observed. Apparently, the presence of a phenylalanine at this position is quite critical. However, the lack of characterizable response for α_1F65A made it impossible to examine how α_1F65 contributes to receptor function and how it may interact with the surrounding residues. We did not envision new information to arise from mutating α_1F65 to other residues. Plus, Padgett et al. (2007) demonstrated that α_1F65 does not participate in cation-π bond. Therefore, this aromatic residue was not studied any further.

A model of the binding pocket centered on GABA-receptor interaction

The current best model of the $GABA_A$ receptor's ligand-binding pocket is derived from the homology model that has been developed based on the crystal structure of the

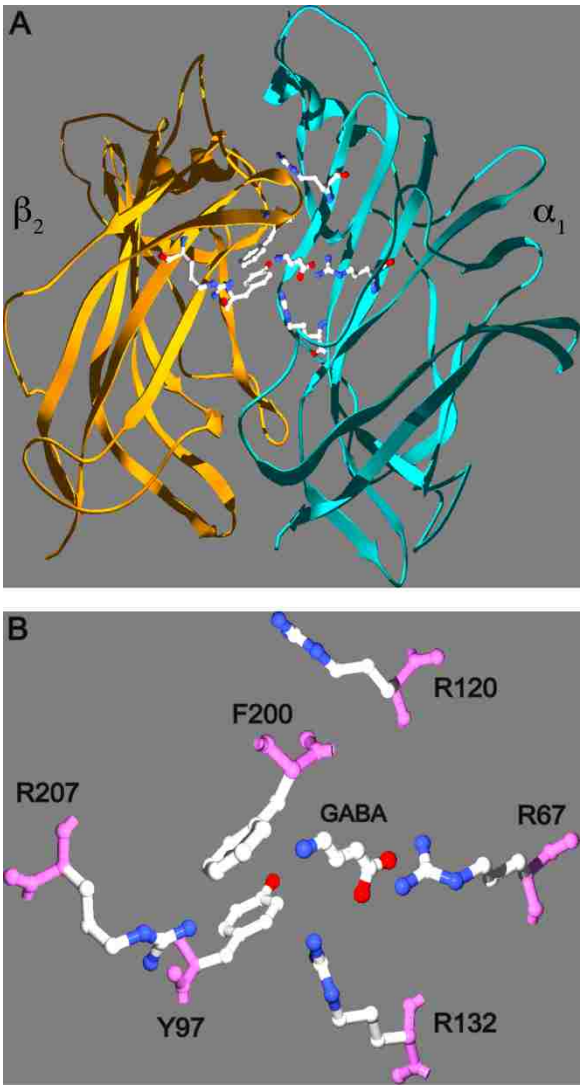

Figure 6.3 Interpretation of our results at the GABA binding pocket: a model of GABA binding pocket based on the homology structure proposed by Cromer et al. (2002). A) Side-view of β/α interface showing the side chains of all the residues mutated in this study. GABA has been manually placed in its proposed orientation between R67 and F200/Y97. B) Zoomed view of panel A with backbone removed. The alpha carbon of each residue has not been moved from its original position in the homology model (Cromer et al, 2002). Several of the side chains have been rotated to alternate stable positions (using the mutate function in Swiss PDB viewer). The side chain of F200 has been slightly rotated using the torsion function in Swiss PDB viewer (see text).

molluscan AChBP (Brejc et al., 2001; Cromer et al., 2002; O'mara et al., 2005) combined with the results of artificial amino acid substitution studied from the Lummis lab (Padgett et al., 2007; Harrison and Lummis, 2006), and SCAM and kinetic studies from the Czajkowski and Jones labs (Boileau et al, 1999; Wagner and Czajkowski, 2001; Boileau et al., 2002; Holden and Czajkowski, 2002; Wagner et al., 2004). In this model (described in Padgett et al., 2007) the amino moiety of GABA is coordinated by a cation-π interaction with β_2Y97 and the carboxyl moiety coordinated by an interaction with either β_2R207 or α_1R67 (or possibly both). Here, we incorporate the results of this

dissertation to modify and add significant detail to this model. The model proposed here includes the following features: a hydrophobic interaction between β_2Y97 and β_2F200, an inter-subunit cation-π interaction between β_2Y97 and α_1R132, a cation-π interaction between the amino group of GABA and β_2F200, hydrogen bond(s) between the carboxyl end of GABA and the guanidinium group of α_1R67, and an interaction between the side chain of β_2R207 and the backbone carbonyl of β_2Y97 (Figure 6.3). The rationale for each feature is discussed below.

β_2Y97/β_2F200/GABA

One major finding from our study is that β_2Y97 and β_2F200 display a tight functional coupling that facilitates binding of GABA. We propose that this tight coupling is underlied by a direct interaction between the two aromatic residues. Our rationale includes several consistent observations. First, both β_2Y97 and β_2F200 were found energetically coupled to β_2R207 (i.e. similar coupling energies). Second, β_2Y97 and β_2F200 are both coupled to α_1R132 with similar but weak coupling energies. Third, in order for β_2Y97 to be functionally coupled to β_2R207, β_2F200 must be intact and vice versa (see triple mutant cycles in Chapter V). Fourth, both β_2Y97 and β_2F200 show no coupling to either α_1R67 or α_1R120. Lastly, β_2Y97 and β_2F200 are energetically coupled for every parameter we considered. For example, β_2Y97 and β_2F200 are coupled when measurements of $EC_{50\text{-}GABA}$, $k_{on\text{-}GABA}$, and $k_{off\text{-}SR}$ were used to drive double mutant cycle analysis.

According to the homology model built by Cromer et al. (2002), the distance between the aromatic rings of β_2Y97 and β_2F200 ranges from 6-9 angstroms when the

side chains are rotated through their stable conformations. This distance is too great to support direct aromatic-aromatic interaction and may appear to be evidence against the tight Y97/F200 interaction proposed here. However, the nature of aromatic-aromatic interaction is still poorly understood. The three lowest energy models are depicted in figure 6.4. Though aromatic-aromatic interactions are commonly thought to be "stacking", it is actually more common to find them interacting at right angles with each other. For example, a previous study looking at aromatic interactions in proteins found that about 60 percent of aromatic side chains participate in aromatic-aromatic pairs, with the phenyl ring centroids separated by distance of 4.5-7 Å and dihedral angles around 90 degrees being the most common pairing features (Burley and Petsko, 1985). The same study also found that 80 percent of these side chains are involved in networks of three or more interacting aromatic side chains. The typical free energy contributed by each pair ranges between -0.6 and -1.3 kCal/mol, depending on how buried the pair is within the protein. Therefore, it is very likely that not only do β_2Y97 and β_2F200 interact, but also they interact at in a perpendicular manner.

β_2F200 is located at the apex of Loop C, a region that aligns very poorly with the AChBP (Cromer et al., 2002) and whose actual structure is likely to differ significantly from the AChBP structure (Ernst et al., 2003). In addition, Loop C appears to be quite flexible (Wagner and Czajkowski, 2001; Bourne et al., 2010). Therefore, we believe our results (Chapter V) have provided a new constraint on the homology model and that future versions of the model should attempt to translate the alpha carbon of β_2F200 a few angstroms so that its interaction with β_2Y97 be clearer.

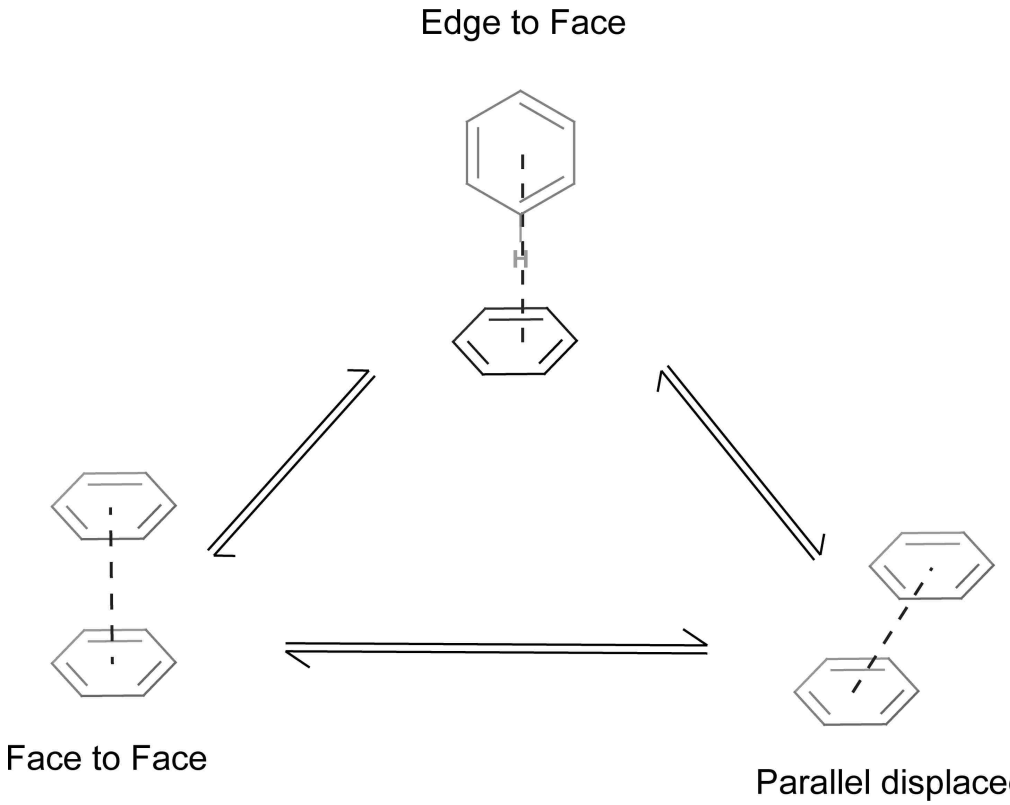

Figure 6.4 Three lowest energy benzene dimers. Two separate studies found the edge to face interaction to be the most stable (Jorgensen and Severance, 1990; Hobza et al., 1996).

The interaction between β_2Y97 and β_2F200 could leave two alternate faces available for cation-π bonding with the amino group of GABA. Because β_2F200 has significantly stronger effect on $k_{on\text{-}GABA}$, we propose that it serves as a docking point for the amino group of GABA. Plus, the flexible nature of loop C may allow it to readily change conformation upon "catching" the amino end of GABA with the aromatic face of β_2F200. This scenario leaves β_2Y97 available for potential cation-π interaction with β_2R207 or α_1R132. The homology model ideally positions α_1R132 for this interaction. Therefore, in our model we chose to depict it thusly, and show β_2R207 contributing via interaction(s) with the backbone carbonyl of β_2Y97, which it perfectly reaches according to the homology model.

A proposed ionic interaction between α_1R67 and the GABA carboxylate

Models for coordination of the carboxyl moiety of GABA have suggested a possible interaction with α_1R67 or β_2R207 (Wagner et al., 2004, Padgett et al., 2007). The main evidence for these interactions has been that mutation of either residue to alanine causes significant increases in $EC_{50\text{-}GABA}$, slowing of the GABA binding rate, and acceleration of the GABA unbinding rate. In addition, they are the only two positively charged residues located in the binding pocket that have these effects. The proposal presented here is supported by the fact that, of the four arginines tested here, mutation of α_1R67 to alanine has the largest effects $EC_{50\text{-}GABA}$. Also, previous work in our lab found that α_1R67A causes the greatest shift in both the GABA binding rate and the GABA unbinding rate (unpublished data). Furthermore, α_1R67A and β_2F200I, as single mutations, have the most severe effects on $EC_{50\text{-}GABA}$ and these effects appear fully additive in the R67A-F200I double mutant. This result supports a model in which α_1R67 and β_2F200 serve as critical and independent sites for GABA docking. Furthermore, as mentioned above, α_1R67 is conserved among cl-LGICs. Functionally, this arginine has been shown to play an important role in both glycine and $GABA_A$ ρ receptors (Grudzinska et al., 2005; Harrison and Lummis, 2006).

Perhaps, in the process of refining the model of ligand-receptor interaction, one can draw useful insights from how the same ligand interacts with distinct classes of known target proteins (i.e. transporters and enzymes). For example, insights can be gained from other proteins that bind GABA, for example. The binding site of the GABA transporter, GAT-1, contains several tryptophan residues that appear to play a crucial role in binding of GABA. One of these tryptophan residues is highly conserved among amino

acid transporters, and has been proposed to interact with the amino group of GABA (Kleinberger-Doron and Kanner, 1994). A different study looking at the interaction at the active site of GABA aminotransferase, the enzyme responsible for GABA degradation in the CNS, synthesized a model in which the carboxyl group of GABA was proposed to interact with an arginine and a lysine residue (Tone et al., 1995). While these interactions may not be identical to those in the $GABA_A$ receptor (i.e. $GABA_A$ binding pocket has no tryptophan), it is clear that distinct groups of amino acid residues coordinate the two ends of the GABA molecule. The idea of the amino end and the carboxyl end of GABA interacting with aromatic and basic residues, respectively, is consistent with the model we proposed here.

A proposed cation-π interaction between β_2Y97 and α_1R132

We propose that a cation-π interaction takes place between α_1R132 and β_2Y97. Results from double-mutant cycle analysis of $EC_{50\text{-}GABA}$ (Chapter V) indicate that β_2Y97 and β_2F200 are functionally coupled to α_1R132. Functional coupling alone is not proof of direct physical interaction. However, we believe that there is sufficient additional evidence to support this claim. Specifically, the homology model shows that α_1R132 and β_2Y97 are ideally positioned for an inter-subunit cation-π interaction and β_2Y97 is known to be involved in a cation-π interaction but the cation partner has not been identified. Other possible cation partners for β_2Y97 include α_1R67, β_2R207 and the amino moiety of GABA. Our data indicates no functional coupling between α_1R67 and β_2Y97; we argue that β_2R207 is interacting with a backbone amino group; and we propose that the amino moiety of GABA is interacting with β_2F200. Additionally, in models that describe binding of glycine to GlyR and GABA to $GABA_A$ ρ receptors, arginines that align with

α_1R132 are suggested to be coordinated by an aromatic side chain (Grudzinska et al., 2005; Harrison and Lummis, 2006). Finally, whether the arginine at this position is mutated in $GABA_A$ αβ type, $GABA_A$ ρ type, or GlyR, generally mild effects on EC_{50} values are seen; such is indicative of a residue that may act as an accessory (helping to position a binding element) as opposed to the large effects one would expect if a residue were responsible for direct coordination of the ligand.

A proposed ionic interaction between β_2R207 and the backbone carbonyl of β_2Y97

As a single mutant, β_2R207A causes the least change in $EC_{50\text{-}GABA}$ compared to β_2Y97A and β_2F200A or β_2F200I (β_2R207A: 10-fold increase; β_2Y97A: 15-fold increase; β_2F200A: 173-fold increase; F200I: 89-fold increase). However, double mutant cycle analysis showed that β_2R207 is functionally coupled to β_2Y97 and β_2F200. Triple mutant cycle analysis (Figure 5.4) further revealed that β_2R207 is actually coupled to the β_2Y97/β_2F200 pair. In the context of "functional coupling reflects interaction", both β_2Y97 and β_2F200 are required for proper interaction with β_2R207. Regarding the influence on $k_{on\text{-}GABA}$, β_2R207A causes less reduction of $k_{on\text{-}GABA}$ compared to either α_1R67A (unpublished data) or β_2F200I (Table 5.2). Combining the observation that β_2R207 is not required to maintain the interaction between β_2Y97 and β_2F200 with the published homology model, in which β_2R207 is favorably positioned for backbone interaction (Cromer et al., 2002), we propose that the role played by β_2R207 is to augment the function the β_2Y97/β_2F200 pair. Specifically, we believe that β_2R207 interacts with the backbone carbonyl of β_2Y97, positioning the β_2Y97/β_2F200 pair for

proper interaction with GABA's amino group. Such a role would also explain for the reduction in $k_{on\text{-}GABA}$ seen with β_2R207 (Table 5.2).

All in all, the model proposed is consistent with the bulk of results to date. Many of the elements described provide a solid basis on which further investigations can be founded. I acknowledge that some of the details provided for the model remain speculative. Nevertheless, this work has lead to an important refinement in the model describing the interaction between the $GABA_A$ receptor and its endogenous ligand, GABA, and has moved us a major step closer to a full understanding of the GABA-$GABA_A$ receptor interaction.

BIBLIOGRAPHY

Ackers KG and Smith RF (1986) Resolving pathways of functional coupling within protein assemblies by site-specific structural perturbation. *Biophys J* **49**:155-165.

Adkins CE, Pillai GV, Kerby J, Bonnert TP, Haldon C, McKernan RM, Gonzalez JE, Oades K, Whiting PJ and Simpson PB (2001) α4β3δ GABAA receptors characterized by fluorescence resonance energy transfer-derived measurements of membrane potential. *J Biol Chem* **276**:38934-39.

Aguayo LG (1990) Ethanol potentiates the GABAA-activated Cl- current in mouse hippocampal and cortical neurons. *Eur J Pharmacol* **187**:127-130.

Aguayo L.G, Peoples RW, Yeh HH and Yevenes GE (2002) $GABA_A$ receptors as molecular sites of ethanol action. Direct or indirect actions? *Curr Top Med Chem* **2**:869-885.

Akabas MH, Stauffer DA, Xu M and Karlin A (1992) Acetylcholine receptor channel structure probed in cysteine-substitution mutants. *Science (Wash DC)* **258:**307-310.

Akabas MH (2004) $GABA_A$ receptor structure-function studies: a reexamination in light of new acetylcholine receptor structures. *Int Rev Neurobiol* **62**:1-43.

Akk G, Li P, Bracamontes J, Reichert DE, Covey DF, and Steinbach JH (2008) Mutations of the GABA-A receptor α_1 subunit M1 domain reveal unexpected complexity for modulation by neuroactive steroids. *Mol Pharmacol* **74:**614-627.

Allan AM and Harris RA (1987) Involvement of neuronal chloride channels in ethanol intoxication, tolerance, and dependence. *Recent Dev Alcohol* **5:** 313–325.

Amin J (1999) A single hydrophobic residue confers barbiturate sensitivity to gamma-aminobutyric acid type C receptor. *Mol Pharmacol* **55:**411-23.

Amin J and Weiss D (1993) GABAA receptor needs two homologous domains of the β subunit for activation by GABA, but not by pentobarbital. *Nature* **366**:565-569.

Bali M and Akabas MH (2004) Defining the propofol binding site location on the GABAA receptor. *Mol Pharmacol* **65:**68-76.

Baulac S, Huberfeld G, Gourfinkel-An I, Mitropoulou G, Beranger A, Prud'homme JF, Baulac M, Brice A, Bruzzone R, and LeGuern, E. (2001) First genetic evidence of $GABA_A$ receptor dysfunction in epilepsy: a mutation in the gamma2-subunit gene. *Nat Genet* **28**:46-48.

Baumann SW, Baur R and Sigel E (2001) Subunit arrangement of gamma-aminobutyric acid type A receptors. *J Biol Chem* **276:**36275-80.

Baumann SW, Baur R and Sigel E (2002) Forced subunit assembly in alpha1beta2gamma2 GABAA receptors. Insight into the absolute arrangement. *J Biol Chem* **277:**46020-5.

Baur R, Minier F, and Sigel E (2006) A $GABA_A$ receptor of defined subunit composition and positioning: concatenation of five subunits. *FEBS Lett* **580**:1616-20.

Beene DL, Brandt GS, Zhong W, Zacharias NM, Lester HA, Dougherty DA (2002) Cation-pi interactions in ligand recognition by serotonergic (5- HT3A) and nicotinic acetylcholine receptors: the anomalous binding properties of nicotine. *Biochemistry* **41:**10262–9.

Beene DL, Price KL, Lester HA, Dougherty DA, and Lummis SC (2004) Tyrosine residues that control binding and gating in the 5-hydroxytryptamine 3 receptor revealed by unnatural amino acid mutagenesis. *J Neurosci* **24:**9097-9104.

Benke D, Fritschy JM, Trzeciak A, Bannwarth W and Mohler H (1994) Distribution, prevalence, and drug binding profile of gamma-aminobutyric acid type A receptor subtypes differing in the beta-subunit variant. *J Biol Chem* **269:**27100-7.

Benke D, Fakitsas P, Roggenmoser C, Michel C, Rudolph U, and Mohler H (2004) Analysis of the presence and abundance of GABAA receptors containing two different types of α subunits in murine brain using point-mutated α subunits. *J Biol Chem* **279:**43654-60.

Bianchi MT and Macdonald RL (2002) Slow phases of GABA(A) receptor desensitization: structural determinants and possible relevance for synaptic function. *J Physiol (Lond)* **544:**3-18.

Bianchi MT, Botzolakis EJ, Lagrange AH, and Macdonald RL (2009) Benzodiazepine modulation of GABA(A) receptor opening frequency depends on activation context: a patch clamp and simulation study. *Epilepsy Res* **85**:212-20.

Boileau AJ, Evers AR, Davis AF and Czajkowski C (1999) Mapping the agonist binding site of the GABAA receptor: evidence for a β-strand. *J Neurosci* **19**:4847-54.

Boileau AJ, Kucken AM, Evers AR and Czajkowski C (1998) Molecular dissection of benzodiazepine binding and allosteric coupling using chimeric gamma-aminobutyric acidA receptor subunits. *Mol Pharmacol* **53:**295-303.

Boileau, AJ, Newell JG and Czajkowski C (2002) GABAA receptor β2 Tyr97 and Leu99 line the GABA-binding site: insights into mechanisms of agonist and antagonist actions. *J Biol Chem* **277:**2931-7.

Boileau AJ, Pearce RA and Czajkowski C (2005) Tandem subunits effectively constrain GABAA receptor stoichiometry and recapitulate receptor kinetics but are insensitive to GABAA receptor-associated protein. *J Neurosci* **25:**11219-11230.

Boulineau N, Baur R, Minier F and Sigel E (2005) Consequence of the presence of two different β subunit isoforms in a GABAA receptor. *J Neurochem* **95:** 1724-31.

Bollan K, King D, Robertson LA, Brown K, Taylor PM, Moss SJ and Connolly CN (2003) GABA(A) receptor composition is determined by distinct assembly signals within alpha and beta subunits. *J Biol Chem* **278:**4747-55.

Bonnert TP, McKernan RM, Farrar S et al. (1999) θ, a novel γ-aminobutyric acid type A receptor subunit. *Proc Natl Acad Sci USA* **96:**9891-6.

Borders CL,Jr, Broadwater JA, Bekeny PA, Salmon JE, Lee AS, Eldridge AM and Pett VB (1994) A structural role for arginine in proteins: multiple hydrogen bonds to backbone carbonyl oxygens. *Protein Sci* **3:**541-548.

Borghese CM, Storustovu S, Ebert B, Herd MB, Belelli D, Lambert JJ, Marshall G, Wafford KA and Harris RA (2006) The delta subunit of g-aminobutyric acid type A receptors does not confer sensitivity to low concentrations of ethanol. *J Pharmacol & Exper Ther* **316**:1360-8.

Bourne Y, Radic Z, Araoz R, Talley TT, Benoit E, Servent D, Taylor P, Molgo J, Marchot P (2010) Structural determinants in phycotoxins and AChBP conferring high affinity binding and nicotinic AChR antagonism. *Proc Natl Acad Sci USA* **107:**6076-81.

Bowery NG, and Smart TG (2006) GABA and glycine as neurotransmitters: a brief history. *British J of Pharm* **147**:S109–S119.

Bowser DN, Wagner DA, Czajkowski C, Cromer BA, Parker MW, Wallace RH, Harkin LA, Mulley JC, Marini C, and Berkovic SF et al. (2002) Altered kinetics and benzodiazepine sensitivity of a GABAA receptor subunit mutation [gamma 2(R43Q)] found in human epilepsy. *Proc Natl Acad Sci USA* **99**:15170 -5.

Brejc K, van Dijk WJ, Klaassen RV, Schuurmans M, van Der Oost J, Smit AB and Sixma TK (2001) Crystal structure of an ACh-binding protein reveals the ligand-binding domain of nicotinic receptors. *Nature* **411:**269-76.

Burley SK and Petsko GA (1985) Aromatic-aromatic interaction: a mechainism of protein structure stabilization. *Science* **229:**23-28.

Casagrande S, Cupello A, Pellistri F, Robello M (2007) Only high concentrations of ethanol affect GABAA receptors of rat cerebellum granule cells in culture. *Neurosci Lett* **414**:273-276.

Casalotti SO, Stephenson FA and Barnard EA (1986) Separate subunits for agonist and benzodiazepine binding in the gamma-aminobutyric acidA receptor oligomer. *J Biol Chem* **261:**15013-16.

Celie PH, van Rossum-Fikkert SE, van Dijk WJ, Brejc K, Smit AB and Sixma TK (2004) Nicotine and carbamylcholine binding to nicotinic acetylcholine receptors as studied in AChBP crystal structures. *Neuron* **41:** 907-914.

Chen S, Hartmann HA, and Kirsch GE (1997) Cysteine mapping in the ion selectivity and toxin binding region of the cardiac Na^+ channel pore. *J Membr Biol* **155**:11-25.

Chiara DC, Xie Y, and Cohen JB (1999) Structure of the agonist-binding sites of the Torpedo nicotinic acetylcholine receptor: affinity-labeling and mutational analyses identify gamma Tyr-111/delta Arg-113 as antagonist affinity determinants. *Biochemistry* **38**:6689-98.

Choi DS, Wei W, Deitchman JK, et al. (2008) Protein Kinase C σ Regulates Ethanol Intoxication and Enhancement of GABA-Stimulated Tonic Current. *J Neuroci* **28:**11890-9.

Colquhoun D (1998) Binding, gating, affinity and efficacy: the interpretation of structure-activity relationships for agonists and of the effects of mutating receptors. *Br J Pharmacol* **125:**924-47.

Colquhoun D and Hawkes AG (1995) The principles of the stochastic interpretation of ion channel mechanisms. In: Single-channel recording (Sakmann B, Neher E, eds), pp 397-482. New York: Plenum.

Connolly CN and Wafford KS (2004) The cys-loop superfamily of the ligand-gated ion channels: the impact of receptor structure on function. *Biochem Soc Trans* **23**:529-534.

Cromer BA, Morton CJ and Parker MW (2002) Anxiety over GABA(A) receptor structure relieved by AChBP. *Trends Biochem Sci* **27:**280-287.

Crowley PB and Golovin A (2005) Cation-π interactions in protein–protein interfaces. *Proteins* **59**:231-9.

Cutting GR, Lu L, O′Hara, BF, Kasch LM, Montrose-Rafizadeh C, Donovan DM, Shimada S, Antonarakis SE, Guggino WB, Uhl GR and Kazazian jr. HH (1991) Cloning of the γ-aminobutyric acid (GABA) ρ1 cDNA: a GABA receptor subunit highly expressed in the retina. *Proc Natl Acad Sci USA* **88**: 2673-77.

Czajkowski C and Karlin A (1995) Structure of the nicotinic receptor acetylcholine-binding site. Identification of acidic residues in the delta subunit within 0.9 nm of the 5 alpha subunit-binding. *J Biol Chem* **270**:3160-64.

Dan B and Boyd SG (2003) Angelman syndrome reviewed from a neurophysiological perspective. The UBE3A-GABRB3 hypothesis. *Neuropediatrics* **34**: 169-176.

Dellisanti DC, Yao Y, Stround CJ, Wang ZZ and Chen L (2007) Crystal structure of the extracellular domain of nAChR α_1 bound to α-bungarotoxin at 1.94 Å resolution. *Nature Neurosci* **10**:953-962.

Deng L, Ransom RW and Olsen RW (1986) 3[H]muscimol photolabels the gamma-aminobutyric acid receptor binding site on a peptide subunit distinct from that labeled with benzodiazepines. *Biochem Biophys Res Commun* **138:**1308-1314.

Dennis M, Giraudat J, Kotzyba-Hibert F, Goeldner M, Hirth C, Chang JY, Lazure C, Chrétien M and Changeux JP (1988) Amino acids of the *Torpedo marmorata*

acetylcholine receptor alpha subunit labeled by a photoaffinity ligand for the acetylcholine binding site. *Biochemistry* **27**:2346-57.

Enz R and Cutting GR (1999) $GABA_C$ receptor ρ subunits are heterogeneously expressed in the human CNS and form homo- and heterooligomers with distinct physical properties. *Eur J Neurosci* **11**:41-50.

Ernst M, Brauchart D, Boresch S, and Sieghart W (2003) Comparative modeling of GABA(A) receptors: limits, insights, future developments. *Neuroscience* **119**:933-43.

Farrar SJ, Whiting PJ, Bonnert TP and McKernan RM (1999) Stoichiometry of a ligand-gated ion channel determined by fluorescence energy transfer. *J Biol Chem* **274:**10100-4.

Feigenspan A, Wassle H, and Bormann J (1993) Pharmacology of GABA receptor Cl- channels in rat retinal bipolar cells. *Nature* **361**:159-162.

Feigenspan A and Bormann J (1994). Differential pharmacology of $GABA_A$ and $GABA_C$ receptors on rat retinal bipolar cells. *Eur J Pharmacol* **288**:97-104.

Fritschy JM, and Mohler H (1995) GABAA-receptor heterogeneity in the adult-rat brain: differential regional and cellular- distribution of 7 major subunits. *J Comp Neurol* **359:**154-194.

Gallivan JP and Dougherty DA (1999) Cation-π Interactions in Structural Biology. *Am Chem Soc* **122:**870-874.

Galzi JL, Revah F, Black D, Goeldner M, Hirth C, Changeux JP (1990) Identification of a novel amino acid alpha-tyrosine 93 within the cholinergic ligands- binding sites of the acetylcholine receptor by photoaffinity labeling. Additional evidence for a three-loop model of the cholinergic ligands-binding sites. *J Biol Chem* **265**:10430–7.

Gleitsman KR, Kedrowski SM, Lester HA and Dougherty DA (2008) An intersubunit hydrogen bond in the nicotinic acetylcholine receptor that contributes to channel gating. *J Biol Chem* **283:**35638-43.

Glykys J, Peng Z, Chandra D, Homanics GE, Houser CR and Mody I (2007) A new naturally occurring GABAA receptor subunit partnership with high sensitivity to ethanol. *Nat Neurosci* **10:**40-48.

Goldschen-Ohm MP, Wagner DA, Petrou S and Jones MV (2010) An epilepsy-related region in the GABA(A) receptor mediates long-distance effects on GABA and benzodiazepine binding sites. *Mol Pharmacol* **77:**35-45.

Grudzinska J, Schemm R, Haeger S, Nicke A, Schmalzing G, Betz H, and Laube B (2005) The β subunit determines the ligand binding properties of synaptic glycine receptors. *Neuron* **45:**727-739.

Haefely W, Kulcsar A, Mohler H, Pieri L, Polc P, and Schaffner R (1975) Possible involvement of GABA in the central actions of benzodiazepines. *Adv Biochem Psychopharm* **11**:131-151.

Harrison NJ and Lummis SC (2006) Locating the carboxylate group of GABA in the homomeric rho GABA(A) receptor ligand-binding pocket. *J Biol Chem* **281**:24455-61.

Hartvig L, Lukensmejer B, Liljefors T and Dekermendjian K (2000) Two conserved arginines in the extracellular N-terminal domain of the GABA(A) receptor alpha(5) subunit are crucial for receptor function. *J Neurochem* **75**:1746-53.

Hedblom E and Kirkness EF (1997) A novel class of GABAA receptor subunit in tissues of the reproductive system. *J Biol Chem* **272:**15346-50.

Hidalgo P and MacKinnon R (1995) Revealing the architecture of a K^+ channel pore through mutant cycles with a peptide inhibitor. *Science* **268:**307-310.

Hobza P, Selzle LH and Schlag WE (1996) Potential energy surface for the benzene dimer. Results of ab initio CCSD(T) calculations show two nearly isoenergetic structures: T-shaped and parallel-displaced. *J Phys Chem* **100:**18790-4.

Holden JH and Czajkowski C (2002) Different residues in the $GABA_A$ receptor α_1T60 – α_1K70 region mediate GABA and SR-95531 actions. *J Biol Chem* **277**:18785-92.

Horovitz A (1996) Double-mutant cycles: a powerful tool for analyzing protein structure and function. *Fold Des* **1:**121-6.

Hosie AM, Wilkins ME, da Silva HM and Smart TG (2006) Endogenous neurosteroids regulate GABAA receptors through two discrete transmembrane sites. *Nature* **444:**486-489.

Johnston GAR (2003) Dietary chemicals and brain function. *Journal & Proceedings of the Royal Society of New South Wales* **135:**57-71.

Johnston GAR (2005) $GABA_A$ receptor channel pharmacology. *Curr Pharm Design* **11:** 1867-85.

Jones MV and Westbrook GL (1995) Desensitized states prolong $GABA_A$ channel responses to brief agonist pulses. *Neuron* **15:**181-191.

Jones MV, Sahara Y, Dzubay JA and Westbrook GL (1998) Defining affinity with the GABAA receptor. *J Neurosci* **18:**8590-8604.

Jones MV, Jonas P, Sahara Y and Westbrook GL (2001) Microscopic kinetics and energetics distinguish GABA(A) receptor agonists from antagonists. *Biophys J* **81:**2660-70.

Jorgensen LW and Severance LD (1990) Aromatic-aromatic interactions: free energy profiles for the benzene dimer in water, chloroform, and liquid benzene. *J Am Chem Soc* **112:**4768-74.

Karlin A and Akabas MH (1998) Substituted-cysteine accessibility method. *Methods Enzymol* **293:**123-145.

Kash TL, Jenkins A, Kelley JC, Trudell JR and Harrison NL (2003) Coupling of agonist binding to channel gating in the GABA(A) receptor. *Nature* **421:**272-5.

Kash TL, Trudell JR and Harrison NL (2004) Structural elements involved in activation of the gamma-aminobutyric acid type A (GABAA) receptor. *Biochem Soc Trans* **32:**540-6.

Kistler J and Stroud RM (1981) Crystalline arrays of membrane-bound acetylcholine receptor. *Proc Natl Acad Sci USA* **78**:3678-82.

Kleinberger-Doron N and Kanner B (1994) Identification of tryptophan residues critical for the function and targeting of the γ-aminobutyric acid transporter (subtype A) *J Biol Chem* **269**:3063-7.

Kloda JH and Czajkowski C (2007) Agonist-, antagonist-, and benzodiazepine-induced structural changes in the alpha1 Met113-Leu132 region of the GABAA receptor. *Mol Pharmacol* **71:**483-493.

Klymkowsky MW and Stroud RM (1979) Immunospecific identification and three-dimensional structure of a membrane-bound acetylcholine receptor from *Torpedo californica*. *J Mol Biol* **128**:319-34.

Krnjević K and Schwartz S (1967) The action of γ-aminobutyric acid on cortical neurones. *Exp Brain Res* **3**:320-36.

Laha KT and Wagner DA (2011) A state-dependent salt-bridge interaction exists across the β/α intersubunit interface of the $GABA_A$ receptor. *Mol Pharm* doi:10.1124/mol.110.068619.

Lester HA, Dibas MI, Dahan DS, Leite JF, and Dougherty DA (2004) Cys-loop receptors: new twists and turns. *Trends Neurosci* **27:**329-336.

Luddens H, Pritchett DB, Kohler M, Killisch I, Keinanen K, Monyer H, Sprengel R, and Seeburg PH (1990) Cerebellar GABAA receptor selective for a behavioural alcohol antagonist. *Nature* **346**:648-651.

Lummis SCR (2009) Locating GABA in GABA receptor binding sites. *Biochem Soc Trans* **37:** 1343-6.

Lummis SC, L Beene D, Harrison NJ, Lester HA, and Dougherty DA (2005) A cation-π binding interaction with a tyrosine in the binding site of the GABAC receptor. *Chem Biol* **12**:993-997.

Luscher B, and Keller CA (2004) Regulation of GABAA receptor trafficking, channel activity, and functional plasticity of inhibitory synapses. *Pharmacol Ther* **102:**195-221.

Maksay G, Bikadi Z and Simonyi M (2003) Bindinginteractionsofantagonists with 5-hydroxytryptamine3A receptor models. *J Recept Signal Transduct Res* **23**:255-270.

McGehee DS (1999) Molecular diversity of neuronal nicotinic acetylcholine receptors. *Ann N Y Acad Sci* **868:**565-577.

McKernan RM and Whiting PJ (1996) Which GABAA-receptor subtypes really occur in the brain? *Trends Neurosci* **19:**139-43.

Mihic SJ, Ye Q, Wick MJ, Koltchine VV, Krasowski MD, Finn SE, Mascia MP, Valenzuela CF, Hanson KK, Greenblatt EP, Harris RA and Harrison NL (1997) Sites of alcohol and volatile anaesthetic action on GABA(A) and glycine receptors. *Nature* **389:**385-9.

Minier F and Sigel E (2004) Positioning of the alpha-subunit isoforms confers a functional signature to gamma-aminobutyric acid type A receptors. *Proc Natl Acad Sci USA* **101:**7769-74.

Miyazawa A, Fujiyoshi Y, Stowell M and Unwin N (1999) Nicotinic acetylcholine receptor at 4.6 A resolution: transverse tunnels in the channel wall. *J Mol Biol* **288:**765-86.

Mohler H (2007). Molecular regulation of cognitive functions and developmental plasticity: impact of GABAA receptors. *J Neurochem* **102:**1-12.

Moragues N, Ciofi, P, Lafon, P, Tramu G, and Garret M (2003) GABAA receptor ε-subunit expression in identified peptidergic neurons of the rat hypothalamus. *Brain Res* **967:** 285-289.

Neelands TR, Fisher JL, Bianchi M, and Macdonald RL (1999) Spontaneous and γ-aminobutyric acid (GABA)-activated GABAA receptor channels formed by ε subunit-containing isoforms. *Mol Pharmacol* **55:**168-178.

Neelands TR and Macdonald RL (1999) Incorporation of the π subunit into functional γ-aminobutyric acid A receptors. *Mol Pharmacol* **56:**598-610.

Newell JG and Czajkowski C (2003) The GABAA Receptor alpha 1 Subunit Pro174-Asp191 Segment Is Involved in GABA Binding and Channel Gating. *J Biol Chem* **278:**13166-72.

Newell JG, McDevitt RA and Czajkowski C (2004) Mutation of glutamate 155 of the GABAA receptor beta2 subunit produces a spontaneously open channel: a trigger for channel activation. *J Neurosci* **24:**11226-35

O'Mara M, Cromer B, Parker M and Chung SH (2005) Homology model of the GABAA receptor examined using Brownian dynamics. *Biophys J* **88:**3286-99.

Padgett CL, Hanek AP, Lester HA, Dougherty DA and Lummis SC (2007) Unnatural amino acid mutagenesis of the GABA(A) receptor binding site residues reveals a novel cation-pi interaction between GABA and beta 2Tyr97. *J Neurosci* **27:**886-892.

Palmer MR and Hoffer BJ (1990) GABAergic mechanisms in the electrophysiological actions of ethanol on cerebellar neurons. *Neurochem Res* **15:**145-151.

Peters JA, Hales TG, and Lambert JJ (2005) Molecular determinants of single-channel conductance and ion selectivity in the Cys-loop family: insights from the 5-HT3 receptor. *Trends Pharmacol Sci* **26:** 587-594.

Pirker S, Schwarzer C, Wieselthaler A, Sieghart W, and Sperk G (2000) GABAA receptors: Immunocytochemical distribution of 13 subunits in the adult rat brain. Neurosci. *Neurosci* **101:** 815-850.

Pless SA, Millen KS, Hanek AP, Lynch JW, Lester HA, Lummis SCR and Dougherty DA (2008) A Cation-π interaction in the binding site of the glycine receptor is mediated by a phenylalanine residue. *J Neurosci* **28**:10937-42.

Price KL, Millen KS and Lummis SC (2007) Transducing agonist binding to channel gating involves different interactions in 5-HT3 and GABAC receptors. *J Biol Chem* **282:**25623-30.

Qi ZH, Song M, Wallace MJ, Wang D, Newton PM, McMahon T, Chou WH, Zhang C, Shokat KM and Messing RO (2007) Protein kinase C epsilon regulates gamma-aminobutyrate type A receptor sensitivity to ethanol and benzodiazepines through phosphorylation of gamma2 subunits. *J Biol Chem* **282:** 33052-63.

Ranganathan R, Lewis JH, and MacKinnon R (1996) Spatial localization of the K^+ channel selectivity filter by mutant cycle-based structure analysis. *Neuron* **16:**131-139.

Reeves D, Sayed M, Chau P-L, Price K, and Lummis S (2003) Prediction of 5-HT3 receptor agonist-binding residues using homology modeling. *Biophys J* **84:**2338-44.

Serafini R, Bracamontes J and Steinbach JH (2000) Structural domains of the human GABAA receptor 3 subunit involved in the actions of pentobarbital. *J Physiol (Lond)* **524 Pt 3:**649-76.

Sergeeva OA, Eriksson KS, Sharonova IN, Vorobjev VS and Haas HL (2002) GABAA receptor heterogeneity in histaminergic neurons. *Eur J Neurosci* **16:**1472-82.

Sieghart W, and Ernst M (2005) Heterogeneity of GABAA receptors: revived interest in the development of subtype-selective drugs. *Curr Med Chem – Central Nervous System Agents* **5:**217-242.

Sieghart W and Sperk G (2002) Subunit composition, distribution and function of $GABA_A$ receptor subtypes. *Curr Top Med Chem* **2:**795-816.

Sigel E, Baur R, Kellenberger S and Malherbe P (1992) Point mutations affecting antagonist affinity and agonist dependent gating of $GABA_A$ receptor channels. *EMBO J* **11**:2017-23.

Sigel E and Buhr A (1997) The benzodiazepine binding site of GABAA receptors. *Trends Pharmacol Sci* **18:**425-9.

Sigworth FJ (1980) The variance of sodium current fluctuations at the node of Ranvier. *J Physiol* **307**:97-129.

Simon J, Wakimoto H, Fujita N, Lalande M and Barnard EA (2004) Analysis of the set of GABA(A) receptor genes in the human genome. *J Biol Chem* **279:**41422-41435.

Sine SM (1997) Identification of equivalent residues in the gamma, delta, and epsilon subunits of the nicotinic receptor that contribute to alpha-bungarotoxin binding. *J Biol Chem* **272**:23521-27.

Sine SM and Engel AG (2006) Recent advances in Cys-loop receptor structure and function. *Nature* **440:** 448-455.

Sine SM, Quiram P, Papanikolaou F, Kreienkamp HJ, Taylor P (1994) Conserved tyrosines in the alpha subunit of the nicotinic acetylcholine receptor stabilize quaternary ammonium groups of agonists and curariform antagonists. *J Biol Chem* **269**:8808-16.

Sinkkonen ST, Hanna MC, Kirkness EF, and Korpi ER (2000) GABAA receptor ε and γ subunits display unusual structural variation between species and are enriched in the rat locus ceruleus. *J Neurosci* **20:** 3588-95.

Sixma TK and Smit AB (2003) Acetylcholine binding protein (AChBP): A secreted glial protein that provides a high-resolution model for the extracellular domain of pentameric ligand-gated ion channels. *Annu Re*v *Biophys Biomol Struct* **32:**311-334.

Sun C, Sieghart W, and Kapur, J. (2004) Distribution of alpha1, alpha4, gamma2, and delta subunits of GABAA receptors in hippocampal granule cells. *Brain Res* **1029:**207-216.

Sundstrom-Poromaa I, Smith DH, Gong QH, Sabado TN, Li X, Light A, Wiedmann M, Williams K and Smith SS (2002) Hormonally regulated α4β2δ $GABA_A$ receptors are a target for alcohol. *Nat Neurosci* **5:**721-722.

Sussman JL, Harel M, Frolow F, Oefner C, Goldman A, Toker L and Silman I (1991) Atomic structure of acetylcholine esterase from *Torpedo californica*: a prototypic acetylcholine-binding protein. *Science* **253**:872-879.

Thompson A, Price K, Reeves D, Chan S, Chau P, and Lummis S (2005) Locating an antagonist in the 5-HT3R receptor binding site using modeling and radioligand binding. *J Biol Chem* **280:**20476-82.

Tone M, Pascarella S and De Biase D (1995) Active site model for γ-aminobutyrate aminotransferase explains substrate and inhibitor reactivities. *Protein Sci* **4**:2366-74.

Tretter V, Ehya N, Fuchs K, and Sieghart W (1997) Stoichiometry and assembly of a recombinant GABAA receptor subtype. *J Neurosci* **17:**2728-37.

Unwin N (1995) Acetylcholine receptor channel imaged in the open state. *Nature* **373:**37-43.

Unwin N (2005) Refined structure of the nicotinic acetylcholine receptor at 4A resolution. *J Mol Biol* **346:**967-989.

Wagner DA and Czajkowski C (2001) Structure and dynamics of the GABA binding pocket: A narrowing cleft that constricts during activation. *J Neurosci* **21:**67-74.

Wagner DA, Czajkowski C, and Jones MV (2004) An arginine involved in GABA binding and unbinding but not gating of the GABA(A) receptor. *J Neurosci* **24:**2733-41.

Wallner M, Hanchar HJ, and Olsen RW (2003) Ethanol enhances α4β3δ and α6β3δγ-aminobutyric acid type A receptors at low concentrations known to affect humans. *Proc Natl Acad Sci USA* **100:**15218-23.

Wei W, Faria LC and Mody I (2004) Low ethanol concentrations selectively augment the tonic inhibition mediated by delta subunit-containing GABAA receptors in hippocampal neurons. *J Neurosci* **24:**8379-82.

Weiner JL and Valenzuela CF (2006) Ethanol modulation of GABAergic transmission: the view from the slice. *Pharmacol Ther* **111:**533-554.

Westh-Hansen SE, Witt MR, Dekermendjian K, Liljefors T, Rasmussen PB and Nielsen M (1999) Arginine residue 120 of the human GABAA receptor alpha 1, subunit is essential for GABA binding and chloride ion current gating. *Neuroreport* **10:**2417-21.

Whiting PJ (2003) GABA-A receptor subtypes in the brain: a paradigm for CNS drug discovery? *Drug Discov Today* **8:**445-450.

Wohlfarth KM, Bianchi MT, and Macdonald RL (2002) Enhanced neurosteroid potentiation of ternary $GABA_A$ receptors containing the δ subunit. *J Neurosci* **22:**1541-9.

Yamashita M, Marszalec W, Yeh JZ, and Narahashi T (2006) Effects of Ethanol on Tonic GABA Currents in Cerebellar Granule Cells and Mammalian Cells Recombinantly Expressing GABAA Receptors. *J Pharmacol Exp Ther* **319:**431-8.

Zacharias N and Dougherty DA (2002) Cation-π interactions in ligand recognition and catalysis. *Trends in Pharmacological Sciences* **23**:281-7.

Zafrakas M, Chorovicer M, Klaman I, Kristiansen G, Wild PJ, Heindrichs U, Knuchel R, and Dahl E (2006) Systematic characterisation of GABRP expression in sporadic breast cancer and normal breast tissue. *Int J Cancer* **118:**1453-9.

Zamyatin, AA (1972) Protein Volume in Solution. *Prog Biophys Mol Biol* **24**:107-123.

Zhong W, Gallivan JP, Zhang Y, Li L, Lester HA, Dougherty DA (1998) From ab initio quantum mechanics to molecular neurobiology: a cation-pi binding site in the nicotinic receptor. *Proc Natl Acad Sci USA* **95**:12088-93.

APPENDIX CHAPTER

DIRECT MODULATION OF $GABA_A$ RECEPTOR BY ETHANOL: PROBING FOR EVIDENCE OUTSIDE-OUT PATCH CLAMP ANALYSIS

Introduction

$GABA_A$ receptors are the major inhibitory receptors in the CNS. By providing inhibitory neuronal transmission, the $GABA_A$ receptors play an important role in normal neuronal processing. $GABA_A$ receptors have been common targets for therapeutic agents treating such disorders as epilepsy and anxiety. Also, $GABA_A$ receptors are known to be modulated by a number of substances such as barbiturates, benzodiazepines, anesthetics, and possibly ethanol. While the basis of modulation by benzodiazepines and general anesthetics are well understood, little progress has been made in deciphering how ethanol may modulate the function of $GABA_A$ receptors, in the past two decades. The reason for this slow progress has to do with the controversial reports from studies that confirm and studies that dismiss the presence of ethanol modulation of $GABA_A$ receptors.

Ethanol as a potential functional modulator of $GABA_A$ receptors

While anaesthetics, barbiturates, and benzodiazepines have become useful therapeutic agents, the role of ethanol has been difficult to define. These important therapeutic agents act allosterically to increase the opening frequency of the $GABA_A$ receptors and, in so doing, provide a mechanism for inducing anxiolytic and sedative effects (Bowery and Smart, 2006). The many effects of ethanol have also put it on the list as a potential $GABA_A$ receptor modulator. For example, at increasing doses, ethanol can cause impaired reaction time and judgment, motor incoordination, coma, and even death. All of these effects are consistent with increased $GABA_A$ receptor function. However, experimental investigations dealing with ethanol modulation of $GABA_A$ receptor function have reported controversial results.

There have been a handful of reports that alcohol, at sobriety-impairing concentrations (3-30 mM), enhances GABA-induced currents in a subset of cultured neurons (Aguayo, 1990; Aguayo et al., 2002) and also in certain neurons in slices (Palmer and Hoffer, 1990). In addition, by measuring $^{36}Cl^-$ flux in synaptoneurosomes, a number of studies assayed that the current flow through $GABA_A$ receptors was increased by ethanol (as reviewed by Allan and Harris, 1987). However, most of these effects were not reproducible by other scientists in the field, using similar or alternative approaches (Borghese et al., 2006; Yamashita et al., 2006; Casagrande et al., 2007).

Some experiments in which recombinant $GABA_A$ receptors were selectively expressed reported that low concentrations of ethanol did not affect $GABA_A$ receptor isoforms that contain the γ_2 subunit (Wallner et al., 2003; Wei et al., 2004). Electrophysiological recording techniques like patch clamp of single neurons, from cultures and from slices preparations, found that most synaptic (γ_2-containing) $GABA_A$ receptors were not affected by low to sobriety-impairing doses (3-30 mM) of ethanol and have very little, if any, effect at concentrations above 100mM (Weiner and Valenzuela, 2006). Such negative results contradicted earlier reports of ethanol's positive modulation of $GABA_A$ receptors. Therefore, some scientists have considered the possibility that the site of ethanol modulation is extrasynaptic, or even intracellular.

Since δ-containing receptors (i.e. $\alpha_4\beta_3\delta$) are known to have higher affinity for such agonists as GABA, THIP, and muscimol as well as known modulators such as general anaesthetics and neurosteroids (Adkins et al., 2001; Wohlfarth et al., 2002), they are thought to be more responsive to ethanol as well. Indeed, it has been reported that $GABA_A$ receptors containing the δ subunit, in particular $\alpha_4\beta_3\delta$ and $\alpha_6\beta_3\delta$ receptors, are

highly modulated by ethanol (Sundstrom-Poroma et al., 2002; Wallner et al., 2003). Glykys et al. (2007) showed that low sobriety-impairing ethanol concentrations (20–30 mM) affected the behavior of wild-type and α_4-deficient mice but not δ-deficient mice, further demonstrating that δ subunit is important for ethanol modulation. However, many labs, including our own, have not been able to detect the effects of ethanol on δ-containing receptors, using similar approaches. All in all, reports from several studies indicated that δ-containing receptors were potentiated by low (3-30 mM) intoxicating concentrations of ethanol (Glykys et al., 2007; Sundstrom-Porama et al., 2002; Wallner et al., 2003). In contrast, several other studies were unable to detect low dose ethanol sensitivity of δ-containing $GABA_A$ receptors (Borghese et al., 2006; Casagrande et al., 2007; Yamashita et al., 2006), indicating that, like γ_2-containing $GABA_A$ receptors, ethanol modulation of extrasynaptic or perisynaptic δ-containing receptors is also variable.

Published recently is a study by Qi et al. (2007), which reported modulation of $\alpha_1\beta_2\gamma_2$ $GABA_A$ receptors by ethanol when receptor phosphorylation was blocked. Qi and colleagues explored the intracellular signaling mechanisms as a potential source for variable results from earlier ethanol studies. They found that ethanol modulation is dependent on the phosphorylation state of the γ_2 subunit of the $GABA_A$ receptors. Specifically, results from this study led to the conclusion that protein kinase C epsilon (PKCε) regulates the sensitivity of $\alpha_1\beta_2\gamma_2$ receptors to ethanol and benzodiazepines through phosphorylation of a serine (S327) located in the large intracellular loop of γ_2 subunit. In other words, dephosphorylation of the S327 on γ_2 subunit will render the $\alpha_1\beta_2\gamma_2$ receptor sensitive to low concentrations (3-30 mM) of ethanol. Another study

(Choi et al., 2008) also found that protein kinase C delta (PKCδ) regulates ethanol potentiation of δ-containing $GABA_A$ receptors. Unlike γ_2 receptors, δ receptors require the presence of phosphorylation for ethanol effect. Overall, both of the above studies offered a potential way to consistently observe ethanol's effects on $GABA_A$ receptors – by controlling the phosphorylation state of the $GABA_A$ receptors. Yet, the ultimate goal is not only being able to measure the effect of ethanol on $GABA_A$ receptors but also finding therapeutic means to treat both acute ethanol intoxication and chronic dependence.

In order to come up with effective strategies to counter the physiological effects of ethanol, assuming that ethanol-elicited effects are mediated by ethanol directly acting on $GABA_A$ receptor, it would be crucial to also understand how ethanol affects the kinetics of $GABA_A$ receptor. Any attempt to control ethanol effect through blocking or enhancing of PKCε or PKCδ, for instance, would be problematic *in vivo* because it would be impossible to target specific kinases without affecting other processes. Logically, it would be simpler to reverse the effects of ethanol on receptor kinetics using agonist or modulator derivatives that specifically target the $GABA_A$ receptors. Thus, it is the objective of the present study to examine the effects of ethanol of the kinetics of $GABA_A$ receptors. A step beyond the focus of this study is to screen various $GABA_A$R-specific for anti-ethanol effects.

Results

The objective of the present study was to verify and describe how ethanol directly modulates $GABA_A$ receptors. We approached this study with the premise that if ethanol directly modulates the $\alpha_1\beta_2\gamma_2$ $GABA_A$ receptor, rapid ligand application patch clamp will get at the underlying mechanism of modulation. Therefore, the experiments were designed to: 1) demonstrate, through isolated outside-out patch, that ethanol directly modulates $GABA_A$ receptors, and 2) gain more details regarding the underlying mechanism(s) of such direct modulation.

Our initial attempts to measure ethanol modulation of $GABA_A$ receptors yielded mostly negative results. We looked at $\alpha_1\beta_2\gamma_2$ and $\alpha_1\beta_2\delta$ receptors' response to ethanol. Less than 20% of the patches from $\alpha_1\beta_2\gamma_2$ cells had current that was potentiated by 50mM ethanol (Figure A.1 A) and none of the patches from $\alpha_1\beta_2\delta$ cells showed potentiated current. Worse, the degree of potentiation of $\alpha_1\beta_2\gamma_2$ was not consistent from patch to patch, for a given dose of ethanol. The cause of this variability was thought to be the different amounts of $\alpha_1\beta_2$ receptors, which are ethanol insensitive, present in each patch. Note that $\alpha_1\beta_2$ receptors are assembled by two α_1 and three β_2 subunits; they are functional $GABA_A$ receptors known to be insensitive to ethanol. For example, when the HEK293 cells are transfected with the cDNAs of α_1, β_2, γ_2 subunits, two types of subunit assembly may occur: $2\alpha_1+2\beta_2+1\gamma_2$ and $2\alpha_1+3\beta_2$. So, when the $\alpha_1\beta_2\gamma_2$ receptors are dominant, ethanol potentiation is observed, otherwise no potentiation would be observed. Additionally, as suggested by Qi et al. (2007), the lack of potentiation could be caused by phosphorylation of γ_2 subunit.

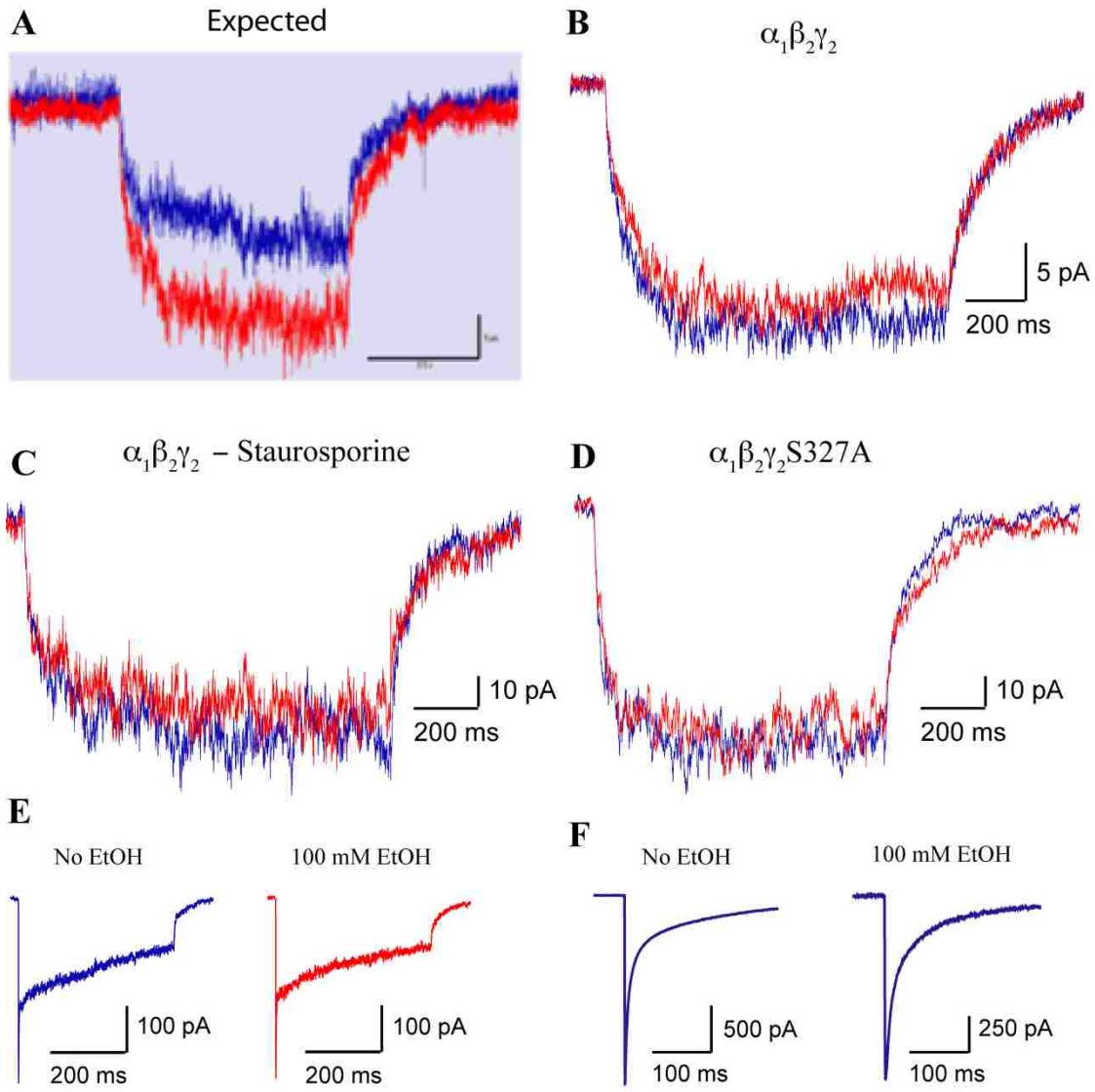

Figure A.1 Ethanol does not directly modulate $\alpha_1\beta_2\gamma_2$ $GABA_A$ receptor. A) The expected potentiation of sub-saturating GABA-induced response by ethanol (not real data): blue - only 3 μM GABA, red - 3 μM GABA and ethanol (mM) co-applied. The degree of potentiation depends on the concentration of ethanol used. B) Ethanol (100 mM) does not modulate $\alpha_1\beta_2\gamma_2$ $GABA_A$ receptors: from the same patch, current elicited by 3 μM GABA (blue) is not different from current elicited by 3 μM GABA with of 100 mM ethanol coapplication (red); n = 13. C) Incubation of cells in staurosporine fails to reveal ethanol modulation. Ethanol coapplication (red) is not different from GABA only current (blue); n = 30. D) Elimination of the previously proposed phosphorylation sites on γ_2 subunit also does not result in ethanol modulation. Current elicited by 10 μM GABA only (blue) is not different from current elicited by 10 μM GABA plus 100 mM ethanol (red); n = 8. E) Coapplication of 100 mM ethanol does not change macroscopic desensitization; n= 5. F) Coapplication of 100 mM ethanol does not change macroscopic deactivation; n = 7.

In the subsequent experiments, two major changes were made to improve the chance of capturing ethanol modulation of $\alpha_1\beta_2\gamma_2$. First, the cDNAs ratio transfected was changed from 1.5 μg(α_1) : 1.5 μg(β_2) : 1.5 μ(γ_2) to 1.5 μg(α_1) : 1.5 μg(β_2) : 4.5 μg(γ_2) to improve the fraction of receptors that are $\alpha_1\beta_2\gamma_2$. Second, prior to patch clamp experiment, the transfected HEK cells were incubated in 20nM staurosporine, a general kinase inhibitor, for 60 minutes to eliminate the basal phosphorylation. Disappointingly, after these two changes in the protocol, still no ethanol modulation of the $\alpha_1\beta_2\gamma_2$ receptor was observed (Figure A.1 B, C).

Then, in an attempt to better control for phosphorylation, S327 residue on γ_2 subunit was mutated to alanine (γ_2S327A), as shown by Qi et al. (2007). Transfection with a ratio of 1.5 μg(α_1) : 1.5 μg(β_2): 4.5 μg(γ_2S327A) was used to yield mainly $\alpha_1\beta_2\gamma_2$S327A receptors. $\alpha_1\beta_2\gamma_2$S327A can serve as a phosphorylation-controlled wild-type for ethanol. As with $\alpha_1\beta_2\gamma_2$ receptors, $\alpha_1\beta_2\gamma_2$S327A receptors were not potentiated by ethanol (Figure A.1 D).

A final strategy used to eliminate phosphorylation was the used of protein phosphatase (PP2A). The catalytic subunit of PP2A was introduced to the intracellular solution (electrode) at 10 nM to control for any residual phosphorylation on the intracellular side of the patch. This approach, too, failed to reveal ethanol modulation of the $\alpha_1\beta_2\gamma_2$ $GABA_A$ receptors.

Throughout the study, measures were taken to ensure enough ethanol exposure. First, we initially used ethanol concentration of 30 mM, which was subsequently replaced by 100 mM. Second, excised patches were exposed to a solution exchange protocol in which the first pulse exposed the patch to a control concentration of GABA (i.e. 500 ms

in 3 uM GABA), return to wash for 20 seconds, and two consecutive pulses exposed the patch to ethanol (i.e. 500 ms in 100 mM ethanol) and immediately to ethanol/GABA combination (500 ms in solution containing 3 uM GABA and 100 mM ethanol). The cycle repeats after a 20-second wash.

Part of this study's objective was to measure how ethanol influences the kinetic parameters of GABA-elicited current. Since no modulation was observed, it was expected that ethanol would not change the macroscopic deactivation and desensitization phases of a GABA-evoked current. Indeed, ethanol did not cause any change in the kinetics of the GABA-evoked current (Figure A.1 E, F).

Discussion

Our initial attempts to measure ethanol modulation of $GABA_A$ receptors yielded mostly negative results. We looked at $\alpha_1\beta_2\gamma_2$ and $\alpha_1\beta_2\delta$ receptors' response to ethanol. Less than 20% of the patches from $\alpha_1\beta_2\gamma_2$ cells had current that was potentiated by 50mM ethanol and none of the patches from $\alpha_1\beta_2\delta$ cells showed potentiated current. Worse, the degree of potentiation of $\alpha_1\beta_2\gamma_2$ was not consistent from patch to patch, for a given dose of ethanol. The cause of this variability was thought to be the different amounts of $\alpha_1\beta_2$ receptors, which are ethanol insensitive, present in each patch. Another possible source of the infrequent and variable potentiation was propofol contamination. Review of the experiment history showed that for those days in which we saw potentiation, the pipes used for ligand application were used in experiments involving propofol perfusion in the previous day. Thus the possibility exist that propofol not ethanol caused the inconsistent cases potentiation.

In summary, the primary goal of this study was to examine how ethanol, at physiologically relevant doses, modulates GABA-induced current. Specifically, we looked at how ethanol altered the kinetics of the $GABA_A$ receptors. We detected no modulation of the $\alpha_1\beta_2\gamma_2$ $GABA_A$ receptor. Thus, our results suggest that ethanol does not modulate the $GABA_A$ receptor at least not through a direct mechanism.